Interfacial activity and membrane interaction of *Duttaphrynus melanostictus* cathelicidin

A Thesis Submitted in Partial Fulfillment of the Requirements for the Degree

of

Doctor of Philosophy

by

Feba Francis

186106004

Department of Biosciences and Bioengineering

Indian Institute of Technology Guwahati

Guwahati, Assam, 781 039, India

Indian Institute of Technology Guwahati

Department of Biosciences and Bioengineering

Declaration

I am pleased to present my thesis titled **"Interfacial activity and membrane interaction of *Duttaphrynus melanostictus* cathelicidin**," which encapsulates my research endeavors in the realm of antimicrobial peptides. This work represents an original investigation into comprehending the peptide-membrane interaction of *Duttaphrynus melanostictus* cathelicidin. Throughout this scholarly pursuit, I have steadfastly upheld the highest standards of academic integrity and ethical standards stipulated by the Indian Institute of Technology and relevant regulatory bodies. All sources of information, including data, ideas, and concepts, have been duly acknowledged and referenced in accordance with the prescribed guidelines of my institution. I affirm that I have not engaged in any form of plagiarism or misrepresentation of others' work. Furthermore, I assert that this thesis is the product of my original research work conducted under the guidance of my esteemed mentors, Prof. Nitin Chaudhary and Prof. Vishal Trivedi, and in compliance with the regulations of my academic institution, the Indian Institute of Technology Guwahati. I declare that this work has not been submitted for any other degree or examination at any other university or institution.

November 16, 2025

Feba Francis
(186106004)

Indian Institute of Technology Guwahati

Department of Biosciences and Bioengineering

Certificate

We hereby certify that the thesis titled **"Interfacial activity and membrane interaction of *Duttaphrynus melanostictus* cathelicidin,"** submitted by Feba Francis under registration number 186106004, has been meticulously prepared under our guidance. This work fulfills the requirements for the Doctor of Philosophy degree at the Indian Institute of Technology Guwahati. The original findings presented in this thesis significantly contribute to the existing knowledge in the field of research. We affirm that this thesis is original and has not been submitted for any other degree or diploma at any other academic institution.

Prof. Nitin Chaudhary

(Supervisor)

Prof. Vishal Trivedi

(Co-supervisor)

November 16, 2025

Table of Contents

Abbreviations

AAMP	Anionic antimicrobial peptide
AMP	Antimicrobial peptide
AMR	Antimicrobial resistance
CD	Circular dichroism
CHL	Cholesterol
DCM	Dichloromethane
DIC	*N,N'*-diisopropylcarbodiimide
$DiSC_3(5)$	3,3'-Dipropylthiadicarbocyanine iodide
DM	*Duttaphrynus melanostictus*
DMAP	4-dimethylaminopyridine
DMF	*N,N*-dimethylformamide
EDTA	Ethylenediaminetetraacetic acid
FESEM	Field emission scanning electron microscopy
Fmoc	Fluorenylmethoxycarbonyl
FRET	Förster resonance energy transfer
HATU	O-(7-Azabenzotriazol-1-yl)-*N,N,N',N'*-tetramethyluronium hexafluorophosphate
HCCA	α-Cyano-4-hydroxycinnamic acid
HDP	Host defense peptide
HEPES	4-(2-hydroxyethyl)-1-piperazineethanesulfonic acid
HNP	Human neutrophil peptide

HOBt	1-Hydroxybenzotriazole hydrate
HPLC	High-performance liquid chromatography
LPS	Lipopolysaccharide
LUVs	Large unilamellar vesicles
M	Molar
MALDI-TOF	Matrix-assisted laser desorption ionization–time-of-flight
POPC	1-palmitoyl-2-oleoyl-*sn*-glycero-3-phosphocholine
POPE	1-palmitoyl-2-oleoyl-*sn*-glycero-3-phosphoethanolamine
POPG	1-palmitoyl-2-oleoyl-*sn*-glycero-3-phospho-(1'-*rac*-glycerol)
SUVs	Small unilamellar vesicles
TFA	Trifluoroacetic acid
WHO	World health organization

Acknowledgement

A few years back, it was only a dream to pursue a Ph.D. in the field of biochemistry. But it was made true due to the hardships and constant support of many individuals in my life. I would like to thank them, although mere acknowledgment would never be enough.

I thank my supervisor, Prof. Nitin Chaudhary, for his immense role in completing this thesis. He chose me when I was just an ordinary student and guided me constantly, with much patience and endurance. His in-depth knowledge of the subject basics and techniques always helped troubleshoot any issues. I will be grateful to you, sir. I also thank my co-supervisor, Prof. Vishal Trivedi, for his guidance and support in times of need. His corrections and encouragement were truly uplifting and motivating.

I want to thank Prof. Sachin Kumar, for his encouragement during this journey. He initially motivated me to pursue this research and guided me to choose my path. Thank you, sir. I thank Prof. Vibin Ramakrishnan for his guidance and support during my progress seminars. His way of dreaming high and aiming for the unreachable always inspired me. I also thank Dr. Shirisha Nagotu for her insightful and constructive feedback, especially during the seminars throughout my course.

My journey in the path would not have been cherished if I didn't have my supportive seniors and some friends. I would like to remember my seniors, Dr. Karabi, Ms. Sravani, Dr. Debika, Dr. Anshuman, and Dr. Vinay, for helping and teaching me different aspects of research. I also owe my juniors Shubhangini, Aishwarya, Nandika, Omkar, Amrita, and Aishee for their love and support during this period. I wish to express my gratitude to Ms. Shubhangini for her dedicated efforts in performing the computational work essential for this thesis. I am ever grateful to my friends and seniors from the MID lab: Dr. Sajitha, Dr. Gaurav, Dr. Gaurav Pandey, Dr. Vivek, Dr. Jahnu, Dr. Yvonne, Dr. Kalpana, Amay, Naveen, Dikshita and Kunal. I also thank Dr. Rafi, Dr. Siddharth, and Dr. Rajendra from the VT lab.

I would be grateful for my friends and coffee mates, Prerana, Sneha, Jaswanth, Sam, Grace, Keerthi, and Anjali. I want to thank Roy sir's family, Pamu sir's family, and Senthil sir's family for constant support in times of need. Their homes were always open for any discussion and guidance. I will never forget your love, correction, and encouragement to make me a better human. I also thank Sunil Anna's and Tittu Chechi's families for being

there for me anytime. I thank all the children in the children's club- Hannah, Harshika, Harshil, Sagiv, Chris, Amy, Dansil, and Russel. I've learned a lot from you, although I was your teacher. It was the most stress-releasing time on campus.

My family had been a stronghold that I could lean on anytime- Words cannot express my gratitude to my father, mother, and my brothers, Jovan and Finny, for their constant love and support. My husband, Jerison, for being my constant companion and partner through every challenge, and for his unwavering support during my thesis period, to my little one, Jeanice, who taught me to smile even through the hardest pain, and my in-laws, Papa, Mummy, Margrette, Rufus, Myrtle, Saby, Reeba, Jaison, and Jerusha, for being my strength and great motivators.

I thank Almighty God, my Father, Lord Jesus, who strengthened me to go through this path, taught me His ways, and comforted me more than a mother. All glory and honor belong to you.

Synopsis

Multicellular organisms live in harmony with microorganisms. Plants grow naturally in the soil, having millions of microbes around. Frogs and toads live and grow in the muddy water without getting infections. They thrive and survive as their body is acquainted with such an unsterile environment. How is it possible? How do natural wounds heal without any signs of infection in such an unsterile environment? This question once disturbed the mind of a scientist, Michael Zasloff, who was working on *Xenopus* oocytes at the US National Institute of Health. Zasloff found that the frogs from which he had taken oocytes by surgical methods did not develop any infection even though they were produced back to non-sterile conditions. Instead, their wounds healed quite fast, rendering them survival. Zasloff hypothesized that specific antibiotic molecules made by their bodies protected them, warding off pathogens and promoting wound healing. This hypothesis led to further investigations into the biomolecule(s) that was/were responsible for antimicrobial activity and wound healing, leading to the discovery of magainin (in Hebrew: shield) (Cannon, 1987). Many antimicrobial peptides were discovered from different species after that. Few have reached the potential target of being a 'drug.' The emergence of antimicrobial-resistant organisms demands the discovery of new antibiotic molecules. As most AMPs are membrane-targeting, microbes find it challenging to develop resistance against them. Limitations like sensitivity to salts and divalent cations, susceptibility towards proteolytical degradation, among others, however, hinder their clinical applications. However, understanding their mechanism of action and engineering them to overcome their limitations can take the AMPs for clinical applications. In this thesis, I have studied a recently discovered toad cathelicidin, cathelicidin-DM, for its action, membrane interaction, and interfacial studies.

Introduction

Host defense peptides are evolutionarily conserved antimicrobial peptides that are ubiquitous. However, anurans are the most widely-studied species in the context of AMPs. Most natural AMPs range from 12-50 amino acids in size and are particularly rich in basic residues that impart them cationicity. Besides, they are rich in non-polar amino acids. The spatial segregation of polar and non-polar residue imparts amphipathicity, which allows interactions with membranes. Anionic AMPs, though far less common than

cationic ones, have also been shown to play an important role in innate immune defense. Maximins were the first reported anionic AMPs (Lai et al, 2002). Expression of AMPs can be inducible and tissue-specific (Tzou et al, 2000) or constitutive. Thus, they not only constitute an integral part of a complex network of molecules in the innate immune system but can also induce adaptive responses. Besides their broad-spectrum antibacterial activity, they also possess inhibitory activity against fungi, viruses, parasites, and even cancer cells (Hoskin & Ramamoorthy, 2008; Mor, 2009; Ballard et al, 2020; Urmi et al, 2023). Natural AMPs have also been reported to exhibit various immunomodulatory roles by stimulating/ modulating host immune responses (Xia et al, 2018; Duarte-Mata & Salinas-Carmona, 2023). AMPs are regulated by post-translational modifications such as phosphorylation, amidation, proteolysis, and ADP ribosylation.

Anuran skins are known for their potential healing ability. Dried skin extracts from certain bufo toads are commonly used in Chinese traditional medicine for wound healing and other diseases. Various bufadienolides are known to have a role in this process (Xu et al, 2014; Li et al, 2015). However, bufo skin extracts have not been explored for AMPs in detail. AMPs from other tissues, however, have been reported for bufo toads (Yi et al, 1996). As the activity of bufo skin extracts was largely attributed to the bufoadeneloids, the skin extracts, unlike other anurans, were probably overlooked for the presence of AMPs.

Anuran AMPs are generally cationic, amphipathic α-helical structures that are found in the granular glands at the dorsal region of the skin. Parotid glands of these species possess a whitish-colored toxic fluid that is enriched with amines, alkaloids, and peptides. The adrenergic stimulation of myocytes, the cells surrounding these granules, stimulates the release of AMPs by a holocrine-like mechanism. The role of host defense peptides is vital in defense against predators and helps them to survive among various pathogenic microbes. The warm and moist habitat of anurans makes them susceptible to various infections by pathogenic bacteria and fungi. Thus, the AMPs have coevolved to ensure protection from these microbes. The traditional folk medicine *Chan su* (*senso*), known for its anticarcinogenic and various other effects, contains the granular secretions of certain anurans (Ko et al, 2005). The pressing need to develop potential antimicrobial peptides is attributed to the emergence of multidrug-resistant strains of various pathogenic microbes. Methicillin-resistant *Staphylococcus aureus* (MRSA), vancomycin-resistant

Pseudomonas, *Klebsiella, Acinetobacter*, and fluoroquinolone-resistant *Pneumococcus* are some of them (Kelly et al, 2024). Antimicrobial peptides from toads are known to lyse the membranes (Boland & Separovic, 2006). It is commonly believed that the mode of action is either through pore formation that facilitates ion conduction or through perturbation of lipid bilayer integrity that leads to the leakage of cell contents (Brogden, 2005).

The emergence of drug-resistant pathogens alongside the slow discovery of antibiotics that succeeded in clinical trials redraws the attention towards the ubiquitous antimicrobials, the AMPs. Recently, an AMP was discovered in the skin of a common Asian toad/Bufo toad: *Duttaphrynus melanostictus*. In this thesis, I investigated the interfacial activity as well as the membrane binding propensity of this peptide using computational methods and experiments. The thesis is divided into six chapters.

Chapter 1: Introduction and Literature review

Chapter 1 summarizes the extensive review of literature about AMPs. It comprises the structural diversity of AMPs, highlighting various structural motifs such as α-helical, β-sheets, α/β, and non-α/β, categorizing them into different families based on their amino acid composition, structural features, and functional characteristics. The review explores the various mechanisms through which AMPs exert their antimicrobial effects, including various membrane models. It also discusses the various limitations and challenges associated with them, their interactions with lipids, and finally, a small section of cathelicidins.

Chapter 2: Material and methods

Chapter 2 elaborates on the materials and methods employed throughout the thesis to investigate the peptide membrane interaction of cathelicidin-DM. This chapter includes methodology about computational methods such as cathelicidin-DM's molecular dynamics simulation in aqueous system, water/cyclohexane biphasic system, and with lipid bilayer models. The methodology about experiments includes peptide synthesis/expression, purification and characterization *via* high-performance liquid chromatography and mass spectrometry, secondary structure characterization using CD spectroscopy, interfacial activity of the peptide, interaction with lipid monolayers and liposomes, and characterization using fluorescence spectroscopy that included spectral

shift in the presence of liposomes, Trp fluorescence quenching, energy transfer to dansyl-POPE-doped vesicles.

Chapter 3: Molecular dynamics simulations predict interfacial activity and membrane-binding of cathelicidin-DM

This chapter presents computational studies involving MD simulations to investigate the behavior of cathelicidin-DM in various environments. The peptide's structure was predicted using QUARK server, and was found to adopt a 3-strand β-sheet. The structural stability was verified by subjecting the predicted structure for 200 ns molecular dynamic simulation. The final structure was used for molecular dynamics simulation in a cyclohexane/water biphasic system. The peptide displays interfacial activity by partitioning from bulk water phase to the water/cyclohexane interface. After establishing the interfacial activity, the interaction of peptide with model lipid bilayers POPC/Cholesterol (10:1) and POPE/POPG (7:3) was carried out. The peptide was found to have transient interaction with zwitterionic lipid bilayer. With POPE/POPG bilayer, however, the peptide does not detach once it binds to membrane. The modes of interaction were also found to be different for these bilayer systems.

Chapter 4: Cathelicidin-DM is a surface-active peptide that preferentially penetrates the negatively charged lipid monolayers

This chapter describes experimental investigations that include surface activity of cathelicidin-DM at air/water interface, compression/expansion isotherms, structural and microscopic analysis of the layers deposited as Blodgett films, and interaction with lipid monolayers. Cathelicidin-DM was found to be highly surface-active. Compression-expansion isotherms exhibited large hysteresis, suggesting that various molecular events could be caused by high surface pressures. It is exciting to observe that the peptide could be compressed to a very high surface pressure (44-45 mN/m). The high surface activity of the peptides predicts the membrane-active nature. The lipid monolayer penetration study also confirmed the membrane activity of the peptide. The peptide could penetrate both POPC/CHL and POPE/POPG monolayers. However, the π_C observed for POPE/POPG lipid monolayers was much higher (~46.7 mN/m) than for POPC/CHL monolayer (~33.2 mN/m), suggesting preferential binding of peptide to negatively charged lipids compared to neutral or zwitterionic ones.

Chapter 5: Cathelicidin-DM interaction with liposomes

Fluorescence spectroscopy is a powerful tool to investigate peptide-membrane interactions. Cathelicidin-DM harbors a Trp residue that can serve as an intrinsic fluorophore and allow membrane binding investigations with liposomes. Interaction with lipid vesicles was investigated using spectral shifts in Trp fluorescence, its quenching in the presence of vesicles, and FRET with acceptor-doped vesicles. Peptide's secondary structure in the presence of lipid vesicles using CD spectroscopy and vesicle perturbation using dye release assay, have been reported. Investigation using Trp fluorescence and quenching in the presence of vesicles clearly indicated that cathelicidin-DM showed preferential binding to negatively charged liposomes. This was further confirmed by FRET analysis. A higher reduction in tryptophan fluorescence emission intensity was observed in POPE/POPG liposomes doped with dansyl-labeled lipids, compared to the POPC/CHL liposomes. Surprisingly, the dye release assay gave a counterintuitive data. The peptide caused rapid dye release from POPC/CHL liposomes without any noticeable dye release from POPE/POPG vesicles.

Chapter 6: Conclusions, Discussion, and Possibilities

This chapter summarizes the findings of the study carried out in this thesis. Future prospects and possibilities are also discussed.

List of conferences

- Participated in Peptide-membrane interactions: Faraday Discussion 2022, organized by the Royal Society of Chemistry (Online mode). Participated in Research and Industrial Conclave-2022 at IIT Guwahati
- Participated in the 9th Indian Peptide Symposium 2023 and Indian peptide show held at BITS Pilani, Goa, and presented a poster.
- Presented a poster at the Research and Industrial Conclave, 2023, at IIT Guwahati.
- Oral presentation in the 4th Student Indian Peptide Symposium-2024 held at Gujarat Biotechnology University.

List of publications

Francis, F., & Chaudhary, N. (2022). 3- Antimicrobial peptides: features and modes of action. In *Antimicrobial Peptides: Challenges and Future Perspectives* (pp. 33–65). Elsevier. https://doi.org/10.1016/B978-0-323-85682-9.00016-7

Chapter 1

Introduction and Literature review

Abstract

Antimicrobial peptides (AMPs) or host defense peptides (HDPs) are short amphipathic, generally cationic, evolutionarily conserved biomolecules that constitute the first line of defense in most living organisms. These peptides display activity against Gram-negative and Gram-positive bacteria, fungi, and some protozoa and viruses. AMPs can be linear or cyclic; the cyclic structure is achieved through end-to-end ligation or disulfide bridge(s) between the Cys residues near the termini. Structurally, AMPs can be classified as α-helical, β-sheets, α/β, and non-α/β. Another useful classification could be disulfide-containing and disulfide-lacking peptides. Most AMPs fold into conformations that introduce amphipathicity, a feature that enables them to interact with membranes. Understandably, a large majority of AMPs exhibit antimicrobial activity through membrane destabilization, which causes leakage of cellular content, thereby causing cell death. Although the exact mechanism of action is an enigma and could be peptide-specific, several models have been proposed for their antimicrobial action. These include the barrel-stave model, the carpet model, the toroidal pore model, and the detergent model. Apart from the antimicrobial activity, AMPs could possess anticancer activity, anti-mycoplasmal activity, spermicidal activity, and cause activation of the immune response and regulation of inflammation. These attributes of AMPs make them promising candidates as an alternative to conventional antibiotics.

1.1. Introduction

Humans and other multicellular organisms have been co-evolving with pathogenic microbes. Evolution is intricately related to the mutations in the genome. Mutations that confer advantages get naturally selected. Mutations that impart the microbe better chances of survival in an antibiotic-containing medium get selected and dominate the bacterial population in the medium. The indiscriminate use of antibiotics has led to the appearance of drug-resistant bacteria. Many clinical bacterial strains show resistance against most known antibiotics, causing difficult-to-treat infections. Survival amid multipotent organisms is the elementary purpose that each organism looks for. Innate immunity provides rapid and non-specific action against pathogenic microbes and protects the cells from infection. Innate immunity, the first line of defense, includes physical barriers such as skin, cilia, and chemical components. One of the various ways

that living organisms employ to combat pathogens is antimicrobial peptides (AMPs). AMPs have been identified in almost all the organisms that have been investigated for their presence. AMPs with antibacterial, antiviral, antifungal, antiparasitic, and antimycoplasmal properties have been reported in the literature (Pasupuleti et al, 2012). Apart from displaying direct microbicidal activity, AMPs may possess other biological activities that include but are not limited to, immunomodulation (Mansour et al, 2014), inhibition of lipopolysaccharide (LPS)-induced inflammation (Lai & Gallo, 2009), wound healing (Mangoni et al, 2016), and antitumor activity (Hilchie et al, 2013). The AMPs, therefore, are often termed host defense peptides (HDPs) as well.

One of the big pluses of the AMPs over conventional antibiotics lies in their mechanism of action. As they kill the microbes primarily through their membrane perturbation, that is, without targeting any molecular receptors in the microbial surface, the chances of bacterial resistance against them are considerably less. According to the 2020 WHO report (Organization, 2020), antibiotic-resistant strains are rapidly increasing, and hardly any solutions succeed in their clinical trials. The increase in multidrug-resistant microorganisms and the decline in new antibiotics' discovery rate constitute a significant healthcare challenge today. As new infectious organisms emerge with high competence, discovering novel antimicrobial agents is the need of the hour. The very fact that all living forms use the AMPs and that they display broad-spectrum antimicrobial activity makes them very promising candidates for developing the next-generation antibiotics. Thus, the increasing resistance of bacteria towards conventional antibiotics accelerated the focus on AMP discoveries as they can potentially overcome the AMR (antimicrobial resistant) strains. Most conventional antibiotics do not disrupt cell membranes. Instead, they target the intracellular organelles after crossing the membrane. They can block peptidoglycan synthesis, inhibit DNA gyrase enzyme that further breaks down double-stranded DNA, trigger autolysins, and so on (Hancock & Rozek, 2002). As far as AMPs are concerned, certain limitations and challenges need to be overcome before they can be taken from the bench to the bed. For example, AMPs may have associated toxicity and hemolytic activity, and they usually have a short half-life (Vlieghe et al, 2010; Mahlapuu et al, 2016). It is, therefore, essential to develop synthetic and long-lasting AMP analogs that display high activity and little toxicity. Let us look into the pioneering studies that brought these fascinating molecules to the forefront.

1.2. Historical perspective

The history of AMPs dates back to the late 1930s when Dubos, in 1939, isolated an antibacterial agent from a sporulating soil Bacillus (Dubos, 1939). The agent displayed bactericidal activity against all the Gram-positive bacteria tested but failed to act against Gram-negative bacteria. It was shown that the agent protected the mice that were infected with virulent pneumococci (Dubos, 1939). Despite the antibacterial agent's success in animal models, it could not be used for treating patients as it was toxic and worked poorly in immunosuppressed individuals. In the following year, Hotchkiss and Dubos isolated gramicidin and tyrocidine as the antibacterial agent's two active ingredients (Hotchkiss & Dubos, 1940; Hotchkiss & Dubos, 1940). Gramicidin was found to be efficient in treating the mice infected with virulent pneumococci (Hotchkiss & Dubos, 1940). The bacterium that produced these antimicrobial agents was later identified as *Bacillus brevis* (Hotchkiss & Dubos, 1941). Gause and Brazhnikova applied Dubos' protocol on the *B. brevis* strains from Russian soil and isolated an antimicrobial agent that they named gramicidin S (Soviet gramicidin) (Gause & Brazhnikova, 1944). Gramicidin and tyrocidine are cyclic decapeptides (Jones et al, 1979; Loll et al, 2014) and exhibit antibacterial activity by disrupting the cell membrane. As they target the membrane, the chance of developing resistance is small. However, both tyrocidine and gramicidin turned out to be poorly selective. They exhibited considerable hemolysis alongside the antimicrobial activity, which in turn reduced their effectiveness and limited their usage to the topical treatments of wounds and ulcers (Loll et al, 2014). Purothionin, an AMP isolated from the plant *Triticum aestivum* by Stuart and Harris in 1942, was found to be effective against fungi and some pathogenic bacteria (Pahr et al, 2013). Later, the studies revealed different classes of purothionin, that is, α-, β- and γ-purothionins (Colilla et al, 1990; Hughes et al, 2000). They are sulfur-rich peptides belonging to thionin family of plant kingdom (Oard & Enright, 2006; Pahr et al, 2013). HDPs from animals were first described in the 1960s by Kiss and Michl in Bombina species. They noted the presence of antimicrobial and hemolytic activity in the skin secretions of *Bombina variegata,* which led to the isolation of antimicrobial peptides, Bombinins (Kiss & Michl, 1962; Simmaco et al, 2009). Subsequently, several HDPs were discovered from various sources. In 1980, Hans Boman and coworkers injected live bacteria into pupae of *Hyalophora cecropia* and isolated AMPs named P9A and P9B that exhibited bactericidal activity against *E.coli* and

other Gram-negative bacteria (Boman, 1981). The sequence and specificity were subsequently determined, and the two P9 peptides were termed cecropins A and B (Steiner et al, 1981). In 1983, Ganz and Lehrer isolated three microbicidal agents from granule-rich sediment of human neutrophils and called them human neutrophil peptides 1-3 (HNP1-3), which were later coined as defensins (Ganz et al, 1985). The discovery of magainins from *Xenopus laevis* is another milestone in the history of AMPs. Zasloff noticed that these frogs seldom developed infection after experimental surgeries despite being in a non-sterile environment. He was curious about this "sterilizing activity" of frog skin and ended up discovering the AMPs called magainins (Zasloff, 1987). Since then, a large number of AMPs have been identified from very diverse sources and are recorded in various AMP databases (Waghu et al, 2015; Wang et al, 2015; Fan et al, 2016).

1.3. Features of AMPs

1.3.1. Diversity

The sequences, structures, and activities of several hundred AMPs have been characterized (Wang et al, 2015; Waghu & Idicula-Thomas, 2020). The analyses of the sequences and the structures show that the AMPs are highly diverse, both in sequence and structure. In terms of length, they range from very short (<10 amino acids) to fairly long (up to around 100 residues). They carry a net positive charge at neutral pH that could go up to +7 or more. Some AMPs are unusually rich in certain amino acids. A large majority of the naturally-occurring AMPs are composed of exclusively L-amino acids (Hwang & Vogel, 1998). However, AMPs with non-natural amino acids are also quite common (Duclohier, 2007). Owing to such diversity in the primary structure, the peptides are rarely classified based on their sequence. However, it is somewhat easier to classify them based on the structure. The diversity in the sequence and the structure is attributed to the diverse activities that the AMPs display. These include, but are not limited to, the spectrum of killing, sensitivity to the salt or divalent cations, mechanism of action, wound healing, and immunomodulatory effects (Sitaram & Nagaraj, 2002; Bowdish et al, 2005; Kumar et al, 2018). Every organism that has been investigated for the presence of AMPs was found to possess them. Even bacteria use peptides called bacteriocins to combat other bacterial strains (Riley & Wertz, 2002; Simons et al, 2020).

1.3.2. Cationicity and Amphipathicity

Despite being exceedingly diverse in the sequences, amino acid compositions, and structures, AMPs harbor two features that are common to most AMPs: cationicity and amphipathicity. AMPs are unusually rich in basic and hydrophobic amino acids. The presence of basic amino acids, especially lysine and arginine, confers them a net positive charge at neutral pH. The cationicity imparts the selectivity to bind the anionic microbial membranes (Brown & Hancock, 2006). Amphipathicity imparts membrane permeabilizing activity to the AMPs (Tossi et al, 2000; Sato & Feix, 2006; Saikia & Chaudhary, 2018; Saikia & Chaudhary, 2018). Unless already folded into an amphipathic structure, the peptides fold upon membrane binding to take up an amphipathic structure that facilitates their insertion into the membranes. Membrane perturbation, therefore, happens to be one of the most common modes of action of the cationic AMPs. Although mostly cationic, anionic AMPs (AAMPs) do exist in nature as a part of the innate defense system. For example, maximin H5 from *Bombina maxima* has a net charge of –2 (Lai et al, 2002). Some AAMPs interact with membranes via divalent cations-mediated bridges (Frederick et al, 2009).

1.3.3. Structure

As AMPs are highly diverse in their primary structure, they could be classified on other structural parameters such as (a) linear or cyclic (b) lacking or harboring disulfide bridges, and (c) secondary structure of the peptide. The cyclic structure is achieved through end-to-end ligation, as in θ-defensins, or via the disulfide bridge(s) between the Cys residues near the peptide termini, as in tigerinins and bactenecin (Romeo et al, 1988; Sai et al, 2001). Cyclic AMPs are less prone to proteolytic degradation and display enhanced structural stability (Trabi & Craik, 2002). As far as the secondary structure of AMPs is concerned, a large majority of them are unordered in solution and fold to take up an amphipathic structure only upon membrane binding. The peptides that have defined three-dimensional (3D) structures usually contain one or more disulfide bridges to impart stability. Based on the recent available data from APD6 database, a total of 535 AMP's has known 3D structures. Among these, 471 structures, accounting for approximately 88%, were elucidated using nuclear magnetic resonance (NMR) spectroscopy (Wang et al, 2025). Based on their secondary structure, AMPs are broadly

classified into four major structural classes (Figure 1.1) (Hancock, 1997). Each chain is color-coded, with blue denoting the N-terminus and red representing the C-terminus.

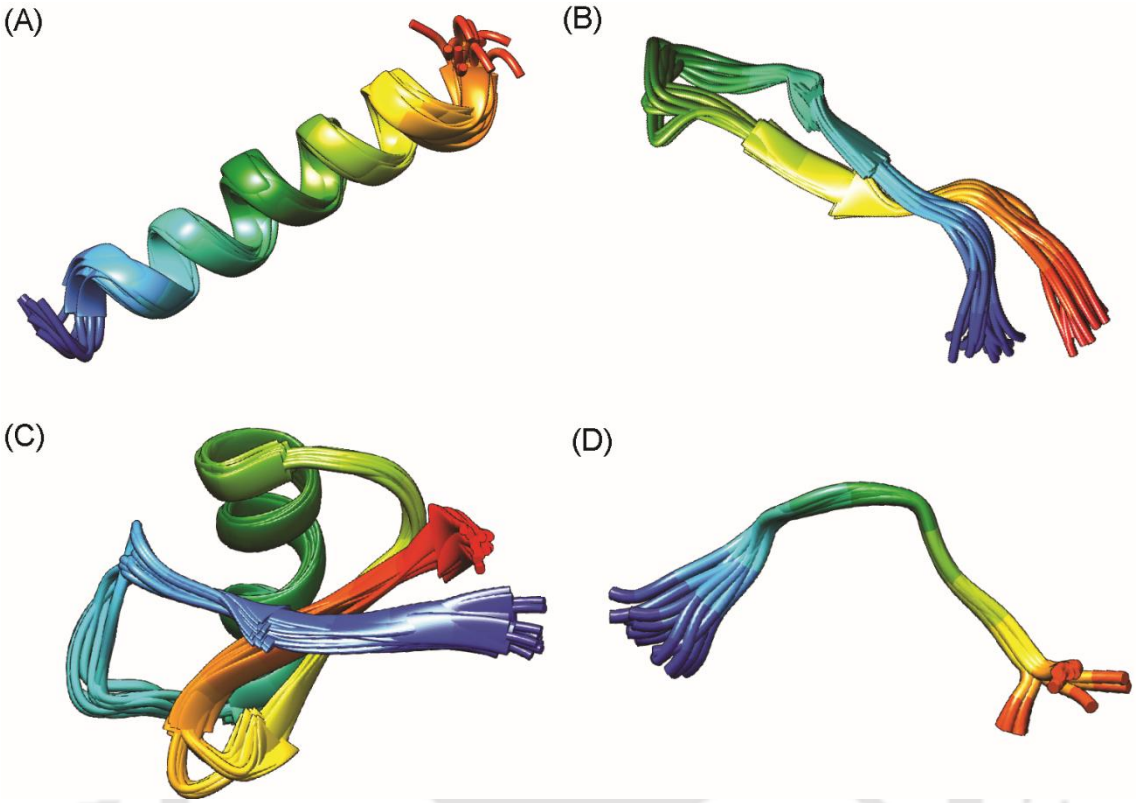

Figure 1.1. Four major classes of AMPs. (A) α-helical structure. e.g., magainin 2 (PDB ID: 2MAG), (B) β-sheet structure, e.g., β lactoferricin B (PDB ID: 1LFC), (C) α/β structure, e.g., plant defensin Psd1 (PDB ID: 1JKZ), and (D) non-α/β peptide structure, e.g., bovine indolicidin (PDB ID: 1G89). The peptide chains are color-coded, with blue and red colors denoting the N and C-termini, respectively.

1.3.3.1. The α-helical antimicrobial peptides

The α-helical peptides constitute the most populous class of AMPs. They are the most widespread among all structural classes and are found in species ranging from invertebrates to higher organisms (Zasloff, 1987; Tossi et al, 2000). They usually adopt an unordered conformation in aqueous solutions but quickly fold into an amphipathic α-helical structure upon membrane-binding or in membrane-mimetic environments such as trifluoroethanol, hexafluoroisopropanol, and sodium dodecyl sulfate micelles (Marion et al, 1988; Lequin et al, 2003; Timmons et al, 2019). Cecropins from insects (Hultmark et al, 1982), magainins from anurans (Marion et al, 1988), and human cathelicidin LL-37 (Johansson et al, 1998) are some of the well-studied α-helical AMPs. Some of the well-

studied AMPs from this structural class are listed in Table 1.1, and the structures for the selected peptides are shown in Figure 1.2. The list was prepared by including peptides that possess a confirmed α-helical structure. They are functionally characterised as they possess antimicrobial/host defense function. AMPs from diverse sources were chosen to elucidate the table.

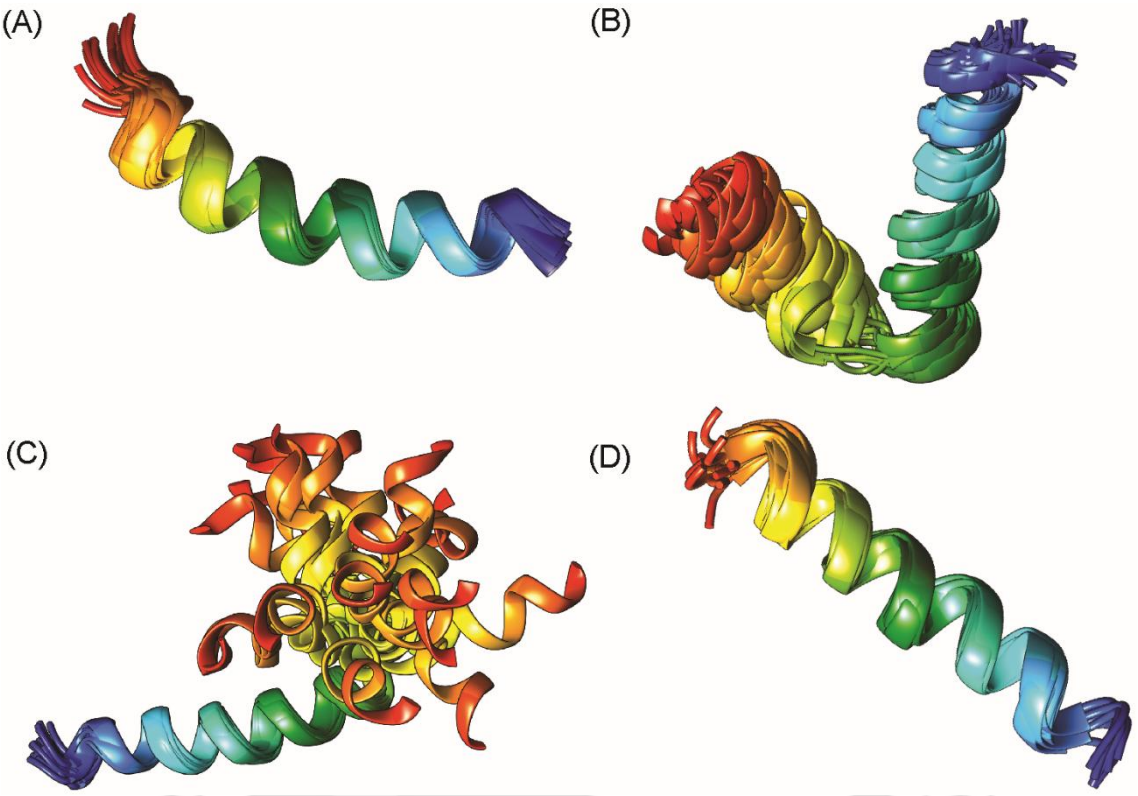

Figure 1.2. The PDB structures of selected α-helical antimicrobial peptides. (A) LL-37 (PDB ID: 2LMF), (B) papiliocin (PDB ID: 2LA2), (C) CB1a (PDB ID: 2IGR), and (D) magainin 2 (PDB ID: 2MAG).

Table 1.1. List of selected α-helical AMPs

AMP	Sequence	Source
Brevinin 1BYa (Pál et al, 2006)	FLPILASLAAKFGPKLFCLVTKKC	*Rana boylii*
Cathelicidin LL-37 (Turner et al, 1998)	LLGDFFRKSKEKIGKEFKRIVQRIKDFLRNLVPRTES	*Homo sapiens*
Cecropins A (Merrifield et al, 1982)	KWKLFKKIEKVGQNIRDGIIKAGPAVAVVGQATQIAK-NH_2	*Hyalophora cecropia*
Clavanin A (Lee et al, 1997)	VFQFLGKIIHHVGNFVHGFSHVF-NH_2	*Styela clava*
Dermaseptins B2 (Charpentier et al, 1998)	GLWSKIKEVGKEAAKAAAKAAGKAALGAVSEAV-NH_2	*Phyllomedusa bicolor*
Dermcidin (Schittek et al, 2001)	SSLLEKGLDGAKKAVGGLGKLGKDAVEDLESVGKGAVHDVKDVLDSVL	*Homo sapiens*
Magainins (Zasloff, 1987)	GIGKFLHSAKKFGKAFVGEIMNS	*Xenopus laevis*
Melittins (Terwilliger et al, 1982)	GIGAVLKVLTTGLPALISWIKRKRQQ-NH_2	*Apis mellifera*
Temporin L (Rinaldi et al, 2002)	FVQWFSKFLGRIL-NH_2	*Rana temporaria*
Aurein 1.2 (Rozek et al, 2000)	GLFDIIKKIAESF-NH_2	*Litoria aurea, Litoria raniformis*
Buforin 2 (Park et al, 1996)	TRSSRAGLQFPVGRVHRLLRK	*Bufo gargarizans*
Piscidin 1 (Lauth et al, 2002)	FFHHIFRGIVHVGKTIHRLVTG	*Morone saxatilis*
Pseudin 2 (Olson et al, 2001)	GLNALKKVFQGIHEAIKLINNHVQ	*Pseudis paradoxa*
Phylloseptin 1 (Zhang et al, 2010)	FLSLIPHAINAVSAIAKHN-NH_2	*Phyllomedusa sauvagei*

1.3.3.2. The β-sheet AMPs

The β-sheet AMPs are made up of two or more β-strands forming at least one β-sheet. The simplest architecture is that of a β-hairpin. The strands in the β-hairpin are often linked through disulfide bonds that impart conformational stability to the otherwise dynamic β-strands (Powers & Hancock, 2003). Tachyplesins isolated from *Tachypleus tridentatus* and protegrins isolated from porcine leukocytes are well-studied β-hairpin AMPs with membrane-disruptive action (Edwards et al, 2017). The HNP-1, the rabbit kidney defensin RK-1, and the bovine neutrophil β-defensin-12 are some examples of β-sheet AMPs with more than two strands. The peptide LCI isolated from *Bacillus subtilis* is a Cys-lacking β-sheet AMP with a novel topology of four-stranded antiparallel β-sheet (Gong et al, 2011). A representative set of peptides was selected that has confirmed beta sheet structure, possesses antimicrobial/host defense function, having structural stability by disulphide bridges, and derived from diverse sources. Selected members of this structural class are presented in Figure 1.3 and Table 1.2.

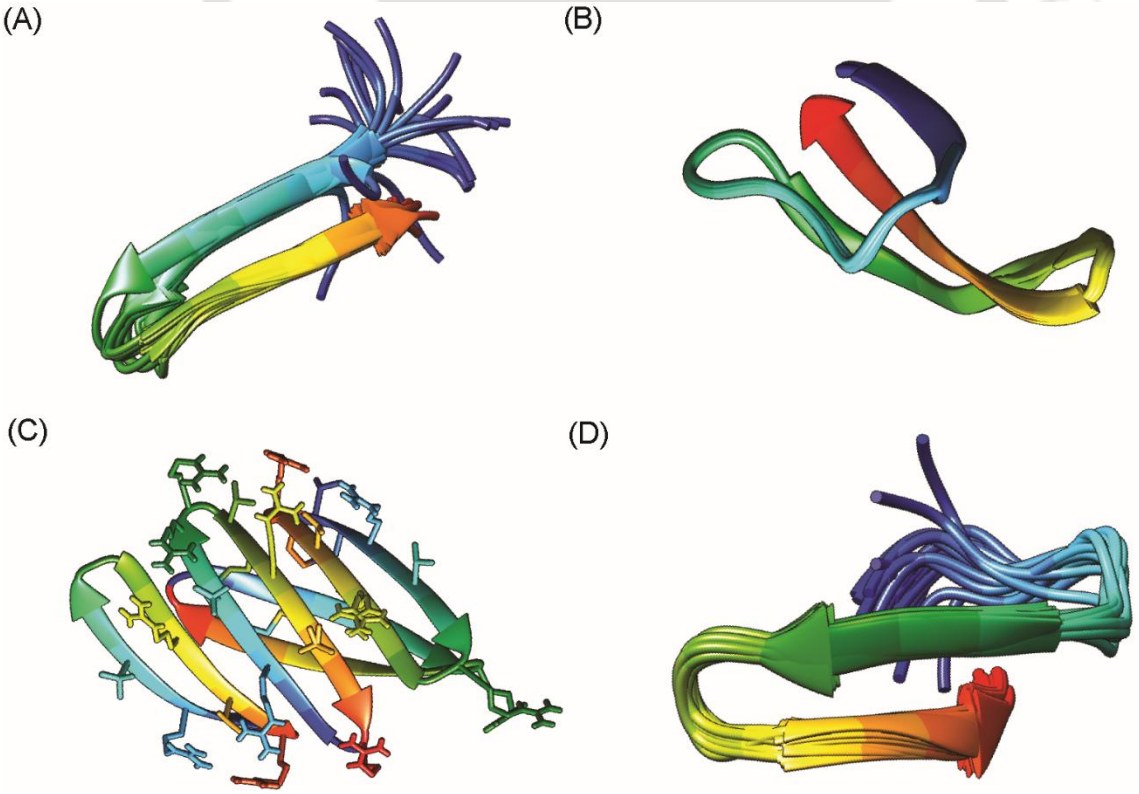

Figure 1.3. β-sheet antimicrobial peptides. (A) Protegrin 1 (PDB ID: 1PG1), (B) human defensin 5 (PDB ID: 2LXZ), (C) antiparallel tetrameric β-hairpin structure of baboon theta defensin 2 (PDB ID: 5INZ), and (D) thanatin (PDB ID: 6AAB).

Table 1.2. List of selected β-sheet AMPs

AMP	Sequence	Source
Protegrin 1(Steinberg et al, 1997)	RGGRLCYCRRRFCVCVGR-NH_2	*Sus scrofa*
Tachyplesin 1 (Nakamura et al, 1988)	KWCFRVCYRGICYRRCR-NH_2	*Tachypleus tridentatus*
HNP-1 (Mizukawa et al, 2000)	ACYCRIPACIAGERRYGTCIYQGRLWAFCC	*Homo sapiens*
Thanatin (Fehlbaum et al, 1996)	GSKKPVPIIYCNRRTGKCQRM	*Podisus maculiventris*
LCI (Gong et al, 2011)	AIKLVQSPNGNFAASFVLDGTKWIFKSKYYDSSKGYWVGIYEVWDRK	*Bacillus subtilis*
Bovine neutrophil β-defensin-12 (Selsted et al, 1993)	GPLSCGRNGGVCIPIRCPVPMRQIGTCFGRPVKCCRSW	*Bos taurus*
Hepcidin (Krause et al, 2000)	ICIFCCGCCHRSKCGMCCKT	*Homo sapiens*
Gomesin (Silva et al, 2000)	ZQCRRLCYKQRCVTYCRGR-NH_2 (Z = pyroglutamate)	*Acanthoscurria gomesiana*
Polyphemusin 1 (Powers et al, 2004)	RRWCFRVCYRGFCYRKCR-NH_2	*Limulus polyphemus*
Microcin J25 (Vincent & Morero, 2009)	GGAGHVPEYFVGIGTPISFYG	*Escherichia coli AY25*

1.3.3.3. αβ antimicrobial peptides

Many AMPs consist of both α-helical and β-sheet structures, some of which are listed in Figure 1.4 and Table 1.3. Human β-defensin 1, for example, possesses an N-terminal α-helical region along with a highly conserved β-sheet (Hoover et al, 2001). Drosomycin is an antifungal peptide derived from *Drosophila melanogaster* with potent activity against filamentous fungi. The 3D structure of drosomycin reveals α-helix and twisted three-stranded β-sheet structure stabilized by disulfide bridges (Landon et al, 1997). Kalata B2, isolated from the plant *Oldenlandia affinis*, is another classic example of the αβ peptides with unusually stable cyclic structure (Jennings et al, 2005). Kalata peptides are prototypic cyclotides with closely packed disulfide core conferring stability against thermal, chemical, and enzymatic degradation (Nair et al, 2006). Recent advances highlight cyclotides, owing to their unique cyclic αβ structure and cystine-knot disulfide core, as exceptionally stable plant-derived scaffolds that resist thermal, chemical, and enzymatic degradation, thereby enabling their use in the design of orally active cyclic peptide therapeutics (Hyun, 2025).

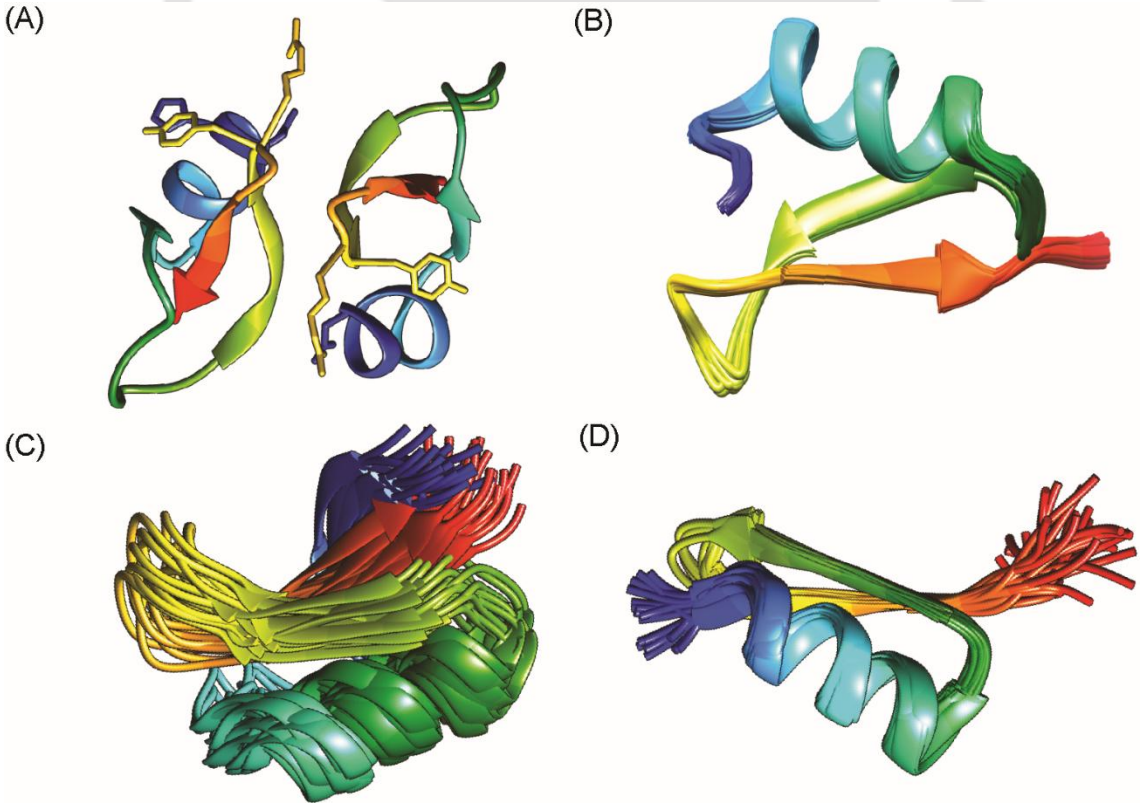

Figure 1.4. αβ-antimicrobial peptides: (A) human β-defensin-1 (PDB ID: 1IJV), (B) defensin MGD-1 (PDB ID: 1FJN), (C) NaD1 (PDB ID: 1MR4), and (D) nasonin 1 (PDB ID: 2KOZ).

Table 1.3. List of selected αβ AMPs

AMP	Sequence	Source
Kalata B2 (Jennings et al, 2005)	GLPVCGETCFGGTCNTPGCSCTWPICTRD	*Oldenlandia affinis*
Plectasin (Mygind et al, 2005)	GFGCNGPWDEDDMQCHNHCKSIKGYKGGYCAKGGFVCKCY	*Pseudoplectania nigrella*
Phormicin (Lambert et al, 1989)	ATCDLLSGTGINHSACAAHCLLRGNRGGYCNGKGVCVCRN	*Phormia terranovae*
pBD-2 (Veldhuizen et al, 2007)	DHYICAKKGGTCNFSPCPLFNRIEGTCYSGKAKCCIR	*Sus scofa*
Drosomycin (Fehlbaum et al, 1994)	DCLSGRYKGPCAVWDNETCRRVCKEEGRSSGHCSPSLKCWCEGC	*Drosophila melanogaster*
Mytilin B (Charlet et al, 1996)	SCASRCKGHCRARRCGYYVSVLYRGRCYCKCLRC	*Mytilus edulis*
Human β-defensin 1 (Bensch et al, 1995)	DHYNCVSSGGQCLYSACPIFTKIQGTCYRGKAKCCK	*Homo sapiens*

1.3.3.4. Non-αβ (extended structure)

The extended AMPs are predominantly rich in specific amino acids such as proline, arginine, glycine, histidine, tryptophan, and have no regular secondary structure. Extended AMPs do not take up stable secondary structures through intramolecular H-bonding and interact with the membrane lipids via the H-bonding and Van der Waals interactions (Powers & Hancock, 2003). The Trp-rich peptide indolicidin, derived from bovine neutrophils, is the best characterized AMP of this class (Powers & Hancock, 2003; Sitaram et al, 2003). Pyrrhocoricin from *Pyrrhocoris apterus* (Cociancich et al, 1994), apidaecin from lymph fluid of *Apis mellifera* (Casteels et al, 1989), and PR-39 from pig are examples of proline-rich AMPs of non-αβ structural class. Histatins are the histidine-rich antifungal peptides present in the salivary secretions of human submandibular and parotid glands (Oppenheim et al, 1988). Majorly, extended AMPs are not membranolytic peptides; instead, they translocate across the membrane and interact with intracellular targets (Renato et al, 2002; Graf et al, 2017). However, some peptides could possess membranolytic activity, for example, indolicidin (Falla et al, 1996). Adepantins are anuran peptides with high glycine content and display high selectivity for Gram-negative bacteria (Ilić et al, 2013). Certain AMPs adopt a loop conformation with one intramolecular disulfide bridge, for example, bactenecin (Radermacher et al, 1993) and lactoferricins derived from bovine lactoferrin (Bellamy et al, 1992). Representative peptides exhibiting extended structures, antimicrobial activity derived from diverse origins are shown in Figure 1.5 and Table 1.4.

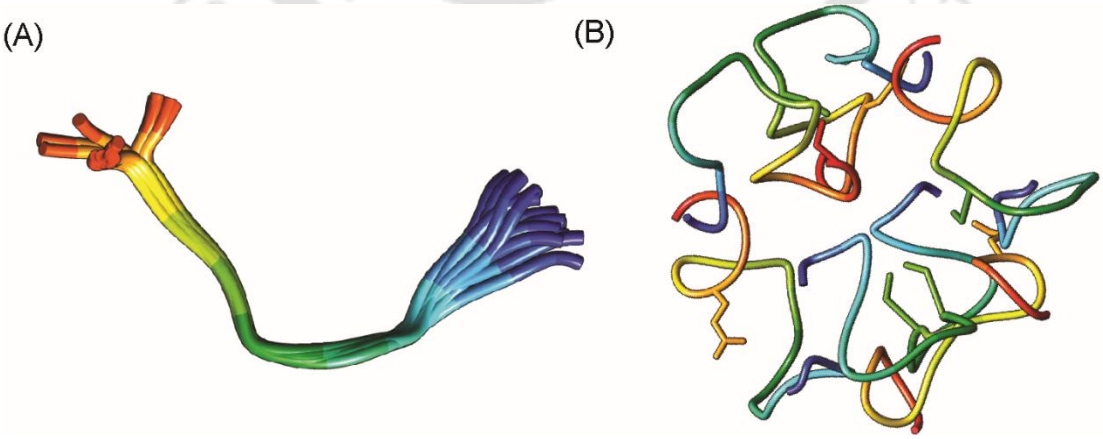

Figure 1.5. Non-αβ antimicrobial peptides. (A) Indolicidin, from bovine neutrophils bound to dodecylphosphocholine micelles (PDB ID:1G89). (B) Tetracyclic structure of mersacidin, a lantibiotic (PDB ID: 1QOW).

Table 1.4. List of selected non αβ- AMPs

AMP	Sequence	Source
PR-39 (Agerberth et al, 1991)	RRRPRPPYLPRPRPPPFFPPRLPPRIPPGFPPRFPPRFP-NH_2	*Sus scrofa*
Indolicidin (Selsted et al, 1992)	ILPWKWPWWPWRR- NH_2	*Bos taurus*
Drosocin (Bulet et al, 1993)	GKPRPYSPRPTSHPRPIRV	*Drosophila melanogaster*
Histatin 5 (Raj et al, 1990)	DSHAKRHHGYKRKFHEKHHSHRGY	*Homo sapiens*
Lactoferricin B (Bellamy et al, 1992)	FKCRRWQWRMKKLGAPSITCVRRAF	*Bos taurus*
Tritrpticin (Lawyer et al, 1996)	VRRFPWWWPFLRR	*Sus scrofa*

As of September 2025, the antimicrobial peptide database (APD6) has expanded to include a total of 5,188 peptides, comprising 3,306 natural AMPs, 1308 synthetic AMPs and 239 predicted AMPs (Wang et al, 2025).

1.4. Biosynthesis and regulation

AMPs are synthesized in two different ways: ribosomally and nonribosomally. The ribosomally synthesized AMPs as the name suggests, are genetically encoded. All species, including bacteria, produce such peptides. Nonribosomally-synthesized peptides, on the other hand, are mainly produced by bacteria using a multifunctional enzyme, known as nonribosomal peptide synthetases (NRPSs) (Finking & Marahiel, 2004; Grünewald & Marahiel, 2013). The genes for the ribosomally-synthesized peptides are mostly present as clusters in the genome, thereby producing multiple AMPs at a single site (Lai & Gallo, 2009). Ribosomally-synthesized AMPs are produced as inactive precursors and require proteolytic cleavage to become active (Bals, 2000; Ongpipattanakul et al, 2022). Their regulation depends not only on their expression but also on the abundance of appropriate proteases (Lai & Gallo, 2009). The AMPs can be expressed constitutively, or they can be inducible. In multicellular organisms, some AMPs are constitutively expressed, where they are stored at high concentrations in granules as inactive precursors and released locally at the site of infection. The expression of other AMPs is induced in response to pathogen-associated molecular patterns, lipopolysaccharides (LPSs), or cytokines (Hancock & Diamond, 2000; Lai & Gallo, 2009). In humans, histatins are expressed constitutively by submandibular, sublingual, and parotid glands (De Smet & Contreras, 2005). On the other hand, drosomycin, a drosophila AMP, gets induced when the fruitfly is exposed to bacteria (Landon et al, 1997). Recent studies have greatly expanded our understanding of developments in AMP biosynthesis and regulation. Mordhorst et al. provided a comprehensive review highlighting the common structural features, post-translational modifications of nonribosomal and ribosomally synthesized peptides, and biosynthetic strategies of ribosomal peptides to imitate the nonribosomal AMPs have been reviewed (Mordhorst et al, 2023).

Nonribosomally-synthesized peptides are synthesized on a large multimodular enzyme complex (Tajbakhsh et al, 2017). One of the classic examples of nonribosomally-synthesized AMPs is peptaibols. Peptaibols are a large class of membrane-active

polypeptides derived from fungi. They show considerable sequence homology, but differ in biological properties and 3D structures (Whitmore et al, 2003; Whitmore & Wallace, 2004). Peptaibols are characterized by the presence of unusual amino acids, principally α-amino butyric acid (Aib), isovaleric acid (Iva), and imino hydroxyl proline. Their antibiotic activity is attributed to their ability to form ion channels (Chugh & Wallace, 2001). Other nonribosomally-synthesized peptides include polymyxins, actinomycin D, and gramicidin S. Polymyxins are an old class of peptide antibiotics that are pentabasic decapeptides nonribosomally-synthesized by *Bacillus polymyxa* (D R Storm et al, 1977). Actinomycin D, the first antibiotic isolated from Streptomyces genus, and gramicidin S from *B. brevis* are also effective AMPs produced by nonribosomal peptide synthetase (NRPS) enzyme (Li et al, 2018). The NRPS genes are organized in a single operon in bacteria and as gene clusters in eukaryotes (Mankelow & Neilan, 2000).

1.5. Some common families of AMPs

A number of peptides can be grouped together into different families. Some of these families are discussed in this section.

1.5.1. Cathelicidins

Cathelicidins constitute one of the major components of the immune systems in vertebrates. Cathelicidins are synthesized as inactive prepropeptides that are stored in the neutrophil granules. The precursors of cathelicidins consist of preprosequences at their N-terminal, followed by an antimicrobial peptide at their C-terminal (Figure 1.6). They are named cathelicidin due to the presence of a common domain, termed cathelin, in their pro-region (Shinnar et al, 2003). Cathelicidins consist of a conserved region, namely the cathelin-like domain, and a highly variable domain, which is the active peptide region (Kościuczuk et al, 2012). Additionally, they have a signal sequence that targets them to the secondary granules of neutrophils. This family of peptides were initially discovered in bone marrow myeloid cells of mammals and therefore, referred to as myeloid antimicrobial peptides (MAP) (Kościuczuk et al, 2012). Cathelin domain shows sequence similarity with the cystatin superfamily of cysteine proteinase inhibitors (Zanetti et al, 1995). Generally, most of the cathelicidins are constitutively expressed, whereas they can also be induced during inflammation, infection, and other pathological conditions.

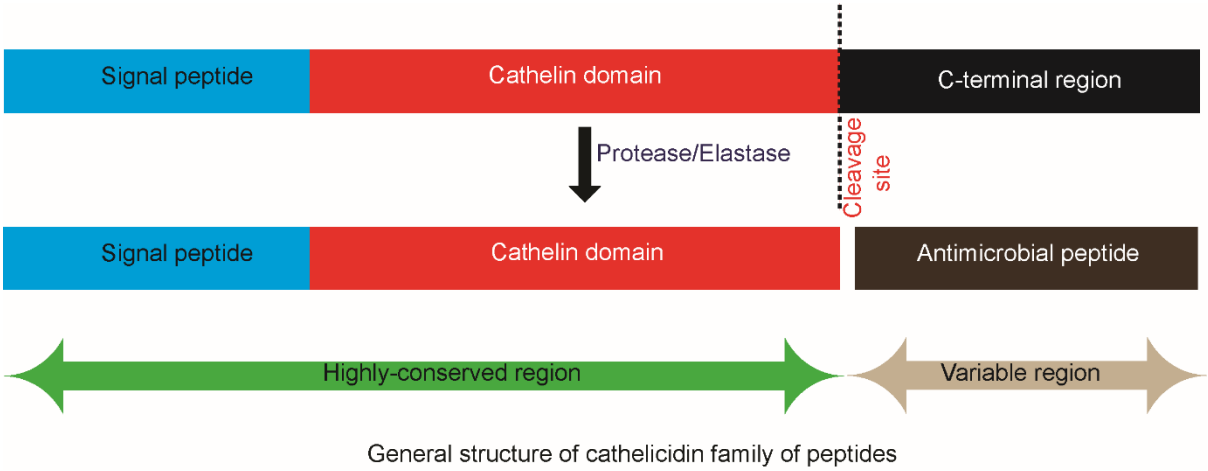

Figure 1.6. Schematic representation of prepropeptides of cathelicidin family.

Cecropin from *Hyalophora cecropia* was the first cathelicidin to be discovered in 1980 (Hultmark et al, 1980). Magainins isolated by Zasloff from the frog *X. laevis* are also cathelicidins (Zasloff, 1987). Bactenecins isolated from bovine neutrophils were among the first cathelicidins isolated from mammals (Skerlavaj et al, 1996). Cathelicidins have now been identified in many vertebrates, including humans and farm animals. The well-studied porcine cecropin P1 is also a cathelicidin (Skerlavaj et al, 1996). Humans have only one cathelicidin, the 37-residue peptide named LL-37. LL-37 is an α-helical AMP that is highly charged; out of the 37 residues, 16 are charged (6 Lys, 5 Arg, 3 Glu, 2 Asp) (Wang, 2008). The peptide, therefore, carries a net charge of +6 at neutral pH. Apart from displaying antibacterial activity through membrane perturbation, LL-37 plays immunomodulatory roles as well that include regulating the inflammatory response (Takahashi et al, 2018), chemo-attracting the immune cells to the site of infection, neutralization of LPS, and wound healing. Moreover, recent studies suggest that it is also involved in the regulation of cancer (Kuroda et al, 2015; Piktel et al, 2016; Wang et al, 2019).

1.5.2. Defensins

Defensins have a common β-sheet core stabilized with three or four disulfide bridges between six or eight conserved cysteine residues, respectively. Mammalian defensins contain three disulfide bridges and are subdivided into α-, β- and θ-defensins based on the linkage pattern of the cysteine residues. In α-defensins, the cysteine connectivity is C^1-C^6, C^2-C^4, C^3-C^5, while the connectivity in β-defensins is C^1-C^5, C^2-C^4, C^3-C^6 (Selsted &

Harwig, 1989; Tang & Selsted, 1993). Several human α-defensins are highly expressed in neutrophils (Ganz et al, 1985), and other α-defensins are produced and secreted by Paneth cells in the small intestine (Ouellette, 2006). The β-defensins are ubiquitous and found in all vertebrates (Lehrer & Ganz, 2002). The human genome has more than 30 genes coding for β-defensins, and the mice genome has even more genes coding for these peptides (Patil et al, 2004). β-defensins are produced mainly in epithelial cells (Jarczak et al, 2013). The cyclic θ-defensins arose from α-defensins after the divergence of primates and have been purified from the leukocytes of rhesus macaques and baboons (Li et al, 2014). These molecules are the only cyclic peptides found in mammals and exhibit antiviral activity as well (Wang et al, 2003; Selsted, 2004). Evidence exists for sequence divergence by both positive and negative selection of mammalian defensin genes following ancestral gene duplication.

1.5.3. Thionins

Plant AMPs are classified into various families: thionins, defensins, hevein- and knottin-type peptides, hairpinins, and macrocyclic peptides (cyclotides). Thionins are cysteine-rich AMPs with antimicrobial and toxic properties (Stec, 2006). They are small in size (around 5 kDa), but happen to be toxic to a wide range of organisms and eukaryotic cell-lines, though they show cell selectivity (H Bohlmann & Apel, 1991). Thionins were first discovered by Ball and coworkers in 1942 when they observed an active ingredient that was inhibiting yeast growth (Balls et al, 1942). They isolated and crystallized the peptide from the wheat endosperm (*T. aestivum*) and termed it purothionin due to its high sulfur content. These compounds were found to have fungicidal and bactericidal properties (Stuart & Harris, 1942). Thionins are classified into five structural classes based on the amino acid sequences and disulfide bond arrangements. Thionins are usually extracted from natural sources by solvent extraction as proteolipid complexes, indicating their association with lipids (Balls et al, 1942). Although purothionin was first crystallized in 1942, the structure of thionin was first reported in 1981 when Hendrickson and Teeter determined the structure of crampin (Hendrickson & Teeter, 1981). Two distinct groups of thionins exist; they are α-/β-thionins and γ-thionins. The γ-thionins, due to their similarity to defensins, are now classified as plant defensins (Stotz et al, 2009).

1.5.4. AMPs rich in specific amino acids.

Another special class of peptides that cannot be considered a family though, is of peptides that have unusual amino acid compositions. These peptides are unusually rich in one or two amino acids. The selected members of this class are discussed here.

1.5.4.1. Tryptophan-rich AMPs

Indolicidin (named as it is an indole-rich peptide) is an AMP isolated from the cytoplasmic granules of bovine neutrophils (Sitaram et al, 2003). It is a tridecapeptide amide with 5 tryptophan residues, and displays remarkable *in-vitro* bactericidal activity (Selsted et al, 1992). It is the only indole-rich peptide in mammalian leukocytes that is amidated and stored in the granules in its mature form (Selsted et al, 1992). Due to the presence of 5 tryptophan and 3 proline residues, it takes up an extended structure. Tritripticin is another tryptophan-rich AMP derived from porcine precursor protein with sequence similarity to indolicidin (Lawyer et al, 1996; Schibli et al, 2006). Puroindolins are tryptophan-rich AMPs found in wheat that exhibit antibacterial and antifungal activities (Day et al, 2006).

1.5.4.2. Proline-rich AMPs

Several peptides are unusually rich in proline residues. PR-39, a 39-residue proline and arginine-rich peptide from porcine, is one such example (Agerberth et al, 1991). Bactenins Bac5 and Bac7 from *Bos taurus*, apidaecin from *Apis mellifera*, and drosocin from *D. melanogaster* are some other examples. PR-39 isolated from the porcine small intestine is a particularly well-studied AMP of this class. Apart from the antibacterial activity, it exhibits various other roles. It is reported to be a neutrophil chemoattractant, indicating its role in inflammation (Huang et al, 1997). It induces syndecan expression in mesenchymal cells (Chan & Gallo, 1998), inhibits neutrophil oxidase (Huang et al, 1997), and induces angiogenesis (Li et al, 2000). PR-39 does not kill the bacterium by membranolytic action; instead, it inhibits the protein synthesis causing cell lysis (Boman et al, 1993).

1.5.4.3. Histatins

Histatins are histidine-rich peptides found in the saliva of humans and higher primates with potent antifungal activity (Oppenheim et al, 1988). They are secreted from the parotid and submandibular glands in humans (Oppenheim et al, 1986). Around 12 fragments of histatins have been identified that are derived from two genes- histatins 1 and 3 by proteolytic degradation (Oppenheim et al, 1986; Troxler et al, 1990). Though histatins do not cause membrane lysis, the exact molecular mechanism of action is not yet clear. Histatin 5, the most potent among all histatins with high activity against *Candida albicans*, is known to target mitochondrial membrane integrity (Helmerhorst et al, 2001).

1.5.4.4. Unusual amino acid containing ribosomally-synthesized AMPs

AMPs produced by bacteria to combat and control invasive microorganisms are termed bacteriocins (Willey & Donk, 2007). They are a small, heat-stable, heterogeneous group of peptides with narrow or broad-spectrum activity towards other bacterial species. Certain bacteriocins contain an unusual amino acid, lanthionine, and exist with thioether rings; they are known as lantibiotics (McAuliffe et al, 2001). Lantibiotics are a class of ribosomally-synthesized AMPs that are post-translationally modified to have unusual amino acids, such as dehydrated and lanthionine residues. Lanthionine, a nonproteinogenic amino acid, consists of two alanine residues that are linked at their β-carbon by thioether links. Nisin is a well-characterized lantibiotic that is commonly used as a food preservative (Hansen, 1994).

1.5. Relationship of structure with function

As AMPs are distributed across the taxonomical hierarchy, they are also diversified in their functions. Higher hydrophobicity is correlated with stronger hemolytic activity (Hollmann et al, 2016). Besides, the high hydrophobicity adversely affects the peptide's antimicrobial activity. High hydrophobicity causes peptide molecules to self-assemble through hydrophobic interactions, thereby adversely affecting their membrane interaction. Hence, an optimum hydrophobicity is required for good antimicrobial activity (Hollmann et al, 2016). In contrast, increased peptide self-association does not affect the peptide's access to the eukaryotic membranes (Lei et al, 2019).

Structure-activity relationship studies of AMPs have revealed that factors such as charge, secondary structure, hydrophobicity, and hydrophobic moment influence the specificity and biological activity of these peptides (Fjell et al, 2011). Each of these factors is intimately related such that altering one can change the other. In general, AMPs interact with their membrane target, change the conformation by self-association, and perturb the membrane, resulting in cell death (Wimley & Hristova, 2011).

Analyzing the 3D structure in solution and the membrane-bound state gives a clear understanding of the action mechanism. NMR spectroscopy happens to be the most useful tool in studying structural details. Due to the short sequences, conventional two-dimensional (2D) NMR is sufficient for solving the structure of many peptides (Wüthrich, 1986). NOESY spectra facilitates high-resolution solution structure determination for these peptides. By studying amide deuterium exchange kinetics or temperature dependence of amide chemical shifts, additional information such as hydrogen-bonding pattern can be known (Baxter & Williamson, 1997). Even though many studies have been carried out to understand the mechanisms of AMP action, the exact sequence of actions remains a mystery. The diversity in the AMP characteristics, in conjunction with the complexity that they encounter on the microbial surface that varies from microbe to microbe, makes it challenging to understand the detailed mechanism of their action.

1.6. Modes of action

Microbial surfaces are decorated with anionic moieties that include negatively charged lipids such as phosphatidylglycerol and cardiolipin, lipopolysaccharides (in case of Gram-negative bacteria), and lipoteichoic acids (in case of Gram-positive bacteria) (Epand & Epand, 2009; Riedl et al, 2011; Teixeira et al, 2012). As most AMPs are cationic in nature, they selectively bind to microbial surfaces. Upon binding, the AMPs have to traverse through the thick peptidoglycan layer in the Gram-positive bacteria and the outer membrane of the Gram-negative bacteria. Once they gain access to the cytoplasmic membrane, they can either disrupt the membrane integrity or translocate across the membrane to act on the intracellular targets (Saikia & Chaudhary, 2018). Several models, however, have been proposed as far as membranolytic action is concerned.

1.6.1. Membrane-mediated action

The binding of AMPs to the cytoplasmic membrane is accompanied by its folding into an amphipathic structure unless they are already folded. The amphipathicity facilitates their insertion into the membrane. This leads to the expansion of the outer leaflet accompanied by local membrane thinning. Besides, the high positive charge causes the crowding of negatively charged lipids around the peptides and their segregation from zwitterionic lipids. This phenomenon is known as "phase separation" or "phase segregation" (Epand & Epand, 2009; Epand et al, 2010; Teixeira et al, 2012). As the concentration of AMPs in the outer leaflet of bacterial membrane increases, several molecular events are triggered, which ultimately lead to cell death; this latter set of events has been proposed to be mediated *via* different models (Sitaram & Nagaraj, 1999; Wiesner & Vilcinskas, 2010; Riedl et al, 2011; Teixeira et al, 2012). The AAMPs can also display antimicrobial action through membrane perturbation. The binding to membrane is aided by metal ions to form cationic salt bridges with negatively charged components of the microbial membrane (Frederick et al, 2009). Interaction of dermicidin with negatively charged bacterial phospholipids is facilitated via Zn^{2+}-dependent oligomeric complex, leading to the ion channel formation, which results in membrane depolarization and cell death (Burian & Schittek, 2015).

The mechanism of AMP action leading to cell lysis occurs in multiple ways. Though the exact mechanism is not clear, various models have been proposed to explain the idea (Figure 1.7). While the mechanism of β-sheet forming peptides has not been clearly elucidated, various models are proposed to demonstrate the pore-forming ability of α-helical AMPs.

1.6.1.1. Barrel-stave model

The first model was proposed by Baumann and Mueller in 1974 to explain the single-channel induced by alamethicin in lipid membranes (Baumann & Mueller, 1974). The model is known as the barrel-stave model (Figure 1.7A). In this model, the amphipathic peptides orient themselves perpendicular to the lipid membrane and form a barrel-like structure. The interior part of the channel is composed of hydrophilic regions of the peptide, while the outer hydrophobic part is surrounded by the fatty-acyl region of the phospholipid bilayer. Thus, the channel acts as a conductance channel that disrupts

transmembrane potential and ion gradients, leading to leakage of cellular components and cell death. The fungal AMP, alamethicin, is one such example of an AMP that penetrates and aggregates to form transmembrane pores (Sato & Feix, 2006).

1.6.1.2. Toroidal pore model

The toroidal pore model describes peptides' action by inducing a bend in the lipid bilayer where the lipid head groups orient themselves to form a pore. The pore is composed of both the peptide and phospholipid (Huang, 2000; Gottler & Ramamoorthy, 2009). The toroidal pore differs from the barrel stave model in that the AMPs are always associated with the lipid head group even when they are perpendicularly inserted into the bilayer (Figure 1.7B). Magainin, protegrins, and melittin are proposed to act through this mode (Hallock et al, 2003).

1.6.1.3. Carpet model

In the carpet model, the peptide molecules align parallel to the lipid bilayer, forming a carpet-like structure. This orientation disrupts the membrane potential by destabilizing the packed phospholipids, forming cracks in the bilayer, thereby disintegrating the cell membrane (Figure 1.7C). A general feature of the carpet model is that the peptide associates with the head groups of lipid bilayer, not with the hydrophobic core of the membrane. Hence, without the insertion of peptide molecules into the membrane core, the membrane gets disrupted/dissolved in a dispersion-like manner and does not involve the formation of pores/channels (Powers & Hancock, 2003). Aurein 1.2 is the exemplary peptide of the carpet model. The peptide displays enhanced interaction with anionic membrane DMPC/DMPG primarily by surface alignment, interaction, and disruption of membrane integrity, resulting in cell lysis (Fernandez et al, 2012).

1.6.1.4. Detergent model

In the detergent model, the peptide disrupts the membrane integrity, causing leakage of cellular content, thereby causing cell death, much like a detergent (Wimley, 2010). It is a non-pore-forming model where the catastrophic collapse of membrane integrity and probe-size-independent leakage of cytosolic components takes place (Figure 1.7D). This

mechanism of AMP action is usually observed at high peptide concentrations (Wimley, 2010).

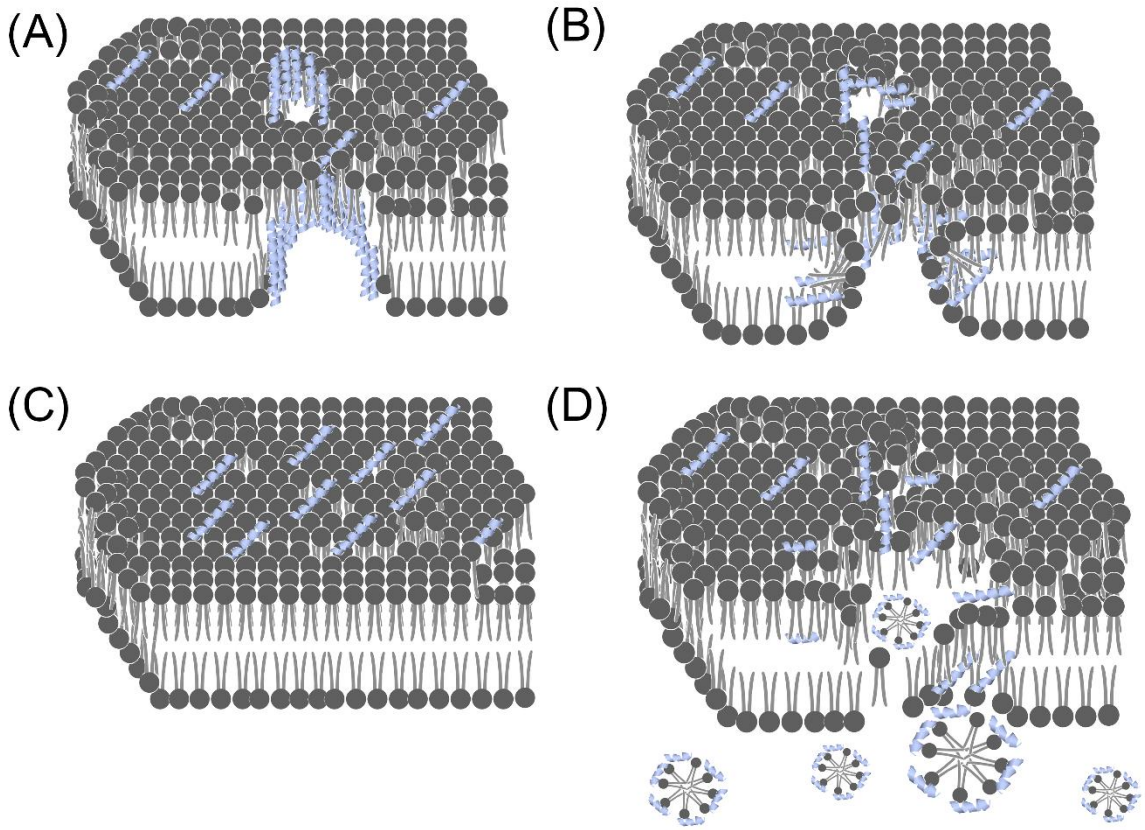

Figure 1.7. Models proposed for the action of AMPs on the microbial cell membrane. (A) Barrel-stave model, (B) toroidal pore model, (C) carpet model, (D) detergent model. (The lipid and peptide cartoons were sourced from Biorender (www.biorender.com) and the figure was created using Adobe Photoshop).

1.6.2. Membrane independent/non-membrane-disruptive mechanisms

Though membrane-permeabilization is often associated with the antimicrobial activity of AMPs, non-membrane-disruptive mechanisms also exist wherein the peptides target intracellular molecules and processes (Cudic & Otvos, 2002; Bera et al, 2003). Unlike membranolytic AMPs, these intracellularly-active AMPs may target DNA/protein synthesis, peptidoglycan synthesis, or any other process, eventually causing cell death (Brogden, 2005). Buforin 2, an AMP derived from Buforin 1 (from toad *Bufo gargarizans*), for example, kills the cell by binding to DNA and RNA after penetrating the cell membrane, thus inhibiting cellular functions. (Park et al, 1998; Muñoz-Camargo et al, 2018). Certain

AMPs have chemotactic properties and induce inflammatory cytokine expression by innate immune cells, e.g., Bac5 exhibits bactericidal activity by inhibiting protein synthesis through cell-mediated immune response (Munshi et al, 2020). Translocated peptides can activate autolysins and phospholipases, cause flocculation, and inhibit septum formation (alter cytoplasmic membrane formation), e.g., PR-39, PR-26, indolicidin (Hsu et al, 2005), microcin 25; inhibit cell wall formation, e.g., lantibiotic mersacidin inhibits peptidoglycan synthesis by interfering with transglycosylation (Brötz et al, 1995); bind to DNA or RNA and alter their functions, inhibit the synthesis of nucleic acid and protein, e.g., buforin 2 (Park et al, 1998) and tachyplesin (Yonezawa et al, 1992); inhibit the enzymatic activity, e.g., salivary histatins inhibit proteolytic activity of matrix metalloproteases enzymes (MMP 2 and MMP 9) that are elevated in periodontal disease (Gusman et al, 2001).

1.7. Multifaceted roles of antimicrobial peptides

Functional diversity is another notable feature of AMPs. Besides having antimicrobial activity, they might possess other biological activities such as anticarcinogenic, antidiabetogenic, and immunomodulatory. Some of the non-antibiotic activities are discussed here.

1.7.1. Anticancer AMPs

Certain AMPs can target the plasma membrane of cancer cells and are, therefore termed anticancer peptides (ACPs) (Deslouches & Di, 2017). Certain mechanisms, both membranolytic and non-membranolytic, have been proposed, but the exact mechanisms by which these peptides kill cancer cells remain unclear (Gaspar et al, 2013). Cancer cells possess a higher amount of phosphatidylserine on their cell surface compared to normal cells. This imparts some selectivity to the ACPs towards cancerous cells (Wang et al, 2017) The AMP dermaseptin PS-1 exhibits anticancer activity by inducing the intrinsic apoptotic pathway (Long et al, 2019). Tumor specificity also plays a key role in the efficacy of the ACPs. Though most ACPs are more cytotoxic to tumor cells than erythrocytes, tumor-selective peptides are not lacking (Deslouches & Di, 2017). Certain peptides target the cancer cells indirectly via an angiostatic mechanism. They inhibit the growth of endothelial cells, thereby inhibiting angiogenesis and the proliferation of cancer cells. Dermaseptins B2 and B3 are two such peptides (van Zoggel et al, 2012). The

peptide pentadactylin induces DNA fragmentation and arrests the cell cycle at the S phase, provoking apoptotic cell death in tumor cells (Libério et al, 2011). Temporin 1CEa elevates the tumor cell membrane's permeabilization, thereby altering its membrane potential in tumor cells, causing cytotoxicity (Wang et al, 2013). Unlike conventional drugs, these peptides trigger diverse mechanisms to target the tumor cell; hence, developing resistance against them is relatively slow.

1.7.2. Wound healing AMPs

The skin, being a highly protective barrier, protects the organisms from infections. Unrepaired skin damage is prone to infection by various opportunistic pathogens. Wound healing is a slow and complicated process that comprises four stages: hemostasis, inflammatory response, cell proliferation, and tissue reconstruction (Martin, 1997). Delayed wound healing, as in the case of diabetes patients, can be life-threatening. Accelerated wound healing, therefore, happens to be a defense mechanism against infections. A number of reports suggest that human AMPs are involved in wound healing (Elgarhy et al, 2015). For example, the wounds in human skin induce expression of human β-defensins 2 and 3. Human cathelicidin LL-37 is another wound-healing peptide. Wound-inflicted human skin shows elevated levels of LL-37 (Dorschner et al, 2001). The levels return to normal once the wound is closed. The mechanism behind wound-healing activity has been reviewed elsewhere (Duplantier & van Hoek, 2013). Porcine cathelicidin PR-39 is another example of a wound-healing peptide (Veldhuizen et al, 2014).

1.7.3. Antidiabetogenic peptides

AMPs are reported to stimulate insulin production upon norepinephrine stimulation. Brevinin 1ITa and 1ITb, the AMPs isolated from the skin secretions of *Rana italica*, induce insulin release from rat pancreatic β-cells (Conlon et al, 2017). Amolopin, a peptide from *Amolops loloensis* skin secretions, stimulates insulin secretion in INS-1 cells (Mo et al, 2014). AMPs temporin A, temporin F, and temporin G from *Rana temporaria* have been reported to cause concentration-dependent stimulation of insulin release without cytotoxicity (up to 3 μM concentration), and the combinational therapy involving temporin A and temporin G is proposed as a promising therapy for type II diabetes treatment (Musale et al, 2018). Peptides from skin secretions of families Pipidae, Ranidae,

and Dicroglossidae show potent insulinotropic activity by stimulating insulin release and lowering blood sugar, thus displaying antidiabetic activity (Conlon et al, 2018).

1.7.4. Anti-inflammatory and immunomodulatory AMPs

HDPs have an imperative role in both innate and adaptive immune responses (Mansour et al, 2014). Nearly all mammalian AMPs have other roles alongside microbicidal activity (Chessa et al, 2020). They can induce various immunomodulatory functions such as chemotactic activity, attracting leucocytes, stimulation of angiogenesis, enhancement of leucocyte/monocyte activation and differentiation, and modulation of the expression of proinflammatory cytokines/chemokines. AMPs AC12, DK16, and RC 11, isolated from *Hypsiboas raniceps* skin secretions, show anti-inflammatory activity (Popov et al, 2019). Esculentin 1GN inhibits inflammatory response induced by LPS (Zeng et al, 2018). Frenatin 2.1S activates the cytotoxic capacity of NK cells (Pantic et al, 2017) as an antitumor immunotherapeutic agent. Frenatin 2D stimulates cytokine-mediated stimulation of adaptive immune response (Conlon et al, 2013). AMPs that predominantly possess immunomodulatory activity usually have little antimicrobial and hemolytic activity (Pantic et al, 2017).

1.7.5. Spermicidal action

Besides killing pathogens causing sexually transmitted diseases, magainins (Reddy et al, 1996) and dermaseptins (Zairi et al, 2008) were observed to possess spermicidal activity. These peptides restricted sperm motility and viability in a dose-dependent manner. The exact mechanism is not known. However, the presence of these peptides altered the permeability of the plasma membrane, leading to cell death. Maximins display spermicidal action by forming pores via detergent-like disruption mechanisms (Lai et al, 2002). The spermicidal activity of these anuran peptides could be promising for the development of safer and natural contraceptives.

1.8. Limitations and challenges

The microbicidal action of cationic peptides and their role in innate immunity was recognized way back in the late 19th century, which drove the development of AMPs as possible new therapeutics. Antibiotic resistance is one of the critical health challenges

today. Microbes develop resistance to antibiotics due to their abuse and improper medication practices. Certain species show cross-resistance to antibiotics, wherein they are more resistant to similar kinds of antibiotics. Strikingly, antibiotic-resistant bacteria show a high rate of collateral sensitivity to AMPs, whereas cross-resistance is relatively rare (Lázár et al, 2018). The main characteristics of innate immunity peptides are that they target nonprotein components, i.e., the bacterial membrane, and also possess auxiliary activities such as immunomodulatory and antiinflammatory activities (Zasloff, 2002). Their effectiveness, biodegradability, and versatile mode of action are notable. The ability to kill the dividing and non-dividing cells, biofilms, and being less prone to induce resistance are some of the striking attributes of AMPs (Peschel & Sahl, 2006; Fjell et al, 2011; Huang et al, 2014). However, they have failed the researchers in terms of their clinical applications. This failure is due to several limitations and hindrances that need to be overcome before AMPs could find clinical applications.

1.8.1. Stability

The AMPs characterized by *in vitro* studies need to be tested for their stability *in vivo* as multiple proteolytic enzymes exist in the serum. Though effective in killing microbes, most AMPs are susceptible to proteolytic degradation, which reduces their half-life (Wang et al, 2015). *In vivo* stability happens to be one of the key requirements of an effective AMP as a drug. Peptide stability is correlated with amino acid composition and lipophilicity of AMPs. Cyclic peptides or disulfide-containing peptides, specific amino acid-rich peptides, tend to be more stable due to their complex structure. Peptide cyclization appears to be an interesting strategy for serum stability without compromising the antimicrobial activity (Anne & Marianna, 2018). The incorporation of nonnatural amino acids also provides protection against proteolytic degradation. As AMPs display their antibacterial activity largely via membrane perturbation, all D-peptides often show comparable activity but very high serum stability. The additional non-antibiotic features, however, are severely affected.

1.8.2. Toxicity

One of the major hindrances in realizing peptides as drugs is their poor selectivity. AMPs display cell selectivity that corresponds to the selective inhibitory action on microbial cells and leaving the mammalian cells intact. The mammalian cells, however, are not

really spared. Many peptides possess strong hemolytic activity. Besides, the selectivity of an AMP depends on its concentration. An otherwise non-cytotoxic AMP can show significant cytotoxicity at higher concentrations. This attribute can lead to deleterious effects (Matsuzaki, 2009). AMPs often lack selectivity in non-native or therapeutic settings but exhibit functional selectivity in their original species due to evolutionary and biological context. (Fjell et al, 2011; Liang et al, 2020). This contrast is an interesting area of research for designing better, more selective AMP-based therapeutics with enhanced selectivity. Recent advances in biosynthetic engineering, such as cyclization, glycosylation, or incorporation of noncanonical amino acids have expanded the structural diversity of AMPs, improving microbial specificity while reducing the host toxicity (Zhu et al, 2014; Mordhorst et al, 2023). Thus, AMP selectivity is both a natural evolutionary adaptation and a property that can be deliberately tuned through synthetic biology approaches (Rossetti et al, 2024). Hence, AMPs can be modified as promising scaffolds for next-generation antimicrobial therapeutics.

1.8.3. Salt-sensitivity

Salt sensitivity poses an obstacle to the development of AMPs as therapeutic agents. Retention of activity under physiological conditions is vital to be an efficient antimicrobial agent. Lee et al. reported that clavanins, the histidine-rich AMPs identified in tunicates show better tolerance to high salt concentration compared to magainin-1 (Lee et al, 1997). Kim and coworkers investigated the antimicrobial role of an α-helical peptide, $[RLLR]_5$, a synthetic analog of buforin 2 that consists of a repeat of C-terminal sequence motif RLLR (Park et al, 2000; Park et al, 2004). They found that the activity of the peptide is severely compromised in the presence of salt. This is attributed to the disruption of the peptide's helical conformation. Capping of peptide with helix-capping motifs was shown to stabilize the helical conformation, thereby causing retention of activity. The structural stability, therefore, is important for both antimicrobial action and peptide's salt tolerance (Tam et al, 2002).

1.8.4. Aggregation propensity

As most AMPs are amphipathic in nature, they have a natural tendency to self-assemble in water to bury their hydrophobic patches. Aggregation is particularly pronounced in the β-sheet peptides as they can readily self-assemble to form long β-sheet rich fibrillar

assemblies (Bellesia & Shea, 2009). Higher aggregation propensity turns out to be a challenge for peptide synthesis as well. The peptides tend to aggregate during synthesis giving poor yields, thereby making synthesis a costlier affair. However, strategies have been devised to reduce aggregation during synthesis (Coin et al, 2007).

1.9. Lipid membranes

Ever since the membrane structure was elucidated by Singer and Nicolson, the field of membrane biology has flourished. Although the proposed structure was way too simple compared to the complexity of real biological membranes, it was the right start of all the remarkable discoveries that followed (Sanderson, 2005). Although AMPs are known to target cell membranes, the actual mechanism behind them is still unclear. They show cell selectivity by targeting microbial cell membranes rather than mammalian cells. One of the major reasons could be due to their lipid composition and the physical properties of the membrane.

The roles of lipid membranes are diverse as they serve different important functions in the cells. They serve as cell boundaries that compartmentalize cellular contents, regulate molecular traffic, act as essential media for cell communications, and participate in signaling processes (Casares et al, 2019). As the membranes are highly dynamic, heterogeneous, and relatively disordered structures, a complete understanding of the membrane structure and organization has not yet been achieved. of the lipids that constitute biological membranes include phospholipids, cholesterol, sphingolipids, and glycolipids. The physicochemical nature of membrane lipids plays a crucial role in the assembly of lipids into structural and functional membranes (Teixeira et al, 2012). The structure of lipids used for the study is shown below (Figure 1.8).

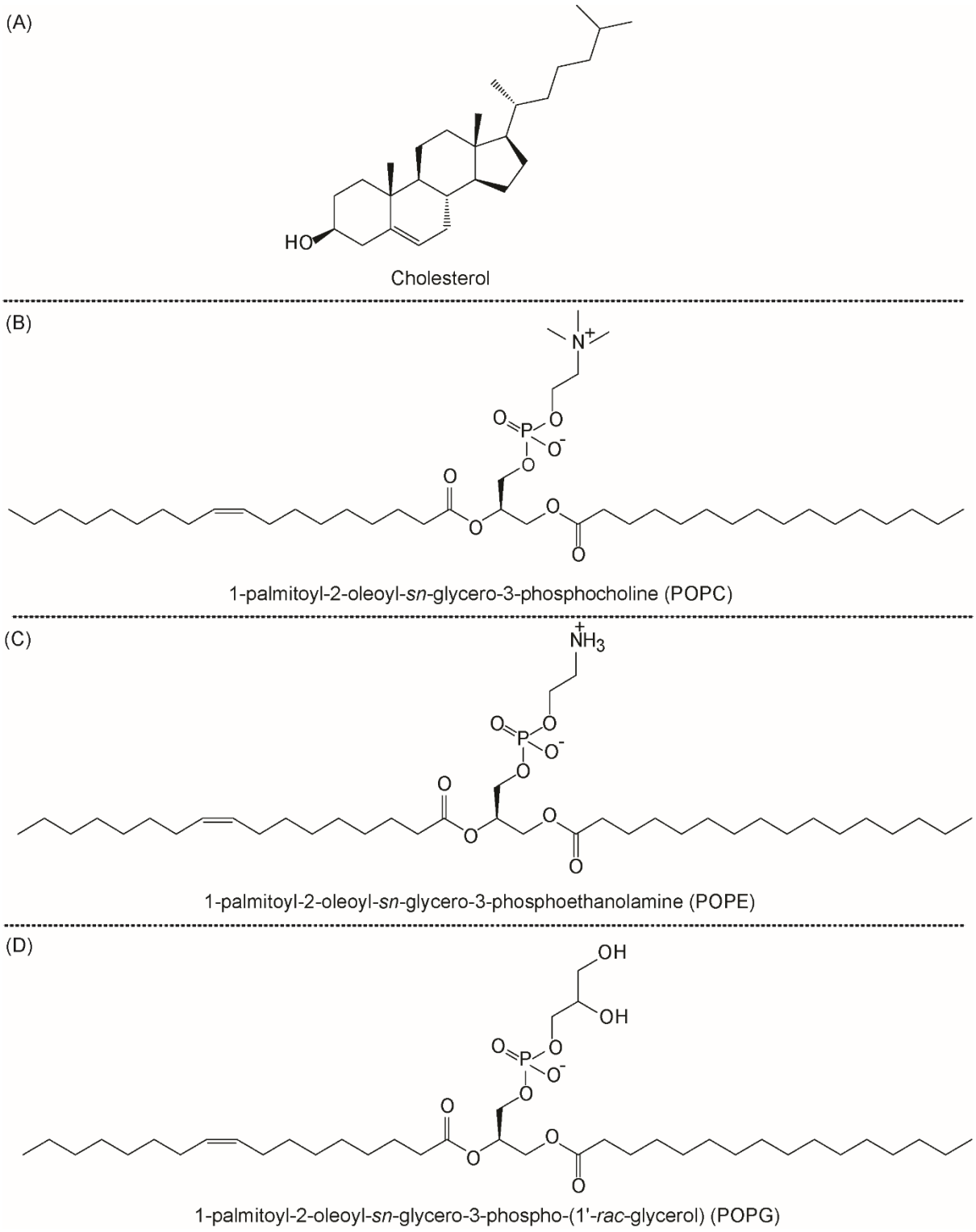

Figure 1.8. The structures of lipids that have been employed in this thesis. (a) Cholesterol, (b) 1-palmitoyl-2-oleoyl-*sn*-glycero-3-phosphocholine (POPC) (c) 1-palmitoyl-2-oleoyl-*sn*-glycero-3-phosphoethanolamine (POPE), and (d) 1-palmitoyl-2-oleoyl-*sn*-glycero-3-phospho-(1'-*rac*-glycerol) (POPG).

Phospholipids are the major lipid components in most cell membranes, except in neural tissues. The composition of phospholipids is tissue-dependent and highly regulated. Although the composition and lipid asymmetry in different types of cell membranes are well known, their influence on function is not clearly elucidated (Yorek, 2018). Yet, it is believed that the variability and asymmetry in lipid composition significantly influence the functions that they get involved in. The interaction of proteins and peptides with membranes is influenced by several factors. The composition, fluidity, and curvature of lipid membranes, as well as the charge, structure, and hydrophobicity of peptides, play very crucial roles.

1.10. Peptide-membrane interactions

Peptide-lipid interactions are essential for various physiological processes, including antimicrobial defense mechanisms, membrane protein insertion, signaling, transport of diverse hormones, toxins, and so on [2]. We have already discussed the different mechanisms of membranolytic peptides. During the host-pathogen interaction, the membrane is the main target of the antimicrobial peptides. For an AMP to be an effective drug molecule, the crucial element is the selective toxicity towards the pathogenic membrane, sparing the host cell intact. The key factor that determines the selectivity of peptide action depends on the composition of the membranes (Sanderson, 2005). Membranes are composed of lipids that self-assemble to form a lipid bilayer, having various proteins attached to it or embedded in it. Membranes of prokaryotes and eukaryotes differ in their membrane lipid composition. This allows the AMPs to distinguish between them, allowing preferential binding to the prokaryotic membranes (Yount et al, 2006). This trait is used to mimic the biological membranes, as far as the membranolytic action of AMPs is concerned, using model membranes of different compositions. Eukaryotic membranes preferentially have phospholipids such as phosphatidylcholine, whereas the bacterial membrane considerably possesses lipids such as phosphatidylethanolamine, phosphatidylglycerol, and phosphatidylserine (Yorek, 2018). The nature of membrane lipids is responsible for the curvature strain on the membrane. The selectivity of lipid membranes is due to the charge (Glukhov et al, 2005). POPC is a zwitterionic lipid having both positive and negative charges, whereas POPG and POPS confer a net negative charge. Cholesterol is present in eukaryotic cell membranes ranging from <5 mol % in the mitochondrial membrane to ~ 40 mol % in the

plasma membranes of the cells. It is absent in the prokaryotic cell membrane (Doole et al, 2022). It gives rigidity and spontaneous curvature to the membrane, thus imparting the ability to withstand the mechanical stresses from the environment.

Research has shown that the length, sequence, and conformation of peptides affect their interactions with lipids. Longer and hydrophobic peptides tend to interact more strongly with the lipid bilayer. Peptides adopting alpha-helical or beta-sheet structures penetrate the lipid bilayer more easily. These interactions are critical in various biological functions, such as membrane protein insertion, signal transduction, and antimicrobial activity. This study investigates the interaction of the recently discovered Bufo skin-derived antimicrobial peptide, cathelicidin-DM, with model membranes mimicking mammalian and bacterial cell membranes.

1.11. Lipid membrane models

The cell is an extremely complex system where every process is connected to many other processes. Understanding or probing a separate entity selectively within the cell is extremely challenging as there are too many parameters to consider while drawing conclusions. Lipid monolayers can be used as a model for flat membranes, while small, large, and giant unilamellar vesicles are used to mimic membranes of different curvatures. While giant unilamellar vesicles have sizes comparable to bacterial size, they are unsuitable for spectroscopic investigations. The large size causes scattering of light. SUVs, therefore, can be used to carry out spectroscopic assays. As model membranes can be synthesized with desired lipid compositions and curvature, they happen to be the most routinely employed systems for investigating membranolytic AMPs. These model membranes have also been employed to elucidate the structural details of peptide-membrane interactions at atomic resolution using techniques such as solid-state NMR and X-ray diffraction. This gives an insight into the underlying molecular mechanism of membrane disruption. This knowledge about the mechanism of membrane disruption and peptide-membrane interaction is essential for engineering the peptides to improve their activity and stability and alleviate their toxicity. Model membranes, therefore, have become an invaluable tool for exploring membrane-associated processes.

1.12. Anuran AMPs

Anurans (frogs and toads) possess various bioactive substances in their skin secretions that provide protection to the organisms. The warm and humid habitat in which anurans reside increases their vulnerability to infections. To thrive in this pathogenic niche, these anurans have specialized skin features and glands. The parotid glands, located behind the head and known for their whitish-colored toxic fluid, are enriched with biogenic amines, alkaloids, various proteins, and peptides (Medeiros, Rego et al. 2019, Carrillo, Boaretto et al. 2024). Additionally, the granular glands on the dorsal region of the skin also contribute to their defense mechanisms. When environmental stress is created due to pathogenic organisms, it causes adrenergic stimulation on myocytes that surround dorsal granules, which further stimulates the release of AMPs in a holocrine-like mechanism (Rollins-Smith et al, 2005). This helps in fighting against the pathogen. Thus, the roles of host defense peptides are vital in defense against predators and help in survival among various pathogenic microbes. Toad venom has been used in anticancer remedies in Chinese traditional medicine as *Chan su* (*senso*) (Rodríguez et al, 2017). *Chan su* is proven to induce apoptosis in human bladder carcinoma T24 cells (Shin Ko et al, 2005). The dried powder of the extracted skin from *B. gargarizans* is also used in another medicine known as Huachansu or Cinobufacini (Meng et al, 2009).

Anuran antimicrobial peptides are the components of the innate immune system. These peptides generally vary in size from 12-50 amino acids. Most anuran AMPs are cationic due to multiple lysine and/or arginine residues, and also contain more than 50% hydrophobic amino acids (Zasloff, 2002). Structurally, they are classified into α-helix, β sheet, β hairpin or loop, α β mixed, and non α β (extended structure) (Zhu et al, 2018). Structural analysis using CD and NMR studies show that most anuran AMPs lack secondary structures in aqueous solution but have a high propensity to fold into an amphipathic α-helical structure in membrane-mimetic solvents. As far as antimicrobial activity is concerned, the cationicity facilitates binding with the negatively charged bacterial surfaces wherein folding occurs to achieve an amphipathic helical conformation (Powers & Hancock, 2003). A few exceptional, biologically-significant AMPs are anionic in nature. Maximins are the first reported anuran anionic peptides from *Bombina maxima* (Lai et al, 2002). These potential defense peptides are produced by immune cells of hematopoietic and epithelial origin. Despite being constitutive, regulation of AMP

synthesis is correlated with any environmental stimuli, such as stress, electrical, and norepinephrine stimulation, and is prominent in response to infection. AMP synthesis was deterred when frog *Rana esculenta* was kept in the sterile microenvironment and restored back in the presence of microbes, which refers to an inducible mechanism of synthesis.

Earlier, the isolation of peptides from frogs was done by sacrificing the animal, followed by extracting the skin. The peptides were then isolated from a very heterogeneous mixture of molecules. Later studies reported skin secretions upon injection of epinephrine or norepinephrine near dorsal glands. This method is pretty fast and reliable, and ethically acceptable (Conlon & Sonnevend, 2010). Identification and characterization of AMPs are carried out by peptidomics and genomic analysis in combination with various other antimicrobial assays. So far, more than 1000 AMPs have been identified from frog species (http://aps.unmc.edu/AP/main.php). The sporadic distribution of these peptides among anurans perceives that AMPs are not inevitable for the survival of species but rather an arsenal, giving protection to the species (Conlon, 2011). The diversity of anuran AMPs is enormous. Each species possesses multiple peptides with structural and functional differences (Vanhoye et al, 2003). Anuran antimicrobial peptides are grouped into various families with unique physicochemical characteristics: Rugosin, Guegurin, Temporin, Ranaalexin, Ranatuerin, Brevenin, Esculentin, Palustrin, Tigerinin, Nigrosin, Japionicin, Melittin related peptides, and so on (Conlon et al, 2004). Interestingly, single peptides have also evolved to have diverse spectra of action for better compatibility. For example, skin secretions of *Rana italica* have both cytotoxic and antidiabetogenic activity (Conlon et al, 2017). Thus, these powerful antimicrobial agents must be investigated further for their unrevealed mysterious actions for the benefit of society.

1.13. Cathelicidin-DM

Cathelicidins are cationic AMPs that are highly diverse and known for their potent antimicrobial activity against a wide spectrum of microorganisms. Apart from their antimicrobial role, cathelicidins have diverse roles, such as anti-inflammatory and immuno-modulatory activities. Various amphibian cathelicidins have been studied for their role in host defense mechanisms. As we looked into the bufo species, we noticed

that a few cathelicidins had been investigated in detail. Some of the Bufo peptides and their amino acid sequences are listed in Table 1.5. The sequence similarity of BG-cathelicidin and cathelicidin-DM is extremely high. BG-cathelicidin is known to kill bacteria through membrane-related activity, similar to other cathelicidins. But the precise mode of action (e.g., pore formation, translocation, intracellular targeting) of BG-cathelicidin has not yet been fully elucidated in the literature.

Cathelicidin-DM is a 37 amino acid cationic peptide identified from *D. melanostictus*, with antimicrobial and wound healing activity (Shi et al, 2020). Structurally, the open reading frame consists of 495 nucleic acids encoding 164 amino acids (including 21 amino acid signal peptide), a highly conserved cathelin region, and a mature peptide with sequence SSRRKPCKGWLCKLKLRGGYTLIGSATNLNRPTYVRA. The chemical structure of cathelicidin-DM is depicted in Figure 1.9. It has been reported to possess antimicrobial activity against *Escherichia coli* (MDR 13A10022), *E. coli* (MDR 13U1780), *E. coli* ATCC25922, and *Citrobacter freundii* (CI 1410UR0112), *Staphylococcus paratyphoid A* (CI 1410UR0112), *Klebsiella pneumoniae* (MDR 13U1752), *K. pneumoniae* (MDR 13A11923), and *K. pneumoniae* (XDR 13A13361). As cathelicidin-DM exhibits antimicrobial activity, leading to cell lysis, and demonstrates wound healing properties by facilitating cell repair, it is imperative to investigate its distinctive membrane interactions. Such a study is essential for understanding the underlying mechanisms governing the dual functionality of cathelicidin-DM.

Table 1.5. List of bufo peptides.

Peptide name	Species	Amino acid length	Sequence
Buforin 1 (Park et al, 1996)	*B. gargarizans*	37	AGRGKQGGKVRAKAKTRSSRAGLQFPVGRVHRLLRKGNY
Buforin 2 (Yi et al, 1996)	*B. gargarizans*	21	TRSSRAGLQFPVGRVHRLLRK
BG-Cathelicidin (Sun et al, 2015)	*B. gargarizans*	37	SSRRPCRGRSCGPRLRGGYTLIGRPVKNQNRPKYMWV
BG-Cathelicidin (5-37) (Sun et al, 2015)	*B. gargarizans*	33	RPCRGRSCSPWLRGAYTLIGRPAKNQNRPKYMWV
Cathelicidin-DM (Shi et al, 2020)	*D. melanostictus*	37	SSRRKPCKGWLCKLKLRGGYTLIGSATNLNRPTYVRA

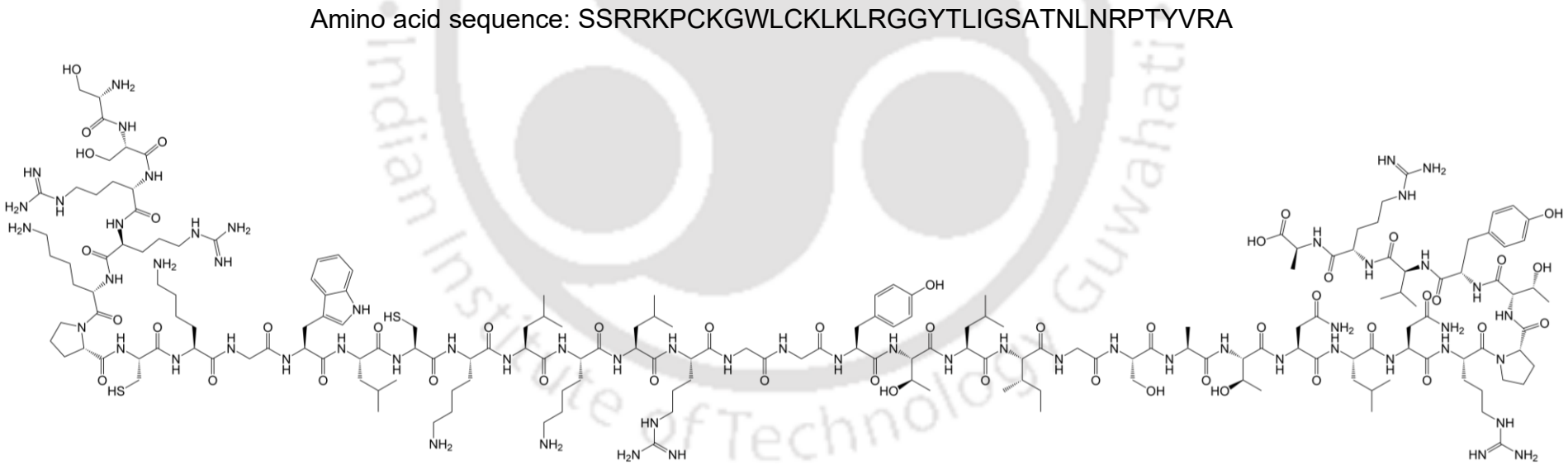

Figure 1.9. The chemical structure of cathelicidin-DM (drawn using ChemDraw).

1.14. Conclusion

Peptides are the ancient defense molecules every living organism uses to combat pathogens. They kill the microbes primarily through a non-receptor mediated mechanism, making it difficult for the microbes to develop resistance. The spectrum of killing is very diverse, and certain AMPs can kill bacteria, fungi, and viruses as well. Another interesting aspect is that they often display synergistic effects in killing the microbes. Despite such features, they have failed to replace conventional antibiotics. There are several limitations and challenges that need to be overcome before peptides can find clinical applications. Several strategies have been devised to overcome the limitations, and peptides have been designed *de novo*. However, there is still a long way to go before the AMPs gain the respect that conventional antibiotics keep enjoying.

Anuran skin is an ocean of antimicrobial peptides with vast medicinal significance. Besides antimicrobial activity, AMPs have various other properties like anticarcinogenic, antidiabetic, wound healing, anti-diabetogenic, immunomodulatory, spermicidal properties, etc. The full potential of these peptides may extend beyond these known functions, with many additional properties yet to be discovered. The diverse spectrum of activity of anuran AMPs renders them promising candidates for developing innovative therapeutic agents. They also show significant potential in addressing challenges posed by antibiotic-resistant strains, biofilms, and persister cells. As AMPs often disrupt bacterial cell membranes directly, they can be effective against resistant strains and help combat biofilms. For that, the peptide potency must be enhanced through modifications, while keeping the mammalian cell cytotoxicity in check. The right way of understanding and application of these potential small molecules could encourage a revolutionary change in the current medicinal research.

1.15. Motivation of the study

The use of frog/toad skin has been observed in different traditional medicines. In northeastern India, the skin of a common Asian toad (*D. melanostictus*, Figure 1.10) is used to cure wounds and infections. While I was investigating the toad secretions, a cathelicidin was reported from this toad (Shi et al, 2020).

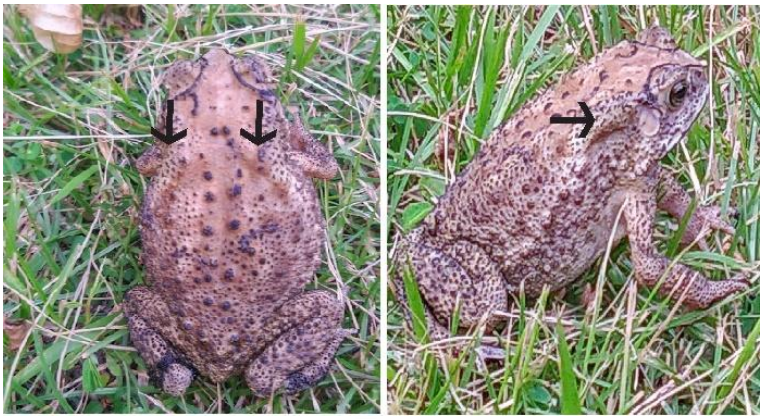

Figure 1.10. *D. melanostictus /* common Asian toad (from IITG campus) bufo toad. Black arrows represent the Parotid glands from which the glandular secretions are taken for traditional drugs.

The peptide cathelicidin-DM was reported to kill several bacteria while healing mammalian wounds. Based on similarity with already known AMPs, membrane perturbation was proposed as the mechanism of antibacterial action. As there was no experimental evidence for the proposed mechanism of action, I chose this as my doctoral thesis. The structure of the peptide was predicted and modeled using the QUARK server and subsequently visualized with CHIMERA. The stability of the structure was assessed using molecular dynamics simulation. Subsequently, the interfacial activity of the peptide was investigated using a water/cyclohexane biphasic system. The peptide turned out to be surface-active. Thereafter, binding with zwitterionic and negatively charged lipid bilayers was investigated. As all computational methods supported membrane-binding, the interfacial activity and interaction with lipid monolayers as well as liposomes were investigated experimentally.

Chapter 2

Material and methods

2.1. Material and resources

NovaPEG Wang resin LL, Fmoc-protected amino acids, and O-(7-Azabenzotriazol-1-yl)-*N,N,N′,N′*-tetramethyluronium hexafluorophosphate (HATU) were purchased from Novabiochem (Darmstadt, Germany). DIC (*N,N′*-diisopropylcarbodiimide), DMAP (4-dimethylaminopyridine) *N, N*-diisopropylethylamine (DIPEA), trifluoroacetic acid (TFA), ethanedithiol, thioanisole, piperidine, acetic anhydride, calcein, 3,3′-dipropylthiadicarbocyanine iodide ($DiSC_3(5)$), and Sephadex G-75 were from Sigma-Aldrich Chemicals Pvt. Ltd. 1-hydroxybenzotriazole hydrate (HOBt), diethyl ether, HEPES, and ethylenediaminetetraacetic acid (EDTA) disodium salt were from Sisco Research Laboratory, India. *N,N*-dimethylformamide (DMF), dichloromethane (DCM) and *m*-cresol were purchased from Merck India. Cathelicidin-DM was purchased from GL Biochem (Shanghai) Ltd. The lipids POPC (1-palmitoyl-2-oleoyl-*sn*-glycero-3-phosphocholine), POPE (1-palmitoyl-2-oleoyl-*sn*-glycero-3-phosphoethanolamine), POPG (1-palmitoyl-2-oleoyl-*sn*-glycero-3-phospho-(1'-*rac*-glycerol) (sodium salt), dansyl-PE (1,2-dioleoyl-*sn*-glycero-3-phosphoethanolamine-N-(5-dimethylamino-1-naphthalenesulfonyl) (ammonium salt), and cholesterol were obtained from Avanti Polar Lipids. LB broth, LB Agar, and acrylamide were obtained from HiMedia. Restriction enzymes, ladder, loading dye, and PCR master mix were from *New England* Biolabs (NEB). Primers were obtained from Integrated DNA Technologies. The computational studies were conducted using IIT Guwahati's supercomputing facility, PARAM ISHAN. Additionally, the QUARK server (https://zhanggroup.org/QUARK/), GROMACS software package (2019.6), and CHARMM-GUI membrane bilayer builder (https://charmm-gui.org/) were employed for *in silico* studies.

2.2. Methods

2.2.1. Cathelicidin-DM modelling and MD simulation

The structure of cathelicidin-DM peptide was predicted and modeled using the QUARK server by submitting the amino acid sequence. The obtained structure was subjected to molecular dynamics simulation on the GROMACS software package (2019.6) utilizing the GROMOS 54a7 force field and a simple point charge (SPC) water model in a cubic box. GROMOS 54a7 is a widely used force field that simplifies molecular interactions by

treating non-polar hydrogen atoms as part of the carbon atoms they're bonded to (Schmid et al, 2011). Cysteine side chains were oxidized, wherein Cys7 and Cys12 formed a disulfide bond. The modeled structure underwent energy minimization using steepest descent logarithm and was equilibrated through NVT and NPT ensembles. The energy-minimized structure was subjected to a 200 ns production MD run. The simulation employed the leap-frog integration method along with the Verlet cutoff scheme. Long-range electrostatic interactions were handled using the Particle Mesh Ewald (PME) method, while bond lengths were constrained with the LINCS algorithm. Periodic boundary conditions were applied throughout the simulation. After completion, the trajectory was analyzed, and the final structure was used for subsequent simulations.

2.2.2. MD simulation of cathelicidin-DM in water/cyclohexane

The interfacial activity of the peptide was investigated by simulating it in a biphasic system. The initial setup involves placing the two immiscible liquids in contact, defining suitable force fields for each component, and running molecular dynamics simulation to observe their behavior over time. The simulation was conducted using GROMACS software with the GROMOS 54a7 force field (Pronk et al, 2013). A cubic box with dimensions (5, 5, 5) was made, and cyclohexane (466 molecules) was added. The system was simulated for 10 ns to stabilize the initial density of cyclohexane (Lemkul et al, 2010). The size of the box was then increased by doubling each of the dimensions while maintaining the cyclohexane density. The box was subsequently extended in z-direction, essentially giving a cuboid with a 1:1:2 ratio of sides, having cyclohexane in the bottom half of the box. Water (simple point charge) was subsequently added to the upper half of the box, giving a biphasic system. The peptide, that was obtained after 200 ns simulation in water as described in the preceding section (2.2.1), was added to the middle of the water phase.

The system was then solvated with water to occupy the empty space that might have appeared while changing the volume of the box. The peptide contains a net +9 charge. Charge neutralization, therefore, was carried out by adding 9 Cl^- ions. The system, containing one peptide molecule, 3728 cyclohexane molecules, 20204 water molecules, and 9 Cl^- ions, was subjected to energy minimization and equilibration with NVT and NPT ensembles (for 500 ps each) before proceeding to the MD production run for 500 ns. The

trajectory was analyzed using VMD, and the densities of water, cyclohexane, and the peptide were calculated before and after the simulation to confirm that no water had penetrated the cyclohexane phase (Wymore & Wong, 1999). Cluster analysis with a 0.2 nm RMSD cutoff was performed on the peptide to identify the most representative structure throughout the simulation.

2.2.3. Modelling of membrane-peptide system

The peptide obtained after 200 ns simulation in water was used to construct the membrane-peptide system using the CHARMM-GUI membrane bilayer builder (Qi et al, 2015). The interaction of cathelicidin-DM peptide was studied with (i) POPE/POPG (7:3) bilayer, a model that mimics bacterial membrane, and (ii) POPC/CHL (10:1) bilayer, a model that represents a mammalian lipid bilayer. The peptide was placed at a 30 Å distance from the center of mass of the lipid bilayers. For the POPE/POPG system, a total of 98 POPE and 42 POPG lipid molecules were added. Similarly, for the POPC/CHL system, 100 POPC and 10 cholesterol molecules were added (Table 2.1). Both systems were set up with a 150 mM NaCl concentration to mimic the physiological ionic strength and solvated with water molecules using the TIP3P water model.

Table 2.1 The parameters of the lipid bilayer systems

Membrane system	Lipid type	Upper leaflet	Lower leaflet	NaCl concentration	Water molecules
POPE/POPG (7:3)	POPE	119	119	150 mM	23621
	POPG	51	51		
POPC/CHL (10:1)	POPC	140	140	150 mM	23430
	Cholesterol	14	14		

2.2.4. Parameters for lipid bilayer simulation

MD simulations were conducted for both peptide-membrane systems utilizing the GROMACS package, employing the CHARMM36 force field. Energy minimization was performed using the steepest descent algorithm and Verlet cutoff scheme. The equilibration of the peptide-membrane system was carried out using NPAT ensemble. Temperature and pressure couplings were done using the Berendsen method. The bond constraints were applied to h-bonds using LINCS algorithm. In the simulation of

membrane proteins, an extended NPT phase is often necessary due to the complex composition of the system. The presence of both water and lipid molecules, which serve as solvents for the protein, introduces heterogeneity that requires a longer equilibration period to achieve stability (Hamedi & Mohammad-Aghaie, 2020). The MD simulation production runs were carried out at 300 K temperature and 1 bar pressure for 500 ns, employing the leap-frog integration method and the Verlet cutoff scheme. Long-range electrostatic interactions were managed using the Particle Mesh Ewald (PME) method. The simulations incorporated periodic boundary conditions. Upon completion of the simulations, trajectory data were processed utilizing GROMACS' built-in utilities and further analyzed using VMD software. Density calculations for the membrane, solvent, and peptide were conducted for initial time point and average over the 500 ns simulation. The RMSD for the peptide was calculated to examine the structural changes, if any, over the course of simulation. Cluster analysis with a 0.2 nm cutoff was performed on the peptide to identify the most representative structure throughout the simulation.

2.2.5. Hydrogen bonding between peptide residues and membrane

The middle structure of peptide's largest cluster in the POPE/POPG system was found to be interacting with the lipid bilayer through its N-terminal region. Therefore, hydrogen bonding interactions of the polar residues viz. Ser1, Ser2, Arg3, Arg4, Lys5, and Lys8 were investigated using UCSF-Chimera. The hydrogen bonds were computed by applying a 0.4 Å constraint for intra-model analysis by selecting the individual residues. A similar analysis was conducted for the POPC/CHL system, but with different residues since the peptide interacted with the lipid bilayer through its C-terminal. Arg31, Thr33, Tyr34, Arg36, and Ala37 were chosen for identifying the hydrogen bonding.

2.2.6. Hydrophobic interactions between tryptophan residue of peptide and cyclohexane (CHX) molecules

The position of tryptophan in the simulated biphasic system was examined for the middle structure of the peptide's largest cluster. Hydrogen bonding and hydrophobic interactions between the tryptophan side chain and the solvents were computed and analyzed using UCSF Chimera. For hydrogen bonding, a 0.4 Å constraint was applied for intra-model analysis by selecting the Trp residue. To assess the hydrophobic interactions,

a van der Waals (vdW) overlap of ≥ -0.4 Å was used, including intra-molecular contacts, by selecting the Trp and CHX residues.

2.2.7. Solid-phase peptide synthesis

The peptide was synthesized manually on Wang resin LL using Fmoc chemistry. The C-terminal alanine was coupled to the resin using DIC and DMAP in anhydrous DCM. Free hydroxyl groups on the resin, if any, were blocked using acetic anhydride and DIPEA after alanine coupling. Subsequent couplings were carried out in DMF using HATU/HOBt/DIPEA activation. After coupling the N-terminal amino acid, Fmoc was removed using 20% piperidine, washed with DMF, and dried using diethyl ether. The peptide was then cleaved from the resin using a cleavage cocktail containing trifluoroacetic acid, ethanedithiol, thioanisole, *m*-cresol, and water (20:1:2:2:2). The peptide was precipitated in ice-cold diethyl ether, and the precipitate was washed multiple times with diethyl ether, each washing followed by centrifugation. After the final wash, the pellet was air-dried. The quality of the synthesized peptide was assessed on a Thermo Scientific Dionex UltiMate 3000 RS UHPLC instrument using a reversed-phase C18 column with a linear gradient of water and acetonitrile (10–100% acetonitrile) containing 0.1% TFA. Purification was carried out using reversed-phase HPLC on a C18 column.

2.2.8. Cloning, expression, and purification of cathelicidin-DM

The synthesis resulted in very low purity. HPLC purification, therefore, resulted in a very low yield, which was insufficient for the assays. I, therefore, attempted to express the cathelicidin-DM in *E. coli*. The amino acid sequence was reverse-translated into nucleotide sequence using tblastn (https://blast.ncbi.nlm.nih.gov/Blast.cgi). *E. coli* K12 was selected as the model organism for codon optimization.

2.2.8.1. Primer design

Forward and reverse primers (FP and RP) were designed with *Nde*I and *Bam*HI restriction sites, suitable T_m, and GC content using SnapGene (https://www.snapgene.com/). Additionally, a GGCCGG nucleotide sequence was added to the 5' end of each primer to facilitate the binding of restriction enzymes. Two sets of

primers were designed: a set of large overlapping primers (Table 2.2) and another set of short primers (Table 2.3). Large primers were used to construct the complete gene through the primer extension method. The short primers were designed for PCR amplification of the gene.

Table 2.2. The designed forward and reverse (overlapping) primers for cathelicidin-DM gene construction

Sequence name	Sequence (5'-3')	No. of bases
Cath-DM-FP-01	GCGCGGGCCATATGTCCAGCAGAAGGAAACCATGCAAGGGGTGGCT CTGCAAGCTGAAGCTAAGAGGAGGTTATACTCTTATCG	85
Cath-DM-RP-02	GCGCGGGCCATATGTCCAGCAGAAGGAAACCATGCAAGGGGTGGCT CTGCAAGCTGAAGCTAAGAGGAGGTTATACTCTTATCG	96

Table 2.3. The designed forward and reverse primers (short primers) for cathelicidin-DM gene amplification

Sequence name	Sequence (5'-3')	No. of bases
Cath-DM-FP-21	GCGCGGGCCATATGTCCAGCAGAAGGAAACCATG	34
Cath-DM-RP-22	GCGCGGGGATCCTTATGCCCTCACGTAGGTAG	32

2.2.8.2. Primer reconstitution

The primers were received in lyophilized form, which were centrifuged at 13000 rpm (11,720 g) for 5 minutes to ensure that any residual powder was collected at the bottom of the vial. After centrifugation, the primers were dissolved in sterile, RNase-free water to obtain 100 µM concentration (Table 2.4). For longer-term storage, the primers were diluted and aliquoted into 10 µL volume (10 µM). This was carried out to minimize

repeated freeze-thaw cycles, which may affect the primer quality. All the primer solutions were stored at -20 °C.

Table 2.4. Reconstitution of primers

Primers	Amount of primer (nmoles)	Volume of RNase-free water added (µL)	Final concentration (µM)
Cath-DM-FP-01	43.6	436	100
Cath-DM-RP-02	98.4	984	100
Cath-DM-FP-21	23.5	235	100
Cath-DM-RP-22	27.3	273	100

2.2.8.3. Gene construct using primer extension method

A gradient PCR was carried out to identify the optimal annealing temperature for gene amplification. A master mix of 60 µL was prepared and aliquoted into six separate PCR tubes (Table 2.5). The PCR for 25 cycles was carried out with annealing temperatures varying from 50°C to 70°C, with 4 °C temperature interval. Following amplification, 10 µL of the PCR products were mixed with 1X gel loading dye, loaded into the wells of a 1.4% agarose gel, and subjected to electrophoresis at 60 V until the dye front migrated approximately 70% of the gel length. The annealing temperature that yielded the most distinct and specific amplification product was selected for subsequent gene amplification. A second PCR was then conducted using this optimized annealing temperature (70 °C) for further amplification of the gene.

Table 2.5. The components used for overlapping primer extension

Constituents	Volume (µL)
GC buffer	12
Cath-DM-FP-01	2.5
Cath-DM-RP-02	2.5
dATP	1.2
dGTP	1.2
dCTP	1.2
dTTP	1.2
DMSO	1.8
Phusion High-Fidelity DNA polymerase (2 U/µL)	0.6
RNase-free water	35.8
Total reaction volume	60

2.2.8.4. Gene amplification using PCR

The gene synthesized by primer extension method was gel extracted using a Monarch gel extraction kit to remove unwanted byproducts that would otherwise hinder the digestion reaction. Briefly, the DNA fragment to be purified was excised from the agarose gel using a scalpel. The excess agarose was removed, and the gel was transferred to a 1.5 mL microcentrifuge tube. After weighing the gel slice, Monarch gel dissolving buffer was added to the tube (4 µL buffer per mg gel). The sample was incubated at 50 °C by inverting periodically until the gel slice was completely dissolved. The column (Monarch® DNA Cleanup Column) was inserted into the collection tube, and the sample was loaded onto the column. After spinning for 1 minute, the flow-through was discarded. The column was re-inserted into the collection tube, and 200 µL DNA wash buffer was added. The process was repeated to wash off the unwanted products. 20 µL of DNA elution buffer was added

to the center of the matrix, and the DNA was eluted. The purified gene was then amplified using short primers, Cath-DM-FP-21 and Cath-DM-RP-22 (Table 2.6). The amplified product was visualized using gel electrophoresis.

Table 2.6. The components used for gene amplification using short primers

Constituents	Volume (µL)
GC buffer	2
Cath-DM-FP-21	1.5
Cath-DM-RP-22	1.5
dATP	0.2
dGTP	0.2
dCTP	0.2
dTTP	0.2
DMSO	0.3
Polymerase	0.1
Amplicon	2.5
RNase-free water	1.3
Total reaction volume	10

2.2.8.5. Preparation of DH5α competent cells

E. coli DH5α cells were inoculated in 3 mL LB broth and grown overnight at 37 °C. A secondary culture was prepared from the primary culture by inoculating the cells, followed by incubation at 37 °C until the cells reached the mid-log phase. The bacterial culture was then centrifuged at 3500 rpm (1040 g) for 15 minutes at 4 °C. The supernatant was discarded, and 5 mL of ice-cold 0.1 M $CaCl_2$ was added to the pellet. The cells were suspended in ice-cold $CaCl_2$ for 30 minutes. The suspension was pelleted down at 3500 rpm (1040 g) for 15 minutes, and the supernatant was discarded. The cells were

finally suspended in 2 mL of ice-cold 0.1 M $CaCl_2$ with 15 % glycerol, and 100 µL aliquots were prepared in 1.5 mL micro-centrifuge tubes and stored at -80 °C.

2.2.8.6. Transformation of E. coli DH5α competent cells with pET21a α-synuclein

1 µL of pET21a α-synuclein vector (100 ng/µL) was added to 100 µL competent cells and incubated on ice for around 30 minutes. Heat shock was given to the cells by incubating the mixture at 42 °C for 90 seconds and transferring immediately back to ice. This enables the bacteria to take up the DNA from the external environment. The cells were incubated in ice for 5 minutes. 900 µL of LB broth was added to the cells and incubated at 37 °C for 1 hour. Centrifugation was carried out at 3500 rpm (850 g) for 5 minutes. The supernatant was discarded, and the pellet was dissolved in 100 µL of fresh LB broth and spread-plated on LB agar media containing ampicillin. The plate was incubated overnight at 37 °C. Negative control was also prepared without a vector.

2.2.8.7. Restriction digestion

Restriction digestion was carried out by mixing the pET21a α-synuclein plasmid with restriction enzymes BamHI and NdeI in NEBuffer™ r3.1 (Table 2.7). The reaction mixture was incubated at 37 °C for 4 hours. After digestion, the DNA was analyzed by agarose gel electrophoresis to confirm the digestion.

Table 2.7. The components and their volume used for restriction digestion.

	Tube 1 (µL)	Tube 2 (µL)	Tube 3 (µL)	Tube 4 (µL)	Tube 5 (µL)
Plasmid	1	1	1	1	1
Buffer r3.1	4	4	4	4	4
*Nde*I (20 units/µL)	0	0.4	0	0.4	0.4
*Bam*HI (20 units/µL)	0	0	0.4	0.4	0.4
RNase-free water	15	14.5	14.5	14	14
Total volume	20	20	20	20	20

2.2.9. Expression and purification of cathelicidin-DM

The cathelicidin-DM cloned in pET-23a(+) in *E. coli* DH5α cells was procured from GenScript. The plasmid was isolated, and the *E. coli* BL21(DE3) cells were transformed.

2.2.9.1. Transformation and peptide expression

100 µL of *E. coli* BL21(DE3) competent cells was taken, and 2 µL of plasmid (100 ng/µL) was gently added to it. The tube was kept on ice for 10 minutes. Heat shock was given by placing the tube at 42 °C for 90 seconds. The tube was immediately transferred back to ice. 900 µL of LB broth was added (without antibiotic) and incubated for 2 hours at 37 °C. LB agar plates were prepared with 100 µg/mL of ampicillin. The mixture containing transformed plasmid was plated to Amp^+ LB plates, and the culture was spread over the agar media. The plate was incubated overnight at 37 °C. The overnight grown primary culture of the transformed cells was diluted 100-fold in LB medium (secondary culture). The secondary culture was grown to mid-log phase (OD_{600} = 0.6). The peptide expression was subsequently induced with different conditions, such as different IPTG induction time (early induction, late induction), varying concentrations of IPTG (0-1.4 mM), and different temperatures (25-40 °C). The overnight grown cells were centrifuged at 5000 rpm (2124 g) for 15 min, and the supernatant was separated. The pellet was suspended in the lysis buffer (20 mM Tris-HCl, pH 8.0, 5 mM EDTA, 1 mM PMSF, and 1% Triton X-100). Following 20 min of lysis at room temperature, the lysates were centrifuged at 20 000 *g* for 45 minutes at 4 °C, and the supernatant was collected. The collected fractions were analyzed by SDS-PAGE.

2.2.10. Peptide oxidation and stock preparation for the assays

As the peptide expression did not give the expected results, the reduced peptide was purchased from GL Biochem (Shanghai) Ltd. Peptide purity and mass were confirmed using reversed-phase analytical high-performance liquid chromatography (RP-HPLC) and matrix-assisted laser desorption/ionization time-of-flight (MALDI-TOF) mass spectrometry.

The peptide was oxidized by air oxidation in 10 mM NaOH. The oxidation was confirmed using HPLC by obtaining the chromatogram every 6 hours. The oxidized peptide was then

purified using reversed-phase HPLC with a 10-100% acetonitrile gradient containing 0.1% TFA. The peptide mass was confirmed using MALDI-TOF mass spectrometry on a Bruker, Autoflex Speed MALDI TOF/TOF. The peptide stock solutions of 0.2–0.5 mM was prepared in deionized water, and their concentration was estimated using a molar absorption coefficient of 8370 $M^{-1}cm^{-1}$ at 280 nm. The molar absorption coefficient (Edelhoch, 1967) was calculated using the following equation 2.1.

$$\epsilon_{280} = (5690 \times n_{Trp}) + (1280 \times n_{Tyr}) + (120 \times n_{S-S}) \quad (2.1)$$

ϵ_{280} is the molar absorption coefficient at 280 nm

n_{Trp} is the number of tryptophan residues

n_{Tyr} is the number of tyrosine residues

$n_{s\text{-}s}$ is the number of disulfide bond

2.2.11. Experimental interfacial activity at air/water interface (surface activity)

The adsorption kinetics of cathelicidin-DM on the air-water interface were examined using the KSV NIMA Langmuir-Blodgett instrument. A 13.2 cm^2 circular polytetrafluoroethylene trough was used for the experiment. The trough contains an opening that allows the sample to be injected into the subphase without disturbing the air-water interface. A magnetic stirrer was used to achieve gentle mixing throughout the experiment. Surface pressure was measured using the Wilhelmy method using a platinum plate, which was attached to the Langmuir Blodgett (LB) microbalance. The experiment was carried out at room temperature using phosphate buffered saline. PBS (137 mM NaCl, 2.7 mM KCl, 10 mM Na_2HPO_4, and 1.8 mM KH_2PO_4, pH 7.4) was used as the aqueous subphase. A compression-expansion cycle was recorded to ensure that the PBS was free of surfactants. The experiment was carried out when the change in surface pressure was within ±0.2 mN/m throughout the compression-expansion cycle. The surface pressure of PBS was initially set to zero. The peptide was then gently injected into the subphase. The increase in surface pressure was monitored over time. Once saturation was achieved, higher amounts of peptide were injected into the subphase.

2.2.12. Compression and expansion isotherms of peptide monolayers and Blodgett deposition

Cathelicidin-DM was deposited on the aqueous subphase by carefully introducing the peptide at the air-water interface. The 200 mL of PBS was taken in a rectangular trough with an initial surface area (fully expanded barriers) of 237 cm^2. Prior to adding the peptide, the surface pressure was set to zero. 20 nmoles of the peptide were added and equilibrated for a duration of 30 minutes to facilitate molecular rearrangements. Three compression/expansion cycles were carried out at the barrier speed of 20 cm^2/min. After three compression/expansion cycles, the fourth compression was carried out, and the peptide was deposited on a quartz slide (12 layers on each side) to obtain Blodgett-deposited cathelicidin-DM.

2.2.13. CD Spectra of Blodgett-deposited films

CD spectra were recorded for the monolayer deposited on a quartz slide. After three compression/expansion cycles, the monolayers were compressed (to the fourth compression isotherm, 4^C) to π ~43-45 mN/m (Fig. 2), and then Blodgett-deposited on a quartz slide by withdrawing at a speed of 1 mm/min. The first layer was deposited with a downstroke, while the second layer was deposited with an upstroke. This results in the deposition of 4 monolayers (2 layers on each face of the slide). This process was repeated two more times to achieve a total of 12 monolayers of the peptide on the quartz substrate. The gradual and even withdrawal ensures that the LB film is deposited uniformly. The secondary structure of the peptide in the LB films was examined using far-UV CD spectroscopy. The spectrum was recorded on a Jasco J-1500 CD spectropolarimeter. 48 accumulations were taken to get a good signal-to-noise ratio as the signal obtained from 12 layers deposited on the two faces of the slide was very small. The spectra were recorded at 100 nm/min scan speed, with a data pitch of 0.05 nm and 1 nm bandwidth. PBS dried on the quartz slide was also recorded as a blank for correcting the Blodgett film spectrum. The obtained graph is smoothened using the Savitzky-Golay algorithm with 2^{nd} polynomial order and 400 window points.

2.2.14. AFM/SEM of Blodgett-deposited films

The cathelicidin-DM was deposited on a silicon wafer using the Langmuir-Blodgett instrument. 200 mL of PBS was taken in a clean Teflon trough with an initial surface area of 237 cm^2 (fully expanded barriers). The surface pressure was set to zero, and 20 nmoles of peptide were loaded over the aqueous subphase and allowed to equilibrate for 30 minutes. Three compression/expansion cycles were recorded, and the surface pressure was monitored. The pre-dipped substrate 'silicon wafer' was withdrawn after the 4^{th} compression at the substrate withdrawal rate of 1 mm/min. The monolayer was evenly spread on the substrate, and the AFM image was captured using an Asylum Cypher AFM microscope in non-contact tapping mode at a scan rate of 1 Hz with a silicon probe. Additionally, FESEM (Zeiss, Gemini) imaging was carried out after depositing an LB film on a glass slide. As AFM and FESEM images are recorded after drying, PBS may not be the ideal subphase. Dried buffer components could be mistaken as peptide structures. The compression/expansion and Blodgett deposition, therefore, were also carried out with deionized water as the subphase.

2.2.15. Penetration of cathelicidin-DM into lipid monolayers

Lipid monolayers POPC/CHL (10:1) and POPE/POPG (7:3) were prepared by mixing the lipid stock solutions in desired ratios from their stock solutions in chloroform. The lipid mixtures in chloroform were added gently at the interface. The chloroform evaporates while the lipids form a monolayer at the interface enabling the monolayer interaction studies with peptide. The initial surface pressures of 5, 10, 15, 20, 25 and 30 40 mN/m were obtained by adding lipid solutions dropwise onto the surface. Once the surface pressure stabilized, 10 nmoles of peptide were gently introduced into the subphase, and the subsequent enhancement in surface pressure was monitored over time.

2.2.16. Preparation of small unilamellar vesicles (SUVs)

SUVs were prepared by mixing POPE/POPG in 7:3 molar ratio and POPC/CHL in 10:1 molar ratio. Additionally, for FRET (Förster resonance energy transfer) experiments, the lipids were doped with 2% dansyl-PE. The solvent (chloroform) was evaporated under a nitrogen stream to obtain a thin lipid film. The dried lipid films were kept for overnight desiccation in a vacuum desiccator. The dried films were hydrated for 6 hours in PBS and

vortexed thoroughly to form cloudy suspensions. The suspensions were sonicated using a probe sonicator with a pulse of 2 seconds on and 10 seconds off cycle with 35% amplitude for 15 minutes. The SUVs are ready once the clear suspension is obtained after sonication. The SUVs were centrifuged at 13,000 rpm (11720 g) for 10 minutes to remove the titanium debris. The clear supernatants contain SUVs of size 30-50 nm (<100 nm), which were further used for circular dichroism (CD) spectroscopy and peptide-membrane interaction studies by fluorescence spectroscopy.

2.2.17. Circular dichroism spectroscopy

The far-UV CD spectra were recorded on a Jasco J-1500 CD spectropolarimeter using a 1 mm quartz cuvette. CD spectra were recorded in PBS without and with SUVs: POPE/POPG (7:3) and POPC/CHL (10:1). With SUVs, the spectra were recorded at 1:50 peptide/lipid ratio. The spectra were recorded with a 1 nm bandwidth, a 100 nm/min scan speed, and a 1 s digital integration time. Each spectrum is an average of 8 accumulations. The spectra were solvent-corrected. As the peptide causes aggregation of POPE/POPG vesicles, very large scattering resulted in very noisy spectrum. and the spectrum recorded in POPE/POPG, therefore, was smoothed using the Savitzky-Golay algorithm with a 2^{nd} polynomial order and window points of 250 (Savitzky & Golay, 1964).

2.2.18. Steady-state tryptophan fluorescence studies

The interaction of cathelicidin-DM with SUVs was investigated using steady-state tryptophan fluorescence. POPC/CHL (10:1) and POPE/POPG (7:3) SUVs were prepared in PBS. Tryptophan fluorescence spectra were recorded in PBS in the absence of SUVs and in the presence of SUVs wherein peptide/lipid ratios of 1:50 and 1:100 were used. The fluorescence emission spectra were recorded from 300-500 nm on a Jasco FP-8500 spectrofluorometer. The samples were excited at 295 nm. The excitation and emission slit widths were set at 2.5 nm and 5 nm, respectively. The corrected spectra were obtained by subtracting the corresponding blanks from the peptide samples.

2.2.19. Tryptophan fluorescence quenching of cathelicidin-DM in the presence of lipid vesicles

Tryptophan fluorescence quenching of cathelicidin-DM by acrylamide was estimated in the absence and presence of POPC/CHL and POPE/POPG SUVs. Peptide solutions in PBS were prepared with and without SUVs (peptide: lipid ratio of 1:100). The emission spectra were recorded from 300 nm to 450 nm after exciting the samples at 295 nm. The samples were then titrated with acrylamide (0.02 M to 0.16 M), and the fluorescence spectra were recorded at each quencher concentration. The excitation and emission slit widths were 2.5 and 5 nm, respectively. Fluorescence intensities at the emission maxima of unquenched samples were extracted, and Stern-Volmer plots were obtained by plotting F_0/F with respect to acrylamide concentration using the following equation (2.2),

$$\frac{F_0}{F} = 1 + K_{SV}\,[Q] \qquad (2.2)$$

F_0 is the fluorescence intensity in the absence of a quencher, F is the fluorescence intensity in the presence of a quencher, K_{SV} is the Stern-Volmer constant, and [Q] is the quencher concentration.

2.2.20. FRET with dansyl-PE-doped SUVs

SUVs with 2% dansyl-PE were prepared to validate the binding of the peptide to lipid vesicles using FRET. Tryptophan and dansyl make a FRET pair wherein tryptophan acts as the donor while dansl moiety acts as the acceptor. Cathelicidin-DM was added to the SUVs (50 μM lipid concentration) to achieve a 1:100 peptide/lipid ratio. The samples were excited at 280 nm, and the emission spectra were recorded from 300-600 nm. Excitation and emission slit width were 2.5 nm and 5 nm, respectively. More peptides were added to the 1:100 peptide/lipid sample to achieve 1:50, 1:33, 1:25, and 1:20 ratios, and fluorescence emission spectra were recorded.

2.2.21. Preparation of LUVs

As cathelicidin-DM has been reported as an antimicrobial peptide that is proposed to cause membrane perturbation, we investigated the membrane perturbation using the dye release assay. Calcein, a polar dye that displays self-quenching at high concentrations, was trapped in LUVs. LUVs composed of POPC, POPC/CHL (10:1), POPC/POPS (7:3), and

POPE/POPG (7:3) were prepared using a mini extruder by lipid extrusion method. The protocol for the preparation of liposomes is depicted in Figure 2.1. Briefly, lipids were mixed in the required ratio and dried under nitrogen gas to get a thin layer of lipids. The lipids were further desiccated overnight. A 103 mM of calcein dye was prepared in 10 mM HEPES-buffered saline, pH 7.4. Dissolution of calcein at the desired concentration was achieved by the addition of a small amount of NaOH, after which buffer was added, and the pH was adjusted to 7.4. The desiccated lipid film was hydrated with 10 mM HEPES-buffered saline, pH 7.4, containing 103 mM calcein dye. The lipid suspension was freeze-thawed for 5 cycles and extruded 80 times by passing through polycarbonate filters of 100 nm pore size. The calcein-encapsulating LUVs were separated from free calcein by size exclusion chromatography using a G-75 sephadex column. The fast-migrating pale yellowish band gave dye-loaded liposomes.

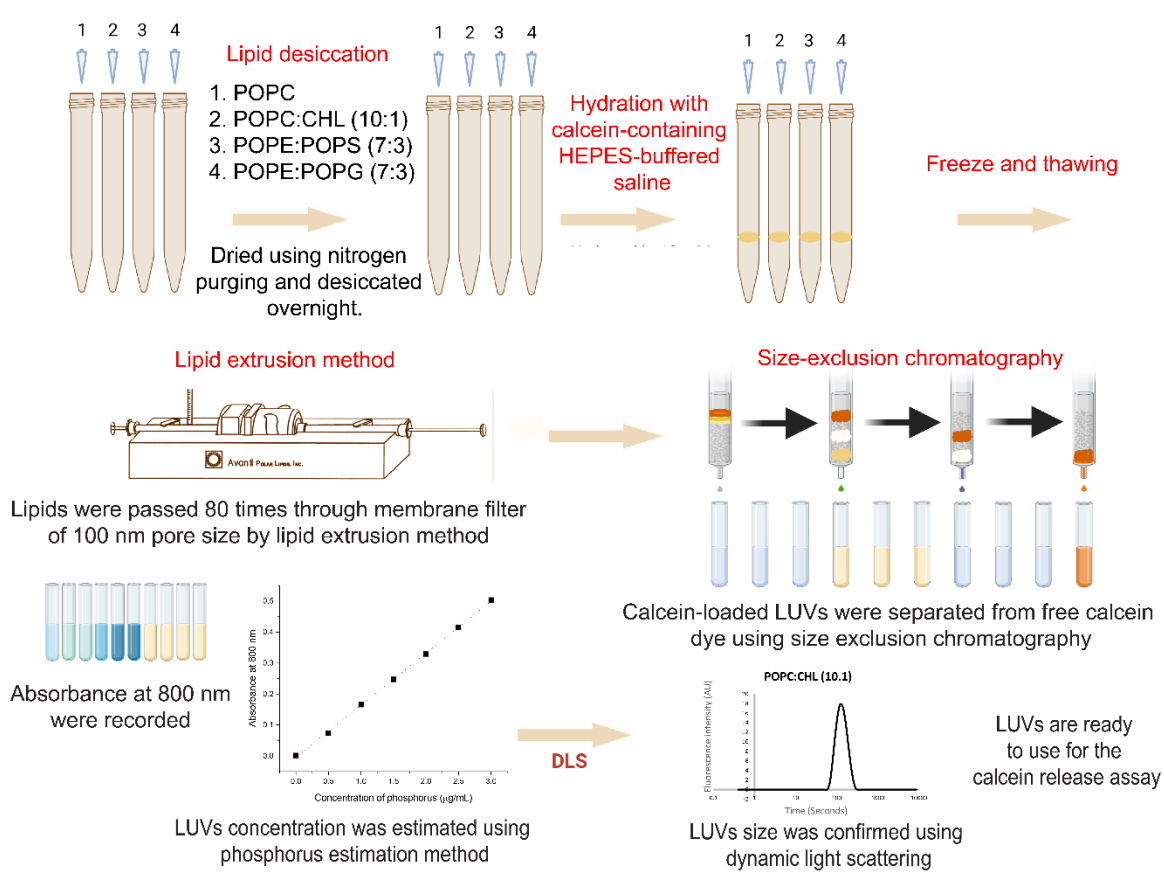

Figure 2.1. The protocol for preparation of liposomes for calcein release assay. The key steps include lipid desiccation, hydration with calcein-containing HEPES-buffered saline, freezing and thawing, lipid extrusion by extruder, size-exclusion chromatography,

concentration determination by the phosphorus assay, and size estimation by dynamic light scattering (DLS).

The collected calcein-loaded LUVs were transferred to clean vials for further characterization. The size of LUVs was ascertained by DLS on a Malvern Zetasizer Nano-ZS instrument at 25 °C using a 173° backscatter configuration. The particle size distribution and polydispersity index (PDI) were determined using instrument's inbuilt software. Phosphorus estimation was used to determine the lipid concentration. The phosphorus content in the phospholipids was determined using the phosphomolybdate method. In this method, phosphate ions react with molybdate ions to form a blue complex, which is then measured using spectrophotometric techniques. Potassium dihydrogen phosphate (KH_2PO_4) was employed as the standard in this assay. KH_2PO_4 was dissolved in deionized water to achieve 50 µg/mL concentrations. Dissolution of Ammonium molybdate was posing challenges. Continuous stirring with intermediate warming was carried out for a long duration to achieve the complete dissolution of Ammonium molybdate. The standards were prepared by diluting the KH_2PO_4 stock solution (concentration ranging from 0 to 3.0 µg/mL). The standard solutions and the LUVs (25 µL and 50 µL each) were taken in different glass test tubes. The samples were then treated with 650 µL of perchloric acid (70%) and incubated in a dry bath at 180 °C for 30 minutes. After cooling down, the samples were diluted with deionized water (3.3 mL). 500 µL each of ammonium molybdate solution (25 mg/mL) and ascorbic acid (100 mg/mL) was subsequently added. The samples were then incubated in a water bath at 75 °C for 10 minutes. A blue-colored complex was formed, and its absorbance was measured spectrophotometrically at 800 nm. The phosphate concentration in the unknown samples was determined by comparing their absorbance readings with those of the standard solution.

2.2.22. Calcein release assay

Calcein release assay was performed on a Jasco FP-8500 spectrofluorometer. The calcein-loaded LUVs were excited at 490 nm, and fluorescence emission intensity was recorded at 520 nm as a function of time. The excitation and emission slit widths were 2.5 and 5 nm, respectively. Cathelicidin-DM was added to calcein-loaded liposomes at the peptide/lipid ratios of 1:70 and 1:200, and the fluorescence were monitored over time. 5

μL of Triton X-100 was added towards the end of the scan to achieve complete lysis of vesicles.

Chapter 3

Molecular dynamics simulations predict interfacial activity and membrane-binding of cathelicidin-DM

3.1. Summary

Molecular dynamics (MD) simulation uses Newtonian physics and statistical mechanics to analyze atomic motions and deduce bulk material properties (Zhou & Liu, 2022). Molecular dynamics simulations have revealed many molecular properties of biological macromolecules and their interactions. Well-developed computational methods are available today to investigate the interfacial properties of biomolecules as well as their binding with lipid bilayers. These simulations provide insights into biological membrane dynamics, essential for understanding physiological processes. Understanding these processes is crucial for biological research, pharmacology, and biotechnology.

The structure of cathelicidin-DM was predicted using QUARK, a protein structure prediction server. The obtained structure closely resembled the one reported by Zhang and coworkers (Shi et al, 2020). Molecular dynamics simulation of the structure resulted in a central antiparallel β-hairpin flanked by polar N and C-terminal unordered stretches. The structure obtained at the end of 200 ns simulation was used for biphasic (water/cyclohexane) simulation. The peptide when kept in the water phase, eventually translocated to the interface. Indicating that the structure obtained after simulation is an amphipathic structure. MD simulations were subsequently carried out with zwitterionic POPC/CHL bilayer and the negatively charged POPE/POPG membranes. Cathelicidin-DM showed transient interaction with POPC/CHL bilayer that caused unfolding of the peptide. Interaction with POPE/POPG bilayer, however, was very stable, as expected from a cationic peptide.

3.2. Results

3.2.1. Modeling and MD simulation of cathelicidin-DM peptide

The structure of cathelicidin-DM was predicted using QUARK (https://zhanggroup.org/QUARK/), an *ab initio* protein structure prediction server (Shi et al, 2020). QUARK was chosen for structure prediction as Zhang and coworkers, the research group that identified cathelicidin-DM, had predicted the structure using the very same structure prediction tool. The structure obtained from QUARK is shown in Figure 3.1A. The structure is very similar to that reported by Zhang and coworkers (Shi et al, 2020). The structure obtained from QUARK was subjected to 200 ns MD simulation in 150 mM NaCl as described in section 2.2.1. The trajectory file was processed and analyzed

using GROMACS' built-in tools. The 200 ns structure had a very similar overall topology to the starting structure (Figure 3.1B). This is also evident from the RMSD plot that displays less than 0.5 nm RMSD throughout the simulation (Figure 3.1C).

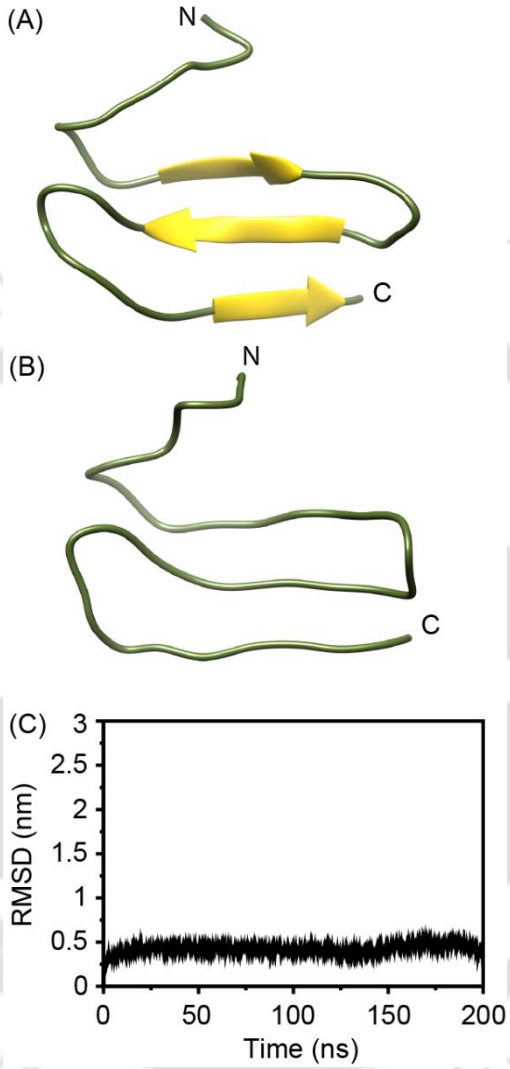

Figure 3.1. (A) Structure of cathelicidin-DM obtained from QUARK server, (B) the 200 ns simulated structure, and (C) RMSD of peptide structure during MD simulation.

3.2.2. Cathelicidin-DM simulation in water/cyclohexane biphasic system

A basic understanding of how a peptide interacts with a membrane interface is that it typically positions its hydrophobic residues within the hydrocarbon region while keeping its hydrophilic residues in the aqueous phase or embedded between polar head groups. This arrangement often leads the peptide to form secondary structures to optimize these interactions. The interfacial activity *i.e.* the propensity to partition to the interface of a

polar/non-polar biphasic system is a useful parameter in predicting the membrane-binding propensity of a molecule (Lee, 2004; Wimley, 2010). To explore the interfacial activity of cathelicidin-DM, an MD simulation was carried out in a biphasic system composed of water and cyclohexane (Aliste & Tieleman, 2005; Cen et al, 2013). The peptide was positioned in the middle of water phase before the start of simulation (Figure 3.2A). During simulation, the peptide eventually moved to the water-cyclohexane interface. Figure 3.2B is the middle structure of the largest cluster. The N-terminal five residues are very polar making this stretch highly hydrophilic. The N-terminal stretch of the peptide at water-cyclohexane interface remains exposed to water phase. The tryptophan residue, that serves as an environment-sensitive intrinsic fluorophore and would be used for experimental studies, was analyzed. The hydrogen-bonding analysis for tryptophan did not form any H-bond, indicating that Trp side chain is shielded from water molecules. The lack of hydrogen bonds implies that Trp side-chain must be interacting with cyclohexane molecule(s). The hydrophobic interaction analysis confirms these interactions. The side chain of Trp in the middle structure was found to interact with four cyclohexane molecules (Figure 3.2C). It is important to note that the peptide undergoes noticeable structural changes at water/cyclohexane interface. The backbone of the middle structure of the largest cluster was overlaid on that of the starting peptide structure (Figure 3.2D). The backbone RMSD between the structures was found to be 0.71 nm.

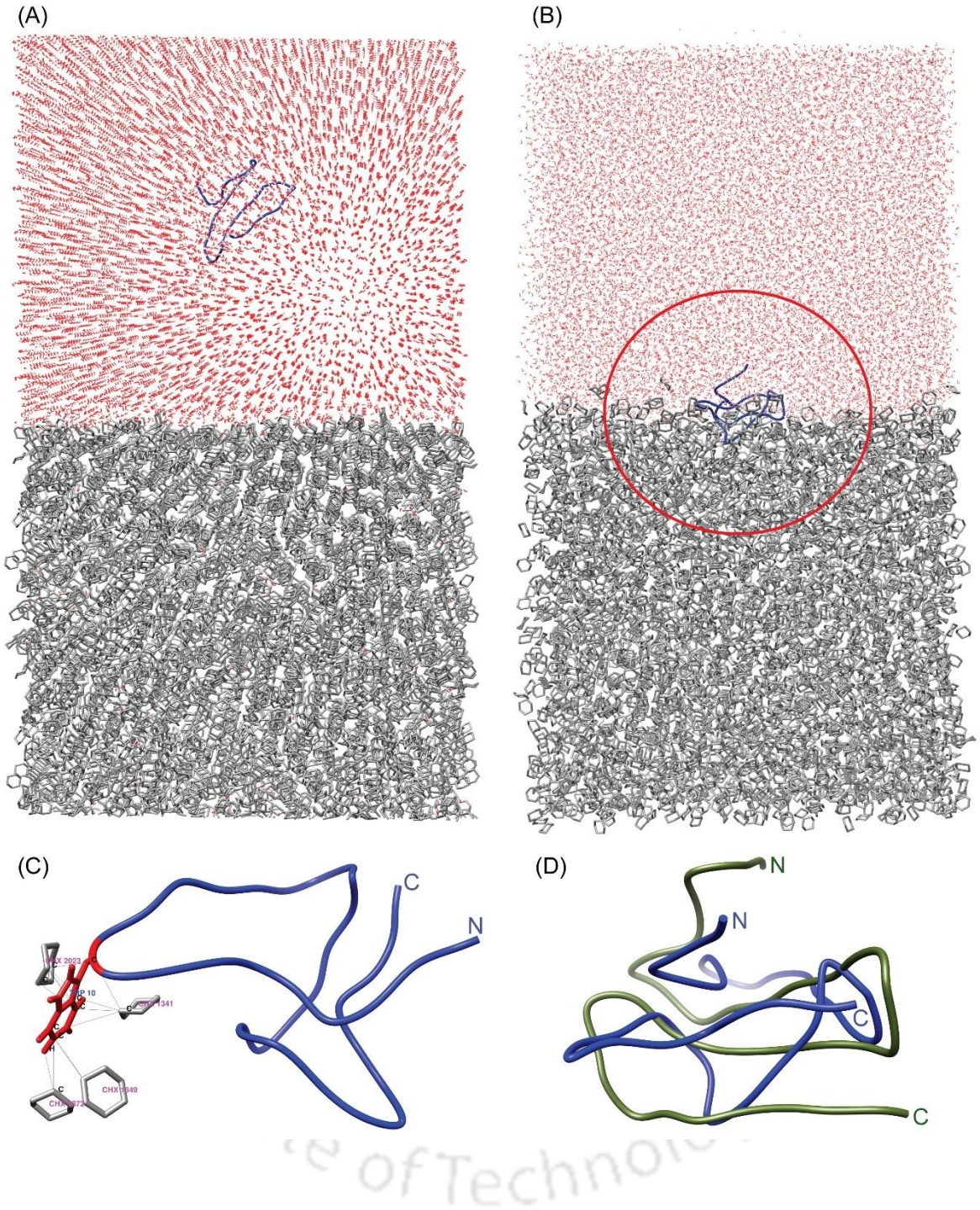

Figure 3.2. MD simulation of cathelicidin-DM in water/cyclohexane at 300 K. (A) The starting system 0 ns, (B) the system with middle structure of the largest cluster of cathelicidin-DM structures at water/cyclohexane interface, (peptide position marked with an oval) (C) the contacts that Trp in the cathelicidin-DM's middle structure makes with cyclohexane molecules, and (D) the 0 ns structure overlaid on the middle structure of the largest peptide cluster.

The RMSD of the peptide was calculated using the MD trajectory. The peptide exhibits a considerable change in conformation, with an RMSD of up to approximately 0.83 nm. (Figure 3.3A). The radius of gyration (Rg) was evaluated to understand how the peptide's mass is distributed about its centre of mass. It provides insights into the molecule's overall compactness and structural configuration. The Rg remains largely constant throughout the simulation, also confirms that the compactness of peptide was maintained (Figure 3.3B). Partial densities of cyclohexane, water, and the peptide were calculated for the initial (0 ns) system and the average over the entire simulation. The density plot also provides insight into the peptide's partitioning into the phases or at the interface. The 0 ns density plot (Figure 3.3C), shows the peptide in the water phase as this is how it was set up before the start of the simulation. However, as the simulation progresses, the peptide moves to the water/cyclohexane interface (Figure 3.3D). The peptide reaches the interface at 53 ns and remained there until the end of the simulation.

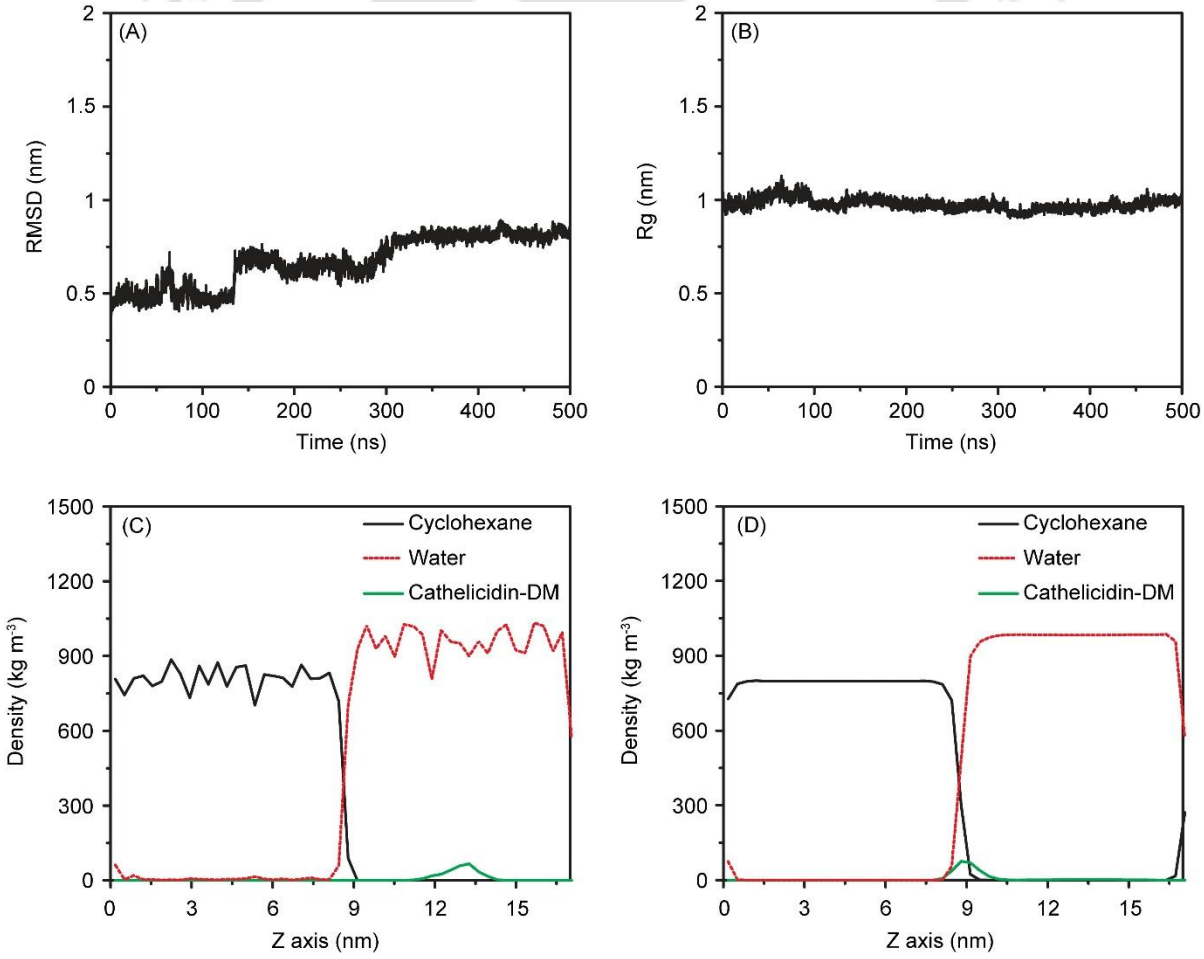

Figure 3.3. (A) The cathelicidin DM RMSD and (B) the Rg plots for MD simulations carried out in water/cyclohexane. (C) The partial densities of the solvents and the peptide at 0 ns

and (D) and the average of the 500 ns simulation, as calculated using gmx density command.

3.2.3. Simulation of membrane-peptide system

The peptide structure obtained after 200 ns simulation was taken to build the membrane-peptide system using CHARMM-GUI as discussed in section 2.2.3.

3.2.3.1. Interaction of cathelicidin-DM with POPC/CHL bilayer

The initial and final structure of the simulation system are shown in Figure 3.4A and B. Analysis of the trajectory revealed that the peptide initially interacts with the POPC/CHL bilayer and then drifts away, indicating that the interaction may not be strong enough to keep the peptide close to the membrane. It is important to note that the peptide's interaction with POPC/CHL bilayer causes unfolding of the peptide, as is evident from the peptide's RMSD (Figure 3.4C) and Rg (Figure 3.4D) data. The RMSD rises to as large as 1.5 nm around 12 ns when the peptide make contact with the lipid bilayer, suggesting large-scale changes in the conformation (Figure 3.4E). After about 20 ns, the peptide moves away from the membrane. After about 50 ns, the RMSD stabilizes to around 0.97 nm with a standard deviation of 0.12 nm. Rg was evaluated to understand how the peptide's mass is distributed about its center of mass. It provides insights into the molecule's overall compactness and structural configuration. The increase in RMSD is accompanied with an increase in Rg, suggesting that initial interaction of the peptide opens up the initially compact structure. The simulation data was subjected to cluster analysis to find out the minimum energy basin. The structure at 288 ns turned out to be the best representative of the largest cluster (Figure 3.4F). This structure was studied to examine the peptide's orientation relative to the lipid membrane. The peptide interacts through its C-terminal stretch, while the tryptophan residue, that precedes the first β-stand in the simulated structure, remains distant from the membrane. The middle structure overlaid is shown in Figure 3.4G. The backbone RMSD between these structures is 0.74 nm. The middle structure interacts with the lipid bilayer through its C-terminal stretch, while the tryptophan residue remains distant from the membrane. These data suggest that the peptide unfolds upon initial contact with the lipid bilayer and exhibits transient interactions with the membrane, typically through its C-terminal.

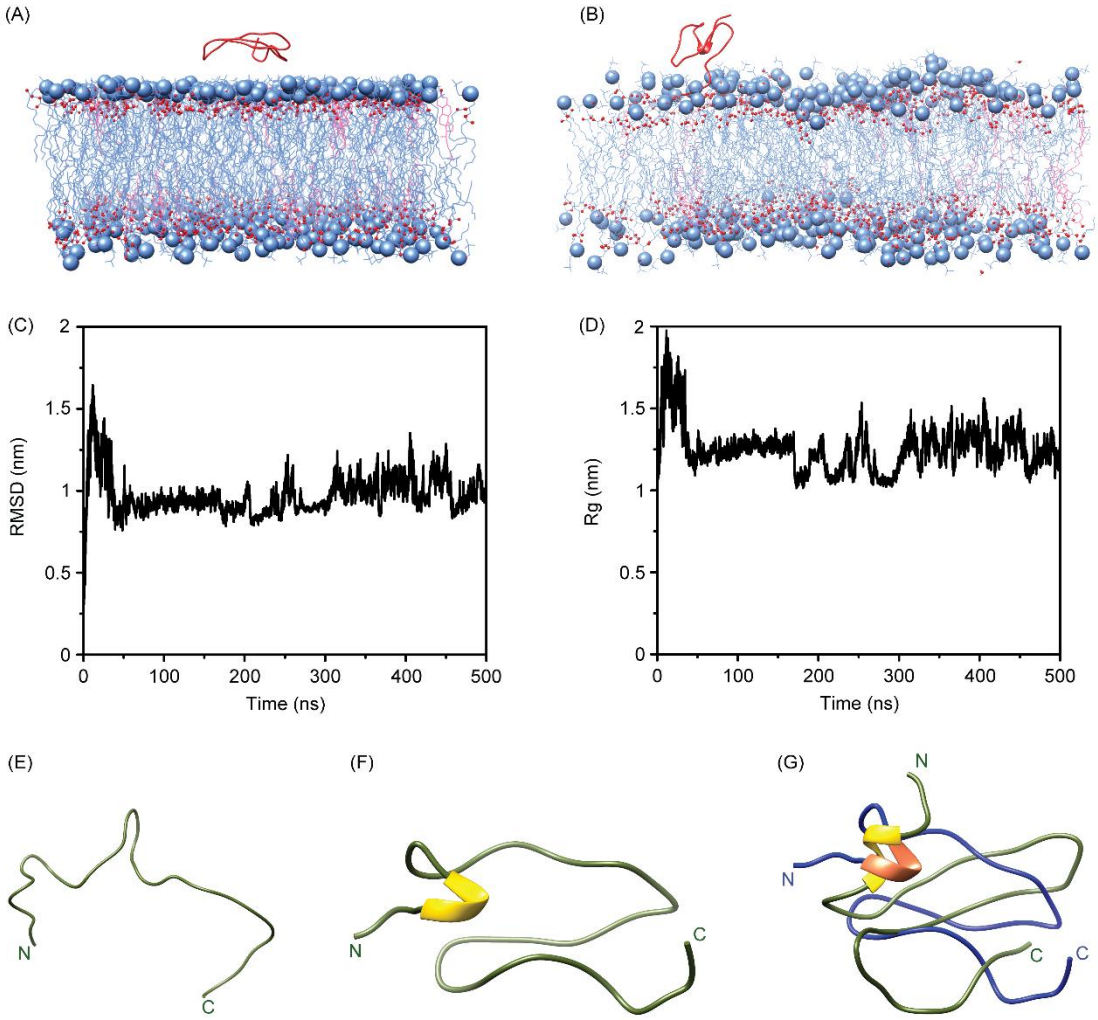

Figure 3.4. Trajectory analysis of the MD simulation for the POPC/CHL system with cathelicidin-DM. (A) The initial and (B) the middle structure of the largest cluster of the system. (C) RMSD and (D) Rg of the peptide. (E) The high RMSD structure observed around 12 ns showing peptide unfolding, (F) the middle structure of the peptides structures' largest cluster, and (G) the 0 ns structure overlaid on the middle structure of the largest peptide cluster.

Partial densities for the membrane, solvent, and peptide were calculated at the beginning and throughout the simulation (Figure 3.5A). The peptide's density indicates that it samples a large depth. It does penetrate deep into the upper leaflet but does not stay there. As cathelicidin-DM interacts with the POPC/CHL bilayer through C-terminal region, the H-bonding between lipid head groups with peptide's C-terminal polar residues as well as the terminal Ala residue (Arg31, Thr33, Tyr34, Arg36, and Ala37) were investigated. The middle structure of the largest cluster obtained for the POPC/CHL

system was used for the analysis. Tyr34, Arg36, and Arg31 were found to participate in hydrogen bonding. The data is shown in (Figure 3.5 B-D)

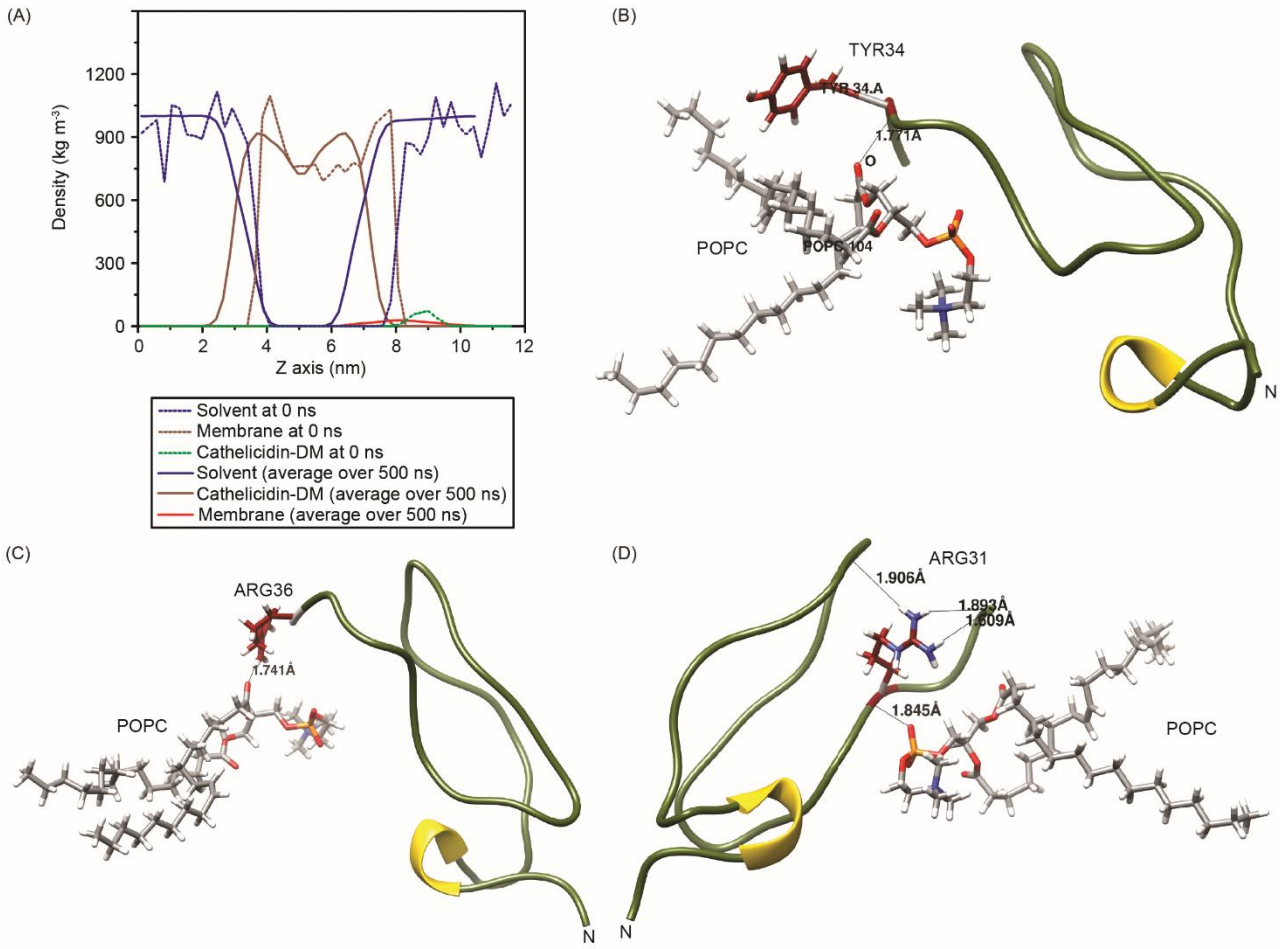

Figure 3.5. (A) The partial density of peptide and POPC/CHL lipid bilayer. (B) Hydrogen-bonding interactions of Tyr34, Arg36, and Arg31.

3.2.3.2. Interaction of cathelicidin-DM with POPE/POPG bilayer

The MD simulation data with the POPE/POPG (7:3) bilayer is shown in Figure 3.6. The initial (0 ns) and the middle structure of the largest cluster of the peptide-membrane system are shown in Figure 3.6A and 3.6B, respectively. Unlike POPC/CHL (10:1) membrane system, where cathelicidin-DM displays unfolding upon initial interaction with the membrane, no dramatic changes in RMSD were observed with POPE/POPG (7:3) bilayer (Figure 3.6C). The peptide displays an average RMSD of 0.64 nm with a standard deviation of 0.08 nm. The middle structure of the peptide structures' largest cluster (329 ns) is shown in Figure 5E. The backbone of the middle structure is overlaid on that of the starting structure (Figure 5F). The backbone RMSD between these structures is 0.48 nm.

The Rg is very stable with an average radius of ~1.15 nm (Figure 3.6D). Unlike as observed for POPC/CHL bilayers, the peptide does not detach from the POPE/POPG bilayer after binding and maintains its orientation throughout the simulation. Cluster analysis of the membrane-peptide system revealed that the peptide interacts primarily through its N-terminal, with the tryptophan residue facing the membrane.

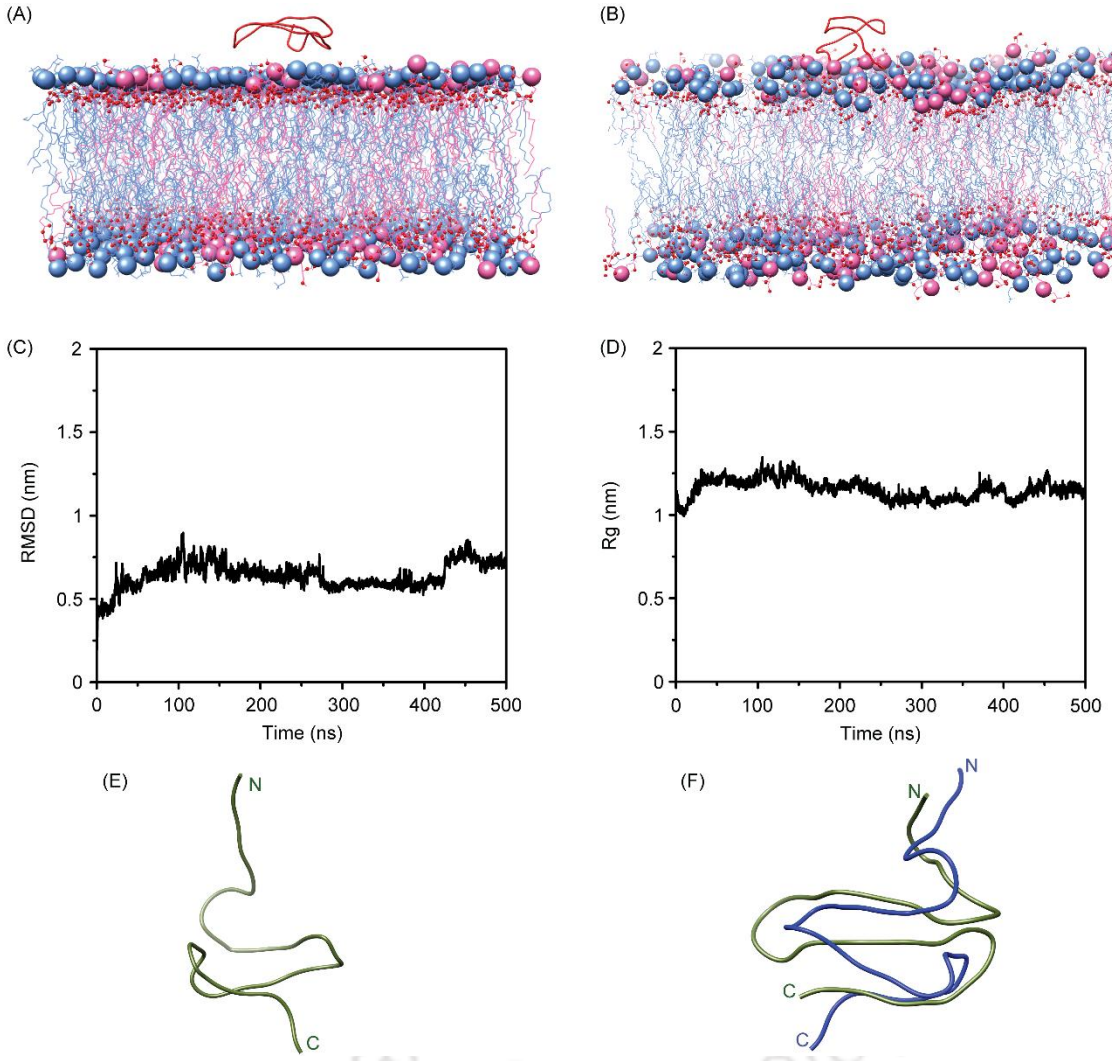

Figure 3.6. Trajectory analysis of the MD simulation for the POPE/POPG system with cathelicidin-DM. (A) The initial and (B) the 200 ns simulated system. (C) RMSD and (D) Rg of the peptide. (E) the middle structure of the largest cluster, and (F) the 0 ns structure overlaid on the middle structure of the largest peptide cluster.

The partial density plot reinforces the stable interaction between POPE/POPG and the cathelicidin-DM peptide, demonstrating that the peptide approaches the membrane during simulation and resides near the membrane interface. The very narrow peptide

density distribution compared to that observed with POPC/CHL suggests that the peptide does not drift away after binding to the bilayer (Figure 3.7).

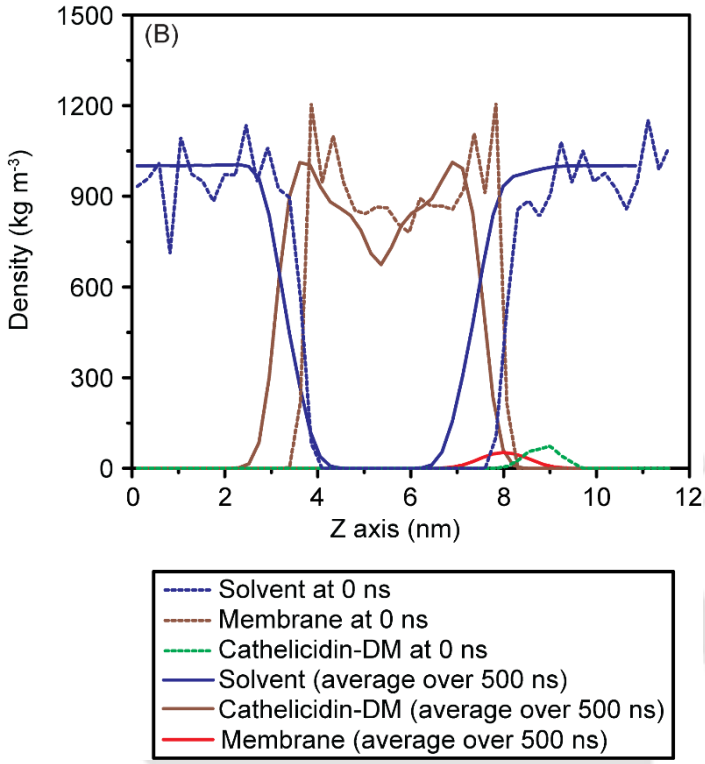

Figure 3.7. The partial density of peptide and POPE/POPG lipid bilayer.

As cathelicidin-DM interacted with POPE/POPG bilayer largely through its N-terminal region, the hydrogen bonding was computed for residues Ser1, Ser2, Arg3, Arg4, Lys5, Lys8, and Trp10. Among these, Ser1 and Arg3 were found to form hydrogen bonds, wherein their side chains acted as H-bond donors to the oxygen atoms in the phosphate groups of the lipids. Ser1 was found to hydrogen bond with the oxygen atoms of POPE (Figure 3.8A), while Arg3 established hydrogen bonds with both POPE and POPG (Figure 3.8B). These interactions align with the observation that cathelicidin-DM exhibits stronger interactions and greater structural stability in the POPE/POPG membrane.

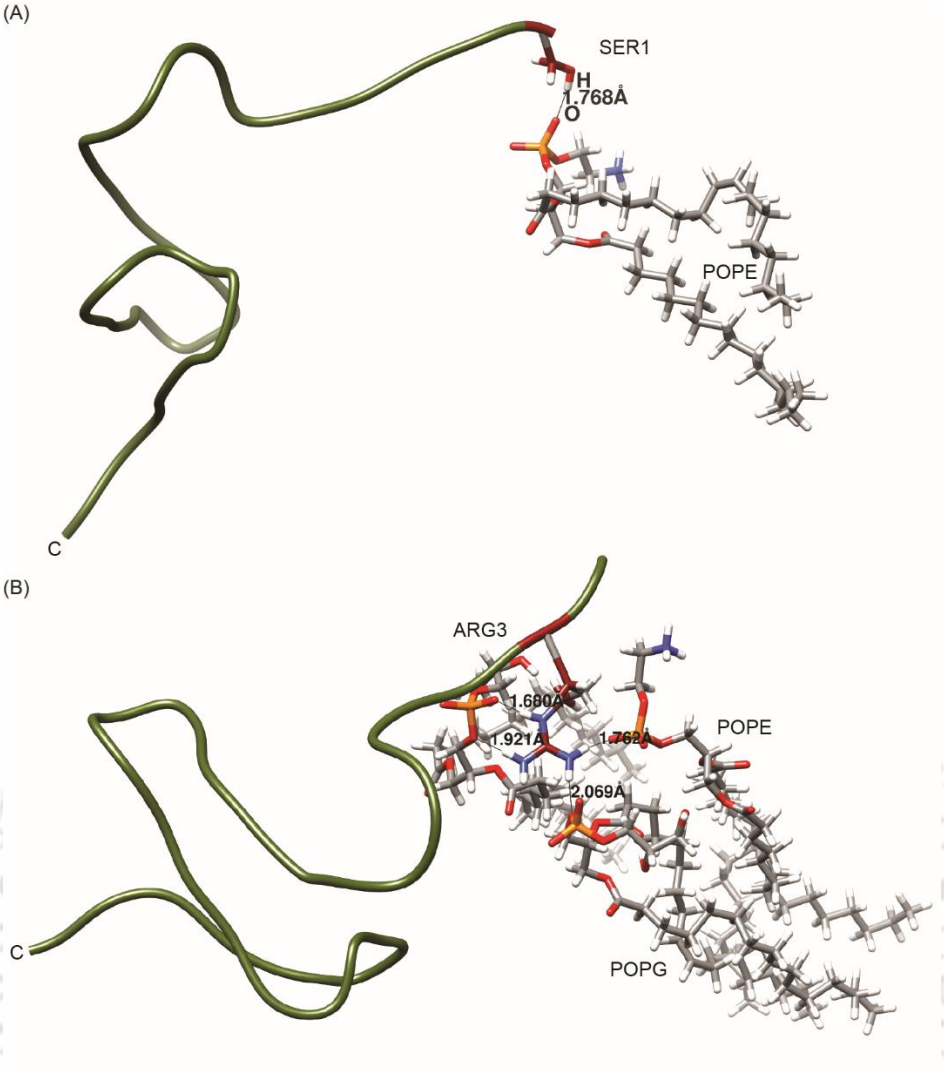

Figure 3.8. Hydrogen-bonding interactions of (A) Ser1 and (B) Arg3 with lipid head groups.

3.3. Conclusion

The modeled structure for cathelicidin-DM was obtained from QUARK server. The obtained structure was simulated for 200 ns that resulted in a similar topology to the starting structure and remained stable throughout the simulation. MD simulation in water/cyclohexane biphasic system shows that the peptide partitions to the interface of the two solvents without any significant conformational change, clearly indicating that the folded structure is an amphipathic structure. MD simulation with POPC/CHL revealed that binding of the peptide with POPC/CHL membrane causes unfolding of the peptide. The partial density plot suggests that the peptide transiently penetrates deep in the membrane. The interaction with the bilayer is mediated largely through its C-terminal

region, wherein Trp10 remains solvent-exposed. Interaction with POPE/POPG lipid bilayer, on the other hand, is mediated via the N-terminal region of the peptide. As the N-terminal region is highly polar and rich in cationic residues, the peptide resides in the interfacial region of the lipid bilayer. The Trp side-chain is oriented towards the lipid bilayer.

Chapter 4

Cathelicidin-DM is a surface-active peptide that preferentially penetrates the negatively charged lipid monolayers

4.1. Summary

The amphipathicity of peptides enables them to be soluble in an aqueous medium such as an extracellular matrix as well as to easily diffuse to non-polar/polar interfaces. Amphipathicity imparts to the peptides a tendency to self-associate, that affects their uptake and action. It can either improve uptake and activity or compromise them by causing aggregation and reducing available hydrophobic patches for membrane interaction (Edwards et al, 2016; Hollmann et al, 2016). Cationic peptides interact preferentially with the acidic lipids, which are abundant in bacterial membrane systems. Therefore, the cell specificity of membrane-targeting AMPs is attributed to the presence of different acidic phospholipids. Antimicrobial activity of AMPs depends not only on specific amino acid sequences and structures but also on the amino acid composition and their physical and chemical properties. Interfacial activity, *i.e.*, the propensity to partition at the interface of two immiscible phases, is important for the AMP membranolytic activity. The peptides bind to microbial membranes, partition into the membrane-water interface, and disrupt the lipid packing and organization. The interaction and the extent of perturbation depend on the peptide's overall hydrophobicity, charge, and amphipathic nature rather than its precise sequence or structural conformation. Hydrophobic residues facilitate deep membrane interaction by engaging with the lipid core, while positively charged residues enhance binding to negatively charged microbial surfaces. This understanding suggests that optimizing these properties, rather than focusing strictly on traditional sequence motifs, could lead to the development of more potent antimicrobial agents.

Interface refers to the boundary separating the two immiscible phases, which are in equilibrium, for example, liquid-liquid phase, liquid-gaseous phase, liquid-solid phase, and solid-solid phase. In this study, I investigated the interfacial activity of peptide cathelicidin-DM at the liquid-gaseous interface. The interface, typically the two-molecule thick region, is where the transition in composition and properties between two bulk phases occurs. Within this narrow zone, the characteristics of the materials differ from those in the respective bulk phases. (McBain et al, 1939). The property of the interface changes with changes in any of the two phases and commonly occurs when a solute is added to the liquid phase. Biosurfactants, such as polymers, proteins, and peptides, reduce surface tension by adsorbing at interfaces between different phases. This

adsorption leads to a decrease in surface tension, and this decrease in surface tension is referred to as surface pressure.

The monolayer technique has been used to study the interfacial properties of AMPs as well as their interaction with the lipid monolayers (Maget-Dana, 1999). The adsorption of peptide to the air-water interface is studied by monitoring the increase in surface pressure after adding the peptide in the aqueous subphase. Different factors, that include peptide length, sequence, net charge, three-dimensional structure, flexibility, and folding propensity at the interface, determine the interfacial activity of peptides. For example, melittin has a random-coiled structure as a monomer, while in its tetrameric form, it adopts an alpha-helical structure (Tatham et al, 1983). The tetramers are composed of α-helical rods with a bent structure, where the hydrophobic core is shielded and the hydrophilic side chains are exposed. This arrangement makes the tetramers less surface-active compared to the monomers. Upon encountering the interface, the hydrophobic core of melittin integrates into the apolar region of the bilayer, making the helical axis parallel to the plane of the bilayer while revealing the hydrophilic region to the aqueous phase (Terwilliger et al, 1982). This integration, which facilitates the change in the surface area of the lipid bilayer, is a vital factor for membrane perturbation and lytic activity of the peptide, arising from peptide's surface activity (Terwilliger et al, 1982). Defensins, another class of AMPs pivotal in immune defense, also adopt dimeric structures. Defensin dimerization, such as that of human α-defensin HNP-3, enables the peptide to effectively interact with microbial membranes (Hill et al, 1991). HNP-1 has been reported in the literature to form dimers and higher order aggregates (Zhang et al, 1992; Suresh & Verma, 2006). The dimeric state often assumes specific structural conformations, facilitating their insertion into the lipid bilayer. This integration disrupts the membrane's integrity, resulting in heightened permeability, leakage of cellular contents, and eventual cell death. It is important to understand that while dimerization is pivotal for the antimicrobial activity of these defensins, not all defensins exhibit dimer formation; their oligomerization state can vary depending on the defensin type and environmental conditions.

Molecular flexibility is an important parameter affecting surface activity. The flexibility allows the polymer to fold/unfold at the interface to minimize the energy. Protein unfolding at the air/water interface is a well-documented problem in cryo-electron

microscopic sample preparation (Noble et al, 2018; Brillault & Landsberg, 2020). Alpha-synuclein, on the other hand, is an intrinsically disordered protein that folds into an amphipathic α-helical conformation at the air/water interface (Mohapatra & Chaudhary, 2021; Mohapatra et al, 2023). If αS were a folded protein with a rigid structure, the surface activity would be determined by the hydrophobic moment of the folded structure. Flexibility, therefore, enables a polymer to optimize its amphipathicity at the interface. The interfacial activity of cathelicidin-DM has not yet been studied. In this chapter, I have investigated the surface activity of cathelicidin-DM, its compression/expansion isotherms, and the Blodgett-deposited peptide layers using CD spectroscopy and microscopy. Subsequently, the lipid penetration propensity has been investigated using monolayers with lipid compositions mimicking mammalian and bacterial membranes.

4.2. Results

4.2.1. Peptide synthesis

Cathelicidin-DM was synthesized using Fmoc chemistry as described in section 2.2.7. The synthesized peptide was characterized by reversed-phase HPLC and MALDI-TOF mass spectrometry. However, the synthesis resulted in a highly impure peptide wherein a cluster of multiple peaks was observed. The synthesis was attempted thrice with minor variations, but no significant improvement was observed. The analytical HPLC chromatogram of the best synthesis is shown in Figure 4.1A. Even though the peaks are poorly resolved, the fractions were collected in different vials and analyzed using MALDI-TOF mass spectrometry. The calculated monoisotopic mass of cathelicidin-DM is 4163.27 Da. MALDI-TOF mass spectrum of the fraction collected around the 26.2-minute peak showed an m/z of 4165.62, among other values (Figure 4.1B). The mass spectrometry data suggests that the late eluting part of the peptide contains the desired peptide alongside some impurities. As purification from such a poor-quality synthesis would yield very small amounts of peptides, a bacterial expression route was explored.

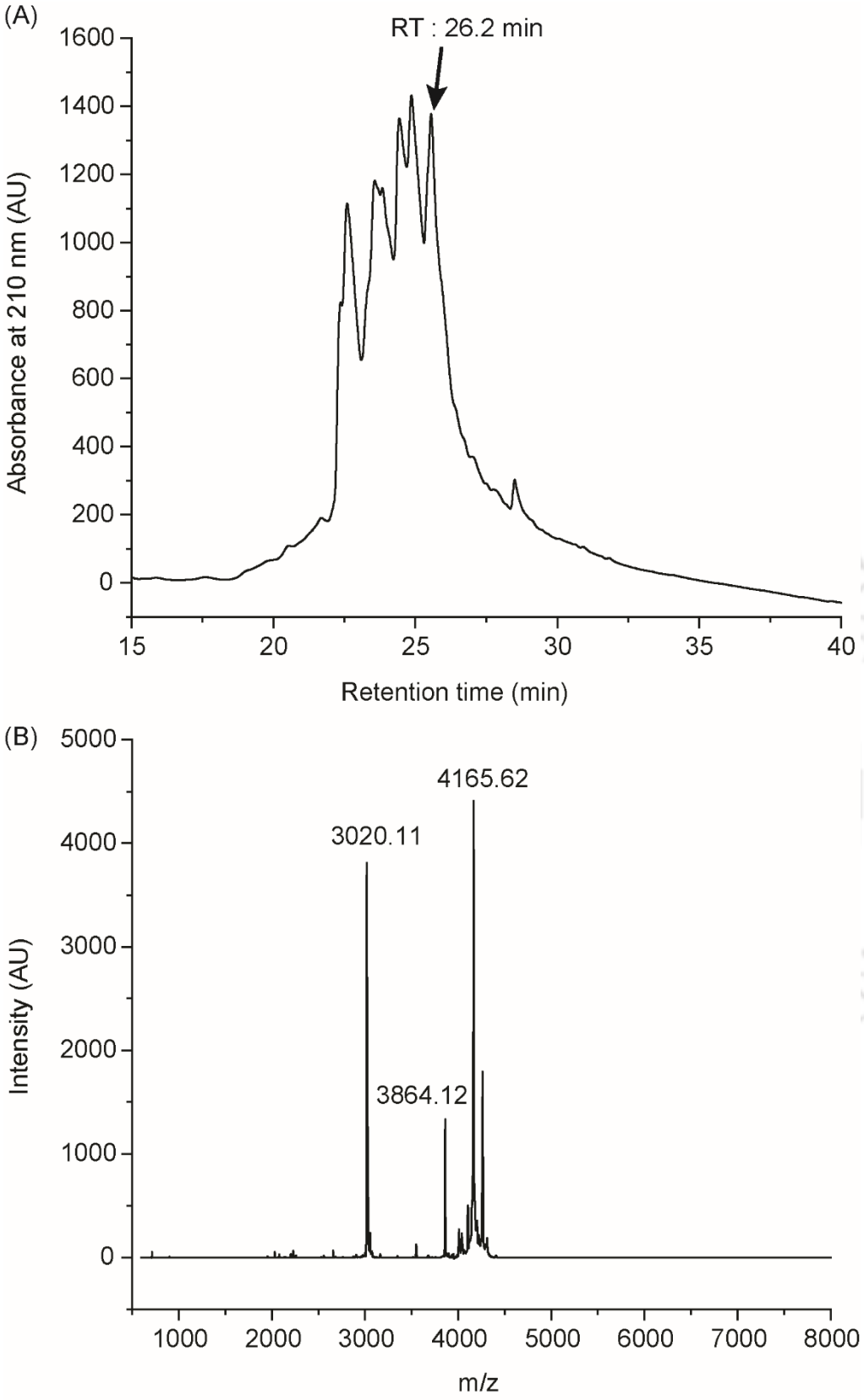

Figure 4.1. The HPLC chromatogram (A) and the mass spectrum (B) of crude cathelicidin-DM peptide.

4.2.2. Cloning, expression, and purification of cathelicidin-DM

Due to a lower purity and yield obtained through multiple attempts at chemical synthesis, I switched to bacterial expression of the peptide. Recombinant DNA technology has significantly improved peptide yields, offering advantages over traditional synthesis methods in terms of yield and scalability. The gene encoding the desired peptide is synthesized using the primer extension method and inserted into an expression vector, which is then introduced into a host organism to produce the peptide of interest. This approach enables high-yield peptide production with improved purity compared to conventional chemical synthesis approaches. The nucleotide sequence of the gene was obtained from tblastn (https://blast.ncbi.nlm.nih.gov/Blast.cgi) by reverse-translation of the peptide sequence (Figure 4.2). The procedures used are described in section 2.2.8.

Duttaphrynus melanostictus cathelicidin-DM mRNA, complete cds

atgaggagctggaggctgtctctgctgctggtctctgcagtcacattacacggctgtctctctgaccctgcagagcctgaggtccaagatggaa
gatctatagaagatgtcatcgacctctacaaccagagggaggggtcacatacttatataaatccctggaccagctgccccctgttccaatgg
aggaggatgagaatccgaacagaagaggctttatcatgaaagagaccgtgtgcctcaaatccgagaatcctgatttaacccagtgtgatttc
aagcctgacggagatgtgaagatctgttctctggatttgggggatgaggatcctgaggatatcatgtgcttcagtctgaacaaggaggtccgta
tgaagcggtccagcagaaggaaaccatgcaaggggtggctctgcaagctgaagctaagaggaggttatactcttatcggcagtgctacaa
acctaaatagacctacctacgtgagggcataa

Complete Protein sequence

MRSWRLSLLLVSAVTLHGCLSDPAEPEVQDGRSIEDVIDLYNQREGVTYLYKSLDQLPPVPMEEDE
NPNRRGFIMKETVCLKSENPDLTQCDFKPDGDVKICSLDLGDEDPEDIMCFSLNKEVRMKRSSRR
KPCKGWLCKLKLRGGYTLIGSATNLNRPTYVRA

Figure 4.2. Nucleotide and amino acid sequences of cathelicidin-DM pre-protein. The amino acid sequence highlighted in red is that of the cathelicidin-DM peptide.

The cathelicidin-DM gene was synthesized using the primer extension method with large primers, as described in section 2.2.8.4. The optimum annealing temperature in gradient PCR was observed to be 70 °C (Figure 4.3A). The gene synthesized was amplified using short primers at the optimized temperature, which also happened to be 70 °C (Figure 4.3B). The pET21a-α-synuclein plasmid was treated with restriction enzymes *Nde*I and *Bam*HI separately as well as together. The plasmid treated with both enzymes did not give the expected product when analyzed by gel electrophoresis (Figure 4.3C). Therefore, no double digestion occurred in the sample.

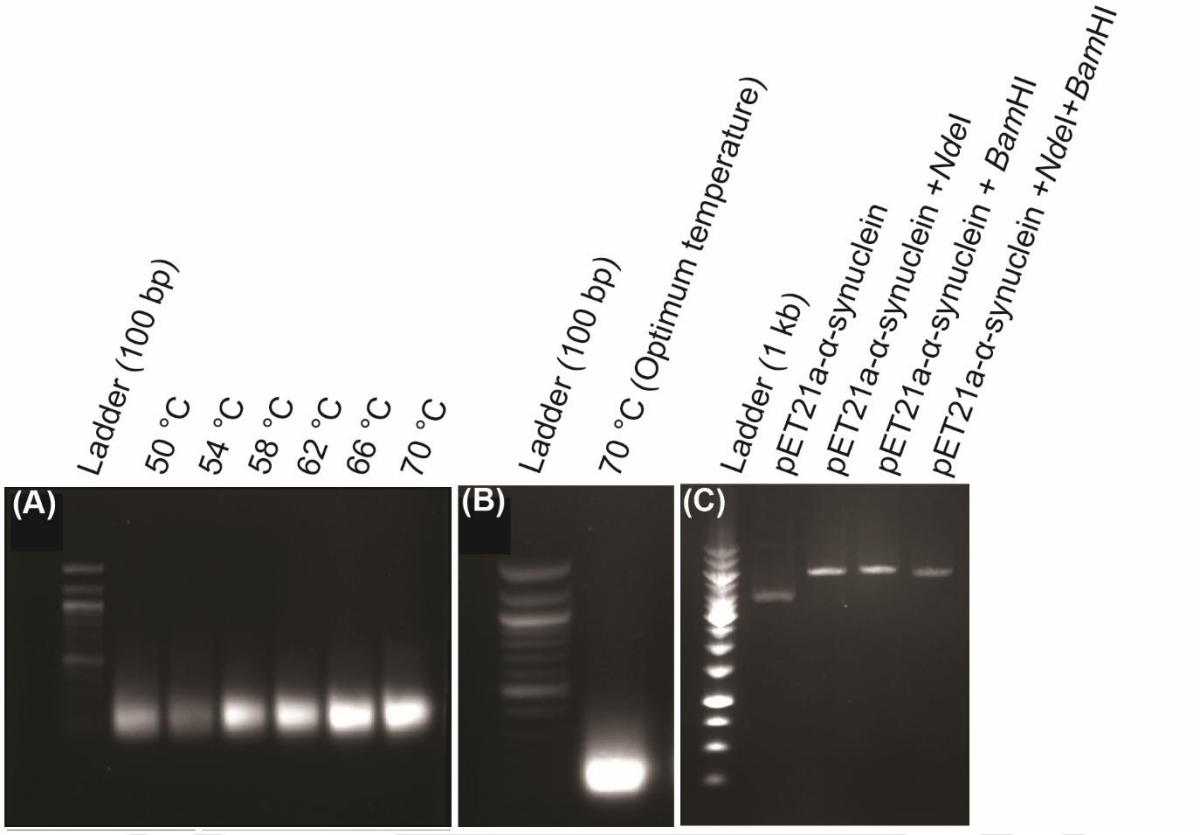

Figure 4.3. (A) Agarose gel electrophoresis of gradient PCR with annealing temperature ranging from 50–70 °C with larger primers. (B) PCR amplification of the gene obtained through primer extension. (C) The gel image of restriction digestion of pET21a-α-synuclein using *Nde*I and *Bam*HI.

4.2.3. Cathelicidin-DM expression

The cathelicidin-DM gene cloned in pET23a(+) plasmid, cloned between *Nde*I and *Bam*HI restriction sites, was procured from GenScript. The peptide expression was attempted in *E. coli* BL21 cells. The cells were transformed as described in section 2.2.9.1. The bacterial colonies were observed in the antibiotic-containing LB agar plates, indicating successful transformation (Figure 4.4A). The secondary culture was obtained in ampicillin-containing LB broth using primary culture inoculum. The cathelicidin-DM expression was induced in the secondary culture. Following centrifugation, the supernatants were collected while the cell pellets were lysed as described in section 2.2.9.1. The supernatants and the cell lysates of induced and uninduced secondary cultures were analyzed by SDS-PAGE (Figure 4.4B). Other parameters varied were the concentration of IPTG at 37 °C (Figure 4.4D), induction temperature at 1 mM IPTG (Figure 4.4E), and

induction time (Figure 4.4C) as described in section 2.2.9.1. Multiple optimization attempts were carried out to obtain the gene of interest. The SDS-PAGE was performed using 15 % polyacrylamide gel. Representative gel images are shown below (Figure 4.4).

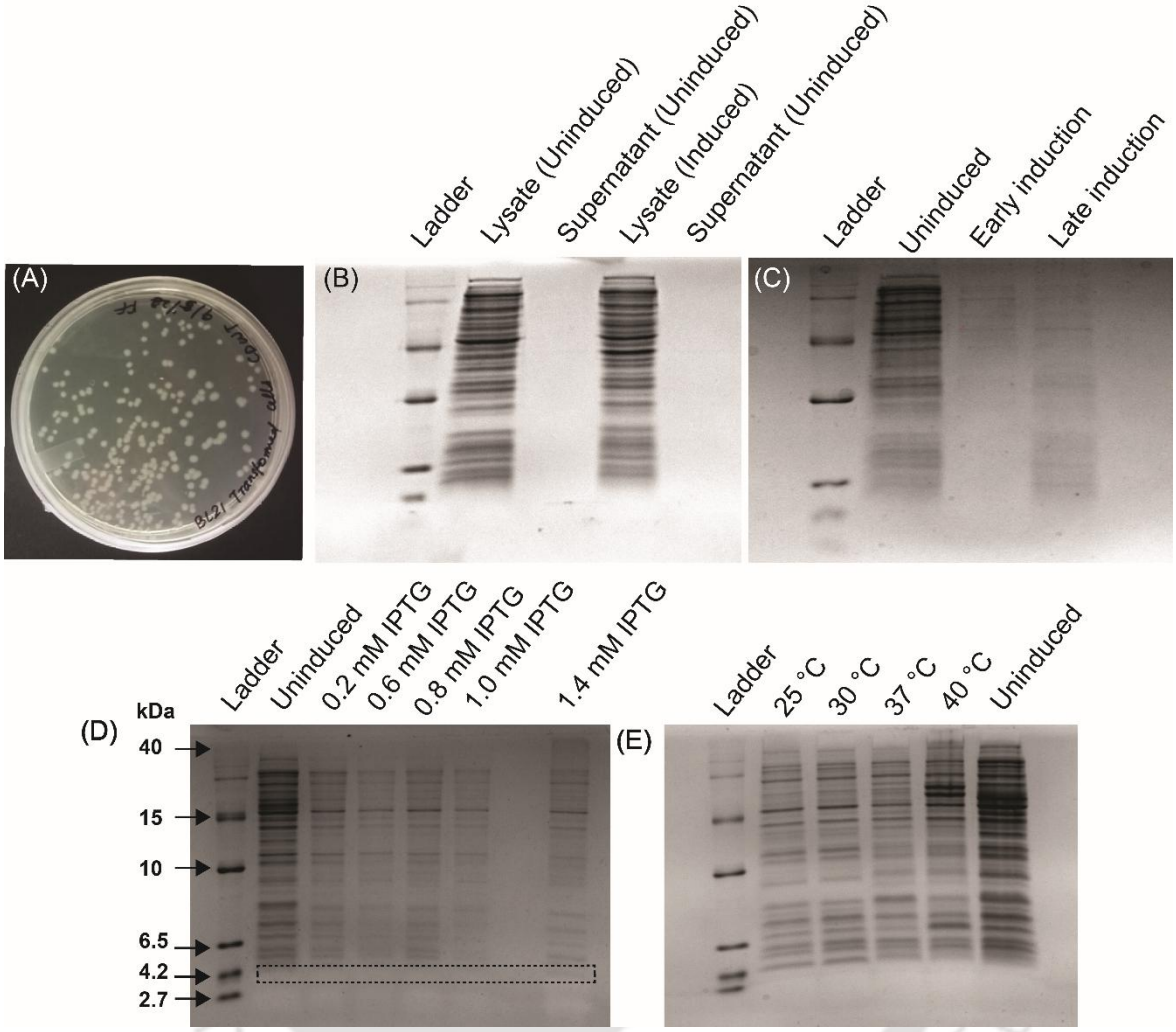

Figure 4.4. (A) The agar plate with transformed colonies with the gene for cathelicidin-DM, Gel electrophoresis images of different optimization conditions used for the expression of the peptide. (B) supernatant and cell lysate with and without IPTG induction at 37 °C, (C) different induction time with 1mM IPTG concentration at 37 °C, (D) different concentrations of IPTG (6 h induction time, 37 °C), and (E) at different induction temperatures (4 h, 1 mM IPTG). The molecular weights of the protein ladder components are labelled in panel D, and the expected peptide position is indicated by a dotted box.

A low-range (3-40 kDa) protein ladder was used to identify the mass of the expressed peptide. No band corresponding to the size of cathelicidin-DM was observed for any sample, indicating no observable expression. One possible reason could be the

antimicrobial activity of the peptide. Short peptides are anyhow difficult to express and are better expressed when fused to a longer host protein sequence.

4.2.4. Peptide oxidation and stock preparation for the assays

Cathelicidin-DM was obtained from GL Biochem (Shanghai) Ltd in its reduced form (as amorphous powder). The peptide was oxidized, as described in section 2.2.10. The oxidation was monitored using HPLC by taking out aliquots every 6 h (Figure 4.5). The HPLC chromatograms resulted in two peaks that correspond to reduced and oxidized forms. With time, the intensity of the oxidized peak increased.

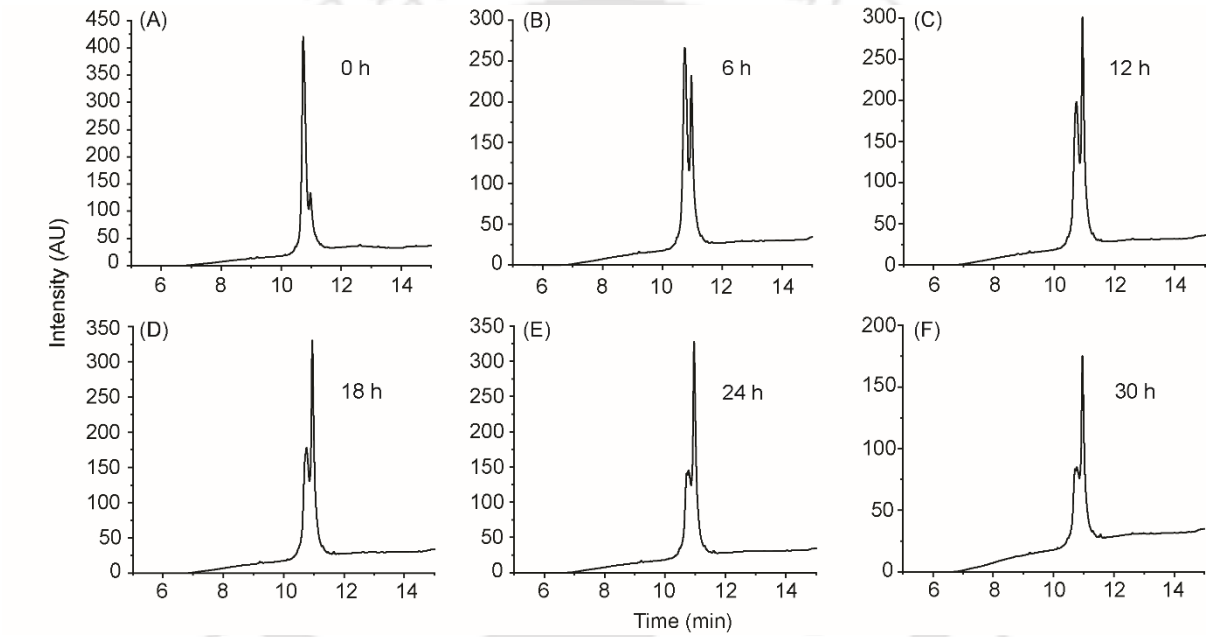

Figure 4.5. Chromatograms depicting the cathelicidin-DM oxidation at various time intervals: 0 h (A), 6 h (B), 12 h (C), 18 h (D), 24 h (E), and 30 h (F).

The average mass and the monoisotopic mass of the oxidized peptide obtained from the peptide calculator (https://www.peptidesynthetics.co.uk/tools/) were 4163.9 Da and 4161.2 Da, respectively, whereas reduced peptide showed the average mass and monoisotopic mass of 4165.9 Da and 4163.2 Da, respectively. The observed mass of reduced and oxidized cathelicidin-DM from MALDI-TOF mass spectrometry was 4168.2 Da and 4166.3 Da, respectively (Figure 4.6).

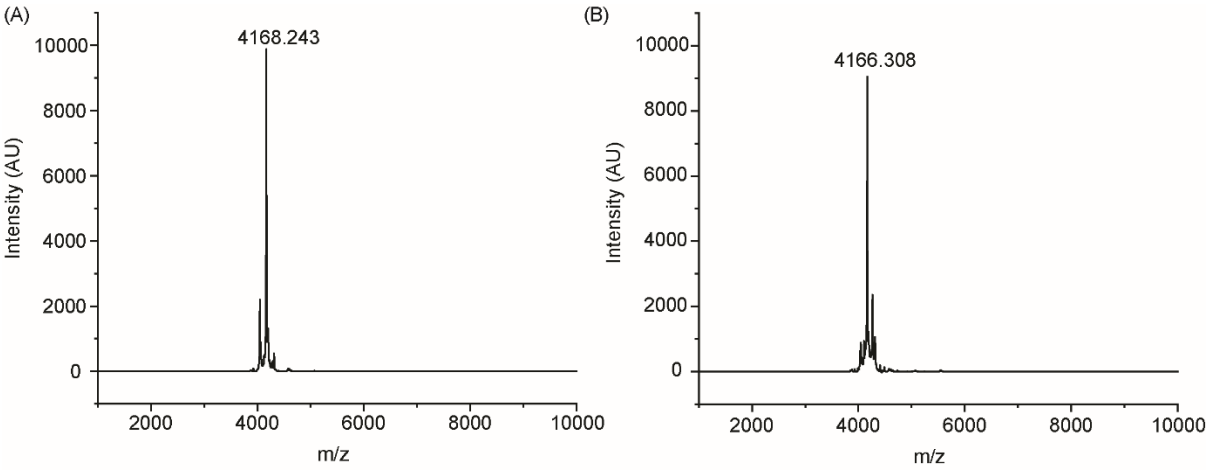

Figure 4.6. The MALDI-TOF mass spectra of the reduced (A) and oxidized (B) cathelicidin-DM.

The oxidized peptide was purified by RP-HPLC (Figure 4.7) and analyzed by MALDI-TOF mass spectrometry on a Bruker, Autoflex Speed MALDI TOF/TOF (Figure 4.7 inset). The stock solution of purified peptide was prepared, and the concentration was estimated as described in section 2.2.10.

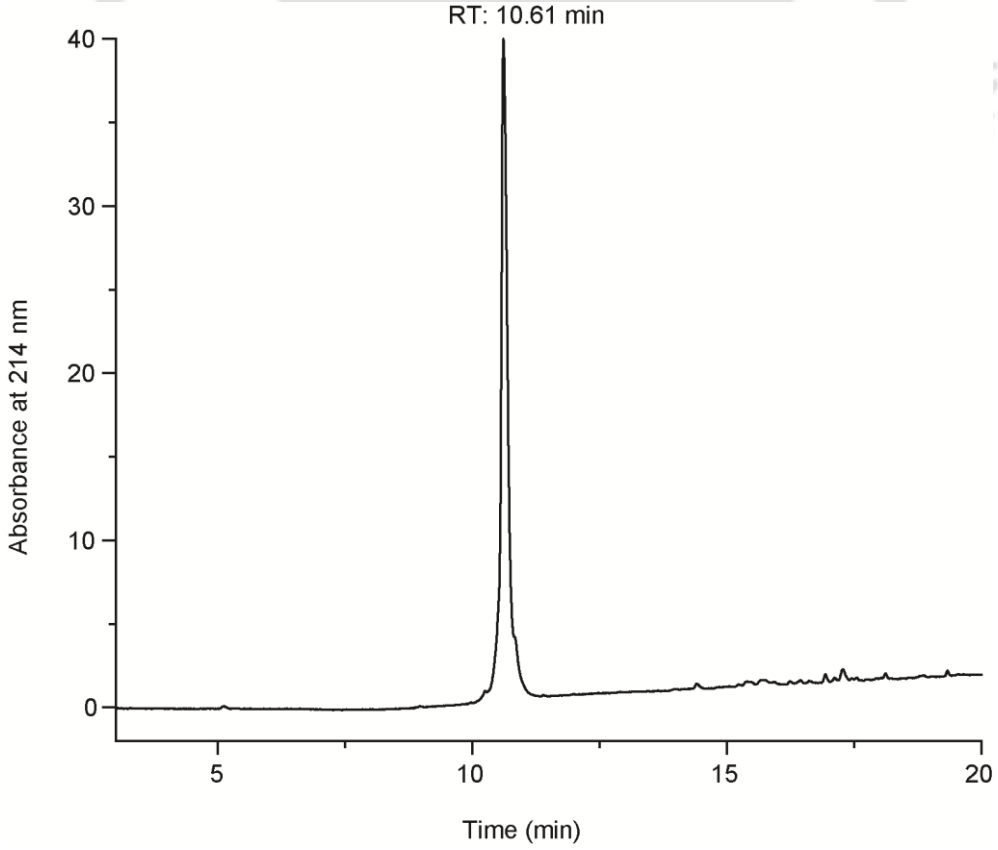

Figure 4.7. The HPLC chromatogram of the oxidized cathelicidin-DM.

4.2.5. Surface activity of cathelicidin-DM

The adsorption of cathelicidin-DM at the air-PBS interface was investigated by measuring the change in surface pressure after introducing the peptide into the subphase. 10 mL PBS was taken as the subphase in a customized PTFE trough, as depicted in Figure 4.8A. The surface pressure was then allowed to stabilize and set to zero. Cathelicidin-DM was added through an orifice without disturbing the air-PBS interface (Figure 4.8A). There was no significant rise in surface pressure when 0.1 nmole of the peptide was added into the subphase (Figure 4.8B). Little enhancement was observed after the subsequent addition of 0.9 nmole. Further addition of 4 nmoles of peptide caused a rapid increase in surface pressure which was around 10-11 mN/m. Cathelicidin-DM showed enhancement in surface pressure with 10 nmoles of peptide. The final concentration was calculated by converting the number of moles in total volume of 10 mL, and the peptide concentration was found to be 1 µM.

- *Convert nmoles to micromoles (µmoles):*

  $10\ \text{nmoles} = 10 \times 10^{-3}\ \mu\text{moles} = 0.01\ \mu\text{moles}$

- *Calculate the concentration in µM:*

Concentration (in µM) is estimated by the formula,

$$\text{Concentration}\ (\mu\text{M}) = \frac{\text{Amount}\ (\mu\text{moles})}{\text{Total volume}\ (\text{L})}$$

Converting 10 mL to liters: 10 mL = 0.01 L

$$\text{Concentration}\ (\mu\text{M}) = \frac{0.01\ (\mu\text{moles})}{0.01\ (\text{L})} = 1\ \mu\text{M}$$

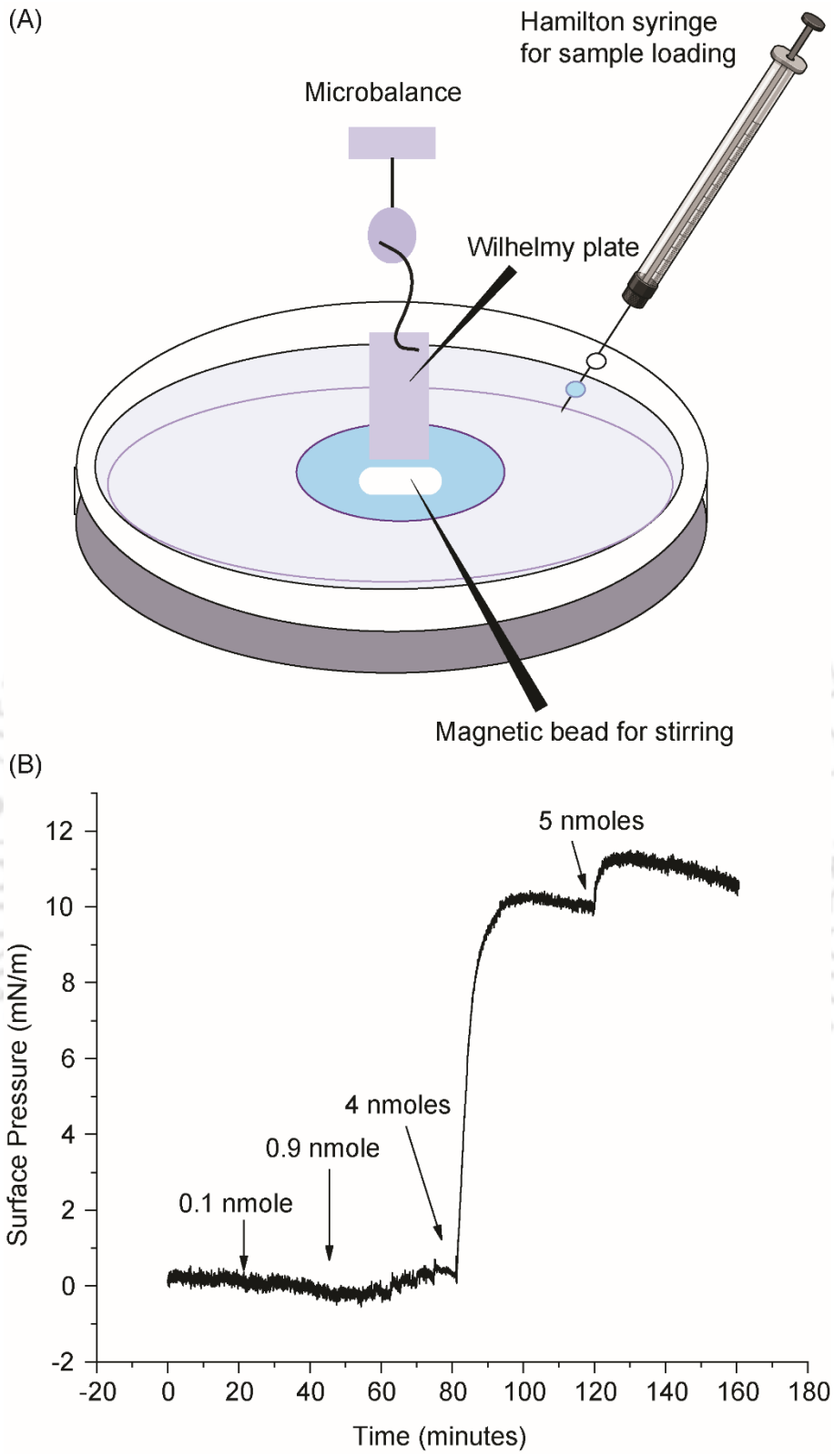

Figure 4.8. The surface activity of the cathelicidin-DM peptide. (A) Customized trough used for the surface activity measurement. (B) The adsorption kinetics at the air-water interface: change in the surface pressure with respect to time after peptide addition to the subphase.

4.2.6. Compression-expansion isotherms of peptide monolayers

Compression-expansion isotherms of cathelicidin-DM monolayers were also investigated. A rectangular PTFE trough with PTFE barriers was used. The initial surface area of fully expanded barriers was 237 cm^2. PBS (200 mL) was taken as the subphase, the surface pressure was allowed to stabilize and then set to zero. Peptide monolayer was established as described in section 2.2.7. Compression-expansion cycles were recorded 30 minutes after peptide deposition. The starting surface pressure was found to be ~12 mN/m (Figure 4.9). The compression of the monolayer causes a steady increase in surface pressure. The change in surface pressure ($\Delta\pi$) was linear up to about 25 mN/m, suggesting a smooth transition from a liquid-expanded (LE) to a liquid-condensed (LC) state. The peptide monolayer could be compressed up to about 44-45 mN/m, where the monolayer displays a collapse. Expansion of the monolayer displays large hysteresis. Such hysteresis has been reported in the literature due to molecular rearrangements, self-assembly, or due to depletion of material from the interface at high surface pressures. Further compressions (2^C-4^C) caused the isotherms to shift towards lower molecular areas. Besides, the 2^E and 3^E expansion isotherms displayed lower than initial surface pressure at the fully expanded barrier position. These data imply that compression caused molecular events that are irreversible on the time scale of the experiment. The linear region of first compression (1^C) isotherm's steep region was extended to find the limiting molecular area (A_0) to be 238 $Å^2$/molecule. After 4^C, 12 layers of the peptide were Blodgett-deposited on a quartz slide (6 layers on each face), and investigated using CD spectroscopy (Figure 4.10). The CD spectrum was noisy but showed a negative band around 220 nm, as can be seen in the smooth trace obtained using Savitzy-Golay algorithm.

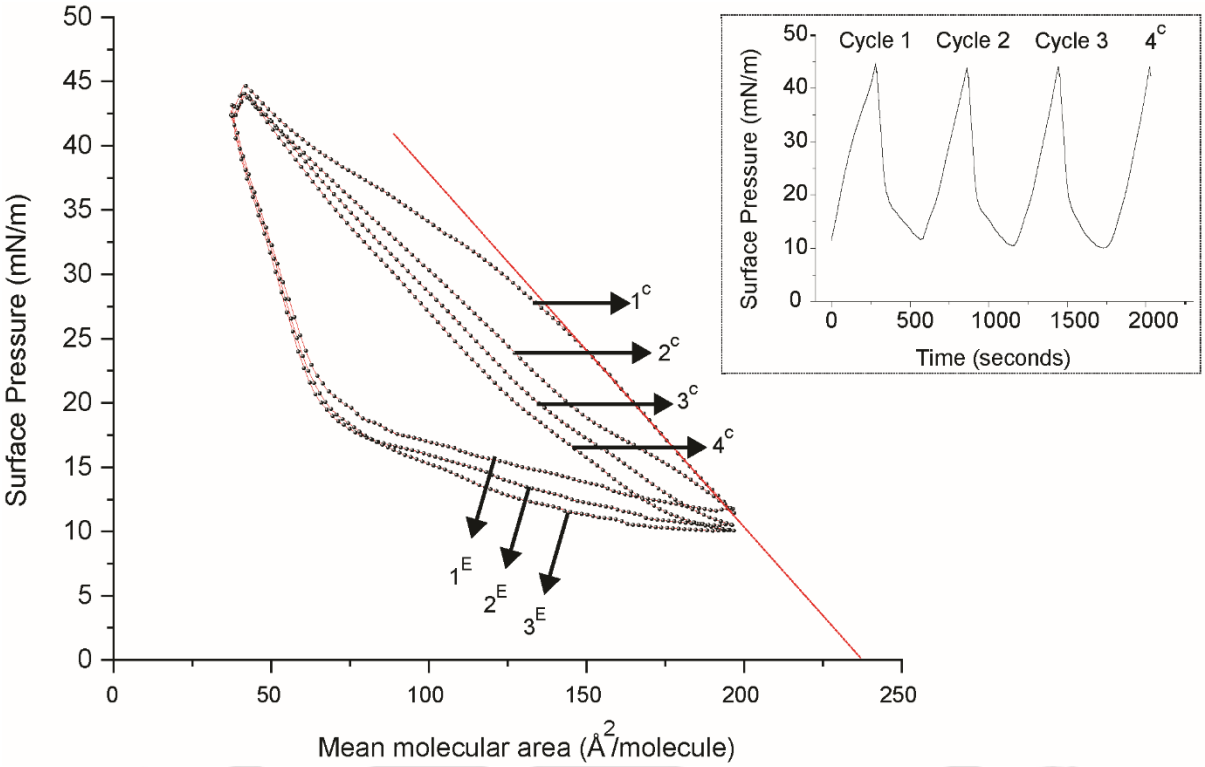

Figure 4.9. The compression expansion isotherms of cathelicidin-DM monolayer on air-PBS interface (Inset: Δπ plotted against time during compression and expansion cycles). The numbers with 'C' superscript represent the compression isotherms, while those with 'E' superscript represent the expansion isotherms.

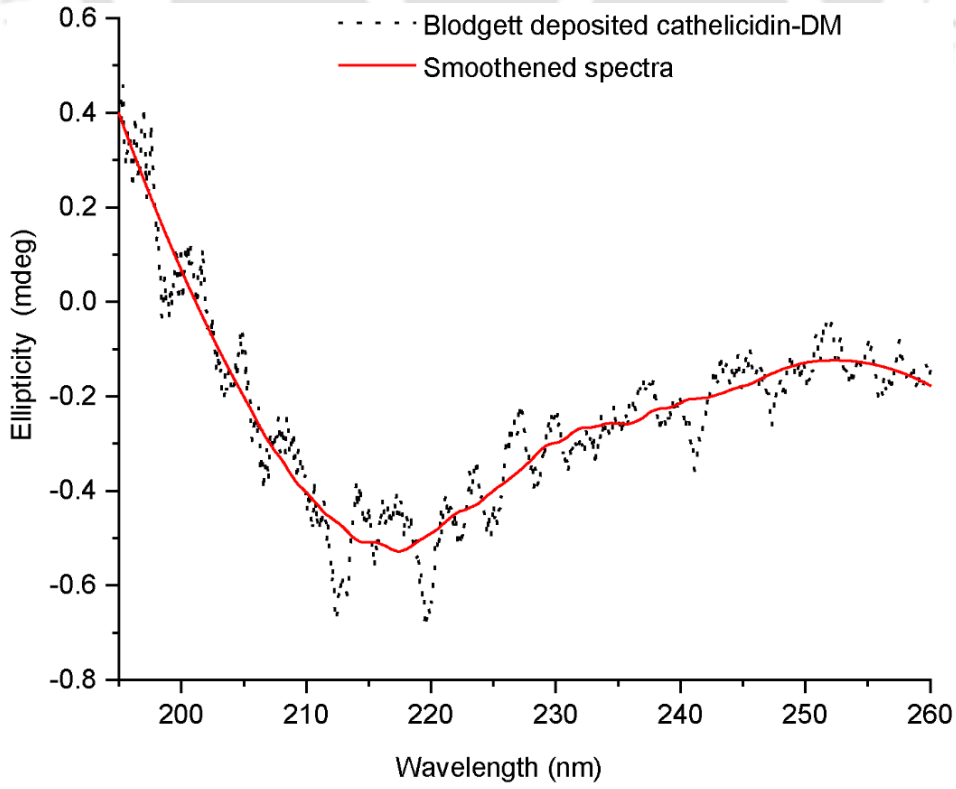

Figure 4.10. Circular dichroism spectrum of the Blodgett-deposit cathelicidin-DM after 4^{C}.

4.2.7. AFM/SEM of Blodgett-deposited films

The cathelicidin-DM monolayer deposited by Blodgett after 4^{C} was also examined using SEM and AFM, as shown in the left panel (Figure 4.11A–C). AFM data reveals a mesh-like structure with intermittent holes alongside some globular structures (Figure 4.11A). The height profile corresponding to the line segment drawn on panel A reveals that the thickness of the mesh-like structure is within 20 nm (Figure 4.11B). FESEM shows flower-like structures that look like crystalline structures (Figure 4.11C). As the peptide was deposited from air-PBS interface, and the drying for microscopic analysis could form salt crystals, the imaging was carried out for the monolayers Blodgett-deposited from the air-deionized water interface. The microscopic data from this monolayer is shown in the right panels (Figure 4.11D–F). The AFM image reveals few globular particles without any mesh-like structure, indicating that the mesh-like structure could be due to the drying of salts from PBS (Figure 4.11D). The height profile of the line segment shown in panel D reveals a sinusoidal pattern (Figure 4.11E) that could be arising from the substrate (silicon wafer). Like AFM, SEM also shows only globular structures (Figure 4.11F). These microscopic data, therefore, revealed only globular structures in the Blodgett-deposited films.

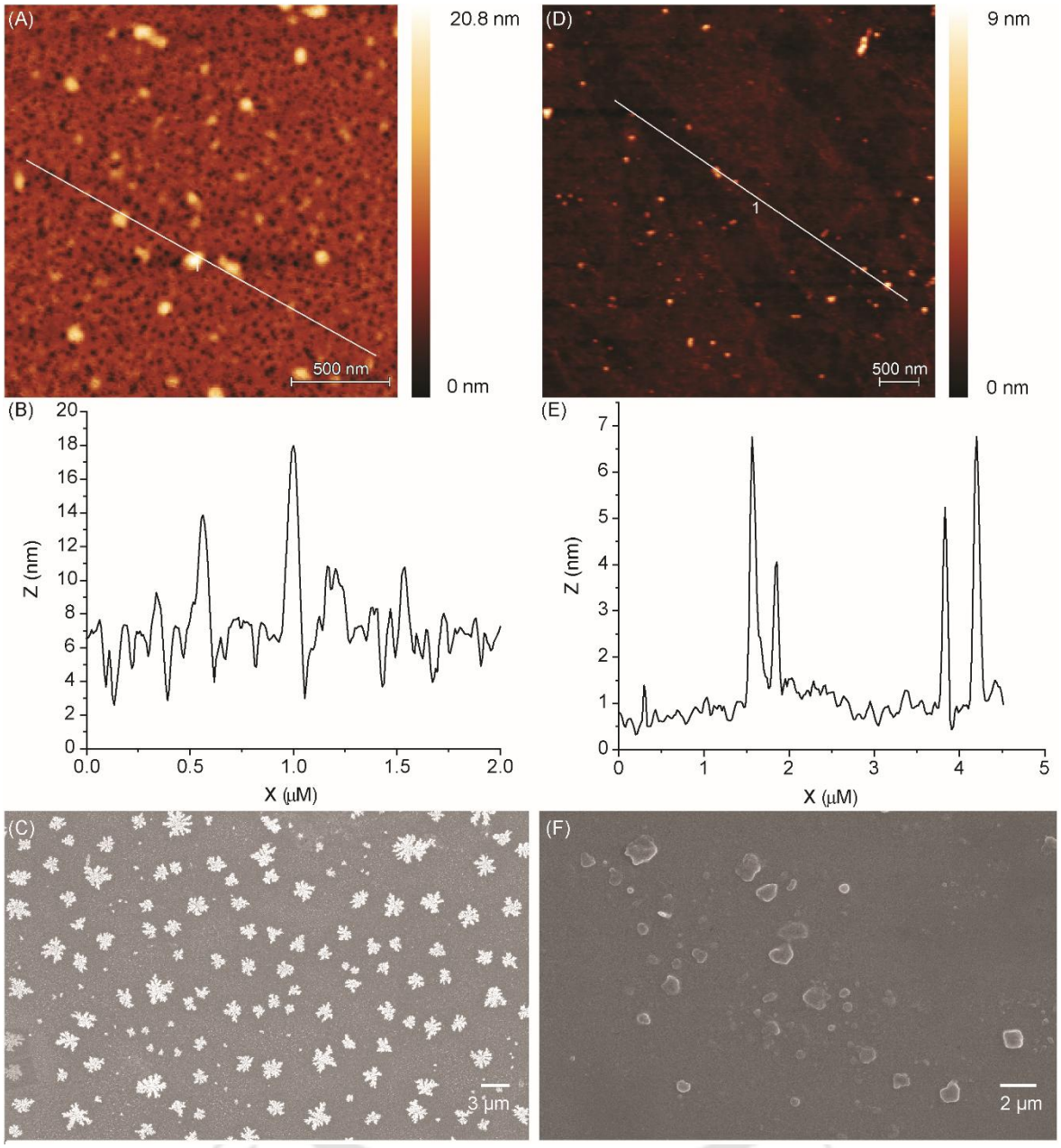

Figure 4.11. The Blodgett-deposited cathelicidin-DM monolayer investigated using AFM and FESEM. AFM images (A and D), the Z-profile of the structures corresponding to the line segment shown on the corresponding AFM images (B and E), and the FESEM images (C and F) of PBS (A-C) and water (D-F) samples.

4.2.8. Penetration of cathelicidin-DM into lipid monolayers

Lipid monolayers are flat membranes and can be prepared with desired packing (surface pressure). They happen to be excellent models for investigating membrane-penetrating molecules. Interaction of cathelicidin-DM with POPE/POPG (7:3) and POPC/CHL (10:1) monolayers was investigated. Lipid monolayers at different initial surface pressures (π_0)

ranging from 5–30 mN/m were prepared. Once the monolayer surface pressure was stabilized, the peptide was gently injected into the subphase without disturbing the surface, and the change in surface pressure was monitored with respect to time. The increase in surface pressure, as expected, displayed a π_0-dependent increase (Figure 4.12). The lower surface pressure lipid monolayers were easily penetrated by the peptide, causing large changes in surface pressure ($\Delta\pi$), whereas lipid monolayers prepared at higher pressures gave smaller $\Delta\pi$.

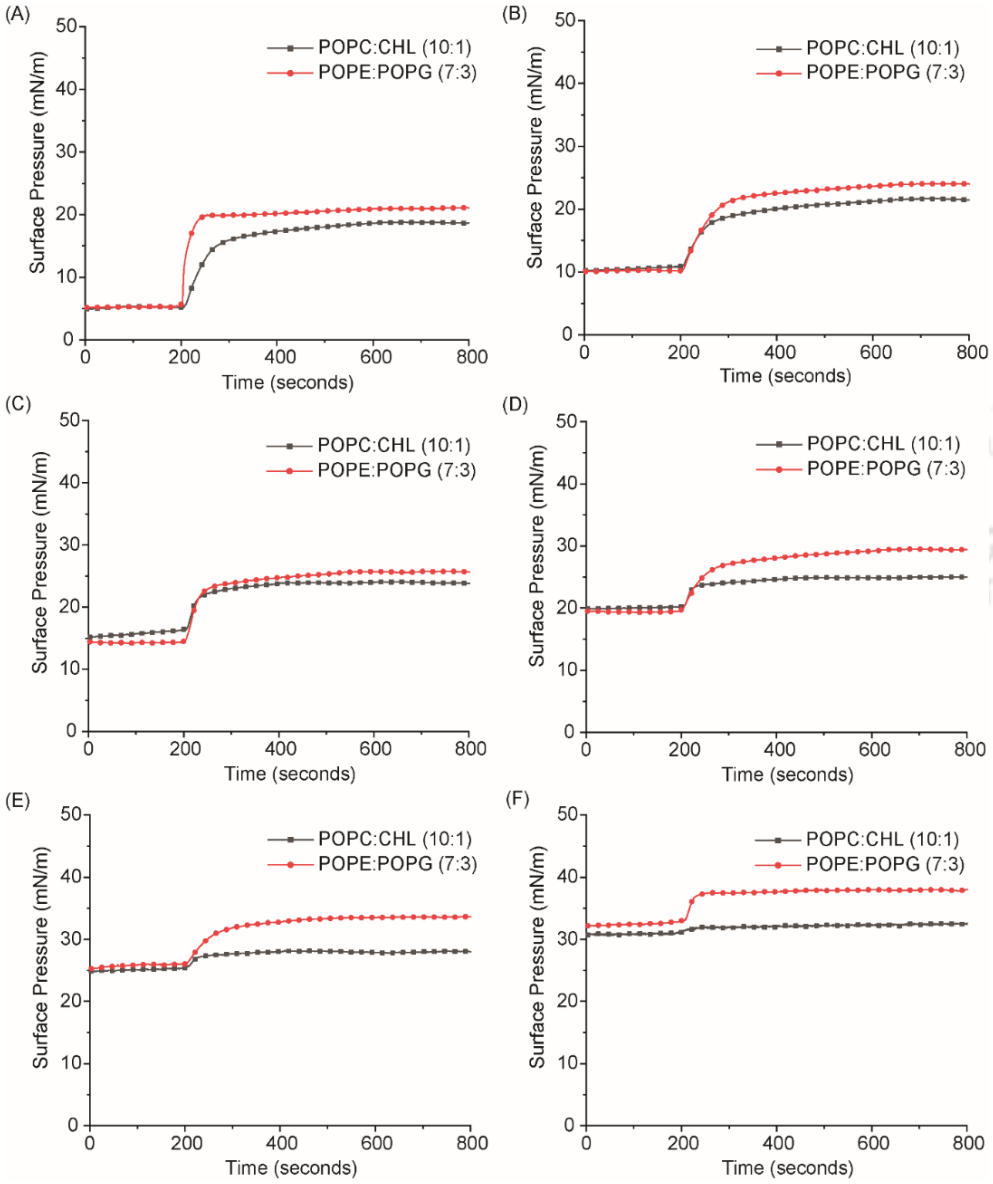

Figure 4.12. The lipid monolayer membrane penetration by cathelicidin-DM at different initial surface pressures, 5 mN/m (A), 10 mN/m (B), 15 mN/m (C), 20 mN/m (D), 25 mN/m (E), and 30 mN/m (F).

The change in surface pressure was observed after peptide addition in the subphase. The change in surface pressure ($\Delta\pi$), ~10 minutes after peptide addition, was plotted against the initial surface pressures (π_0) of POPC/CHL and POPE/POPG monolayers (Figure 4.13). The increase was higher in POPE/POPG monolayers at all initial surface pressures with respect to POPC/CHL monolayers, establishing better penetration of negatively charged monolayer. The data was fit using linear regression and extrapolated to find the intercept at π_0. The π_0 intercept is known as the critical insertion pressure (π_C) *i.e.* the maximum initial pressure at which the peptide can penetrate the membrane. The π_C for POPC/CHL and POPE/POPG monolayers were found to be 33.16 mN/m and 46.66 mN/m, respectively. These data conclude that cathelicidin-DM has a higher propensity to penetrate the bacterial membrane-mimicking monolayer than the mammalian membrane model.

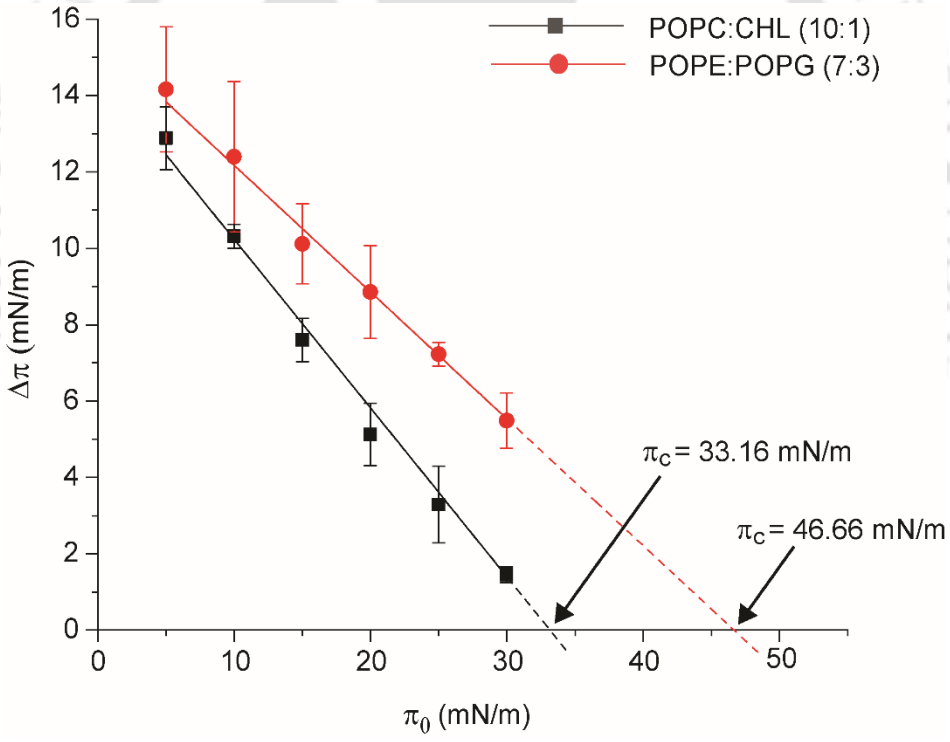

Figure 4.13. $\Delta\pi$ plotted against π_0. The data was fit linearly and extrapolated to intersect with the π_0 axis. The π_0 intercept is the critical insertion pressure for a given monolayer.

4.3. Conclusion

In this chapter, the interfacial activity of cathelicidin-DM was investigated. The peptide was found to be surface-active. Compression-expansion isotherms displayed large

hysteresis, suggesting molecular events triggered by high surface pressures. It is interesting to note that the peptide could be compressed to a very high surface pressure of about 44-45 mN/m. A peptide with high surface-activity is expected to be membrane-active. Lipid monolayer penetration study established membrane-activity of the peptide. The peptide could penetrate both POPC/CHL and POPE/POPG monolayers. However, the π_C observed for POPE/POPG lipid monolayers is much higher than that observed for POPC/CHL monolayers, suggesting that the peptide would show preferential binding to negatively charged lipids compared to neutral or zwitterionic ones. This outcome is very much expected from a peptide that contains a net charge of +9 at physiological pH.

Chapter 5

Cathelicidin-DM interaction with liposomes

5.1. Summary

The results in chapter 4 establish the penetration of cathelicidin-DM into lipid monolayers. The interaction with lipid bilayers has been described in this chapter. The secondary structure of the peptide with and without liposomes was studied using CD spectroscopy. Cathelicidin-DM harbours a tryptophan residue that can serve as an intrinsic fluorescent probe for investigating membrane binding. Tryptophan emission is strongly dependent on the polarity of the local environment. In water, tryptophan displays an emission maximum around 350 nm. A decrease in polarity is manifested in the blue shift of emission spectrum. Binding of cathelicidin-DM to liposomes could place tryptophan into relatively non-polar environment, causing a blue shift. Besides, partitioning into lipid bilayers makes tryptophan less accessible to aqueous quenchers like acrylamide and potassium iodide. Both these data supported preferential binding to negatively charged liposomes. This is further supported by FRET analysis. Liposomes doped with dansyl-labeled lipid caused reduction in tryptophan fluorescence emission intensity, suggesting that tryptophan excitation energy is transferred to the dansyl moiety. Perturbation of liposomes was investigated using dye-release assay. Surprisingly, the results were counterintuitive: the peptide caused rapid dye release from POPC/CHL liposomes without any noticeable dye release from POPE/POPG vesicles.

5.2. Results

5.2.1. CD spectroscopy

Far-UV CD spectra of peptide were recorded in PBS without or with SUVs (1:50 peptide/lipid ratio). In PBS, the peptide displayed a negative band around 202 nm and negative-to-positive CD crossover around 196 nm (Figure 5.1A). This data is suggestive of a mixture of unordered as well as folded elements. The spectra recorded in lipid vesicles displayed little change in the conformation (Figure 5.1B). Addition of peptide to POPE/POPG vesicles caused instant clumping that could be easily seen with naked eye. This suggests that the peptide could cause clumping of negatively charged vesicles. As the sample caused large scattering, a very noisy spectrum could be recorded (Figure 5.1C). The data was analyzed using BESTSEL (https://bestsel.elte.hu/index.php), an online server for secondary structure deconvolution using CD data (Micsonai et al, 2018). The secondary structures derived from the CD deconvolution are shown in Table 5.1, and

support the interpretation of very similar secondary structure content. Even though the data in the presence of POPE/POPG SUVs contains very large noise, and CD deconvolution may not be very reliable, surprisingly, the CD deconvolution predicted very similar secondary structural content.

Table 5.1. Secondary structural content predicted from CD deconvolution data

Sample	α-helix	Antiparallel β-sheet	Parallel β-sheet	Turn	Others
Peptide in PBS	3.5	31.9	0	12.4	52.2
Peptide in POPC/CHL SUVs	4.8	33.2	0	10.7	51.3
Peptide in POPE/POPG SUVs	6.9	32.2	0	12.2	48.7

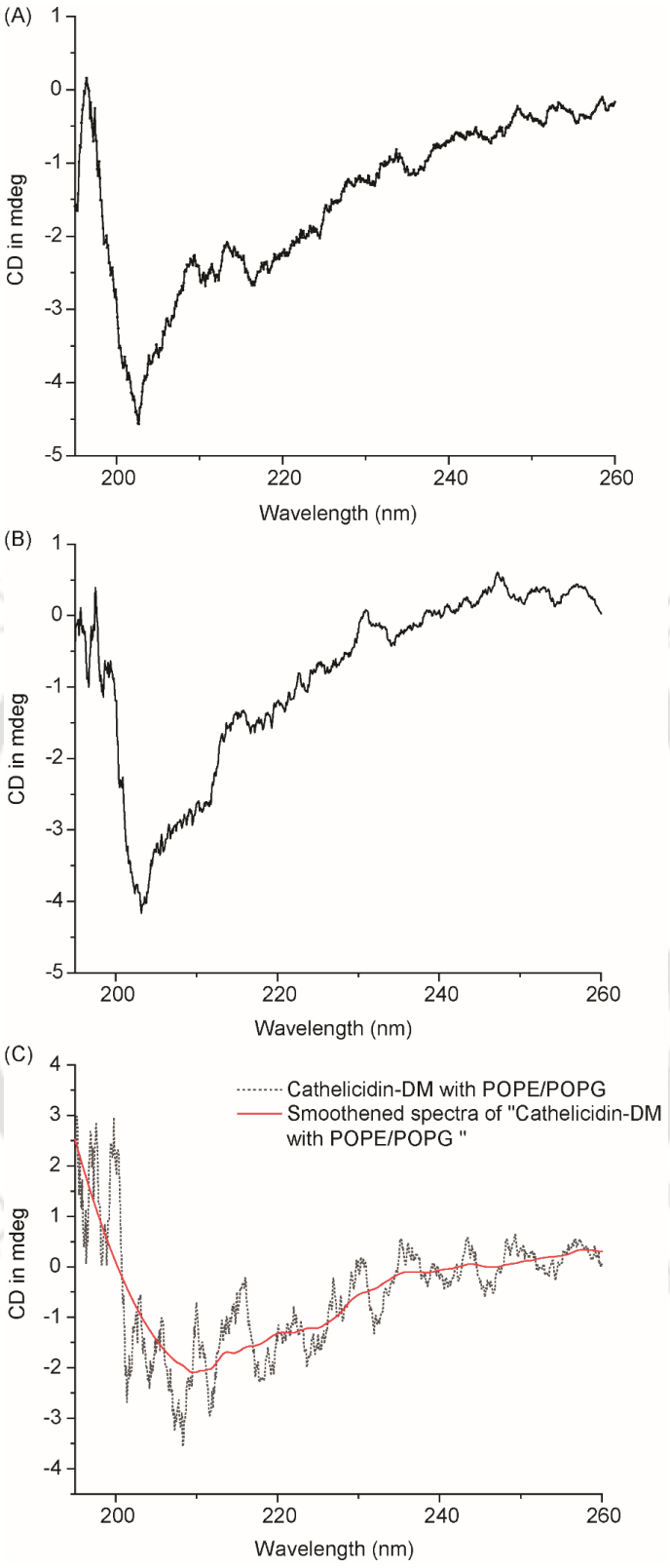

Figure 5.1. Circular dichroism spectra of the cathelicidin-DM peptide in PBS (A), in the presence of POPC/CHL SUVs (B), and in the presence of POPE/POPG SUVs (C). As the spectrum in panel C is noisy, a smooth trace is also shown on top of the noisy spectrum.

5.2.2. Steady-state tryptophan fluorescence

Binding of cathelicidin-DM to POPC/CHL (10:1) and POPE/POPG (7:3) liposomes was investigated using steady-state tryptophan fluorescence. The spectra were recorded in PBS with or without SUVs (Figure 5.2). In the absence of vesicles, the peptide displays fluorescence emission with λ_{max} around 350 nm. A small enhancement in fluorescence intensity with very little blue shift was observed with POPC/CHL liposomes at 1:50 and 1:100 peptide/lipid ratios. A large enhancement in fluorescence emission intensity along with ~12 nm blue shift in λ_{max} was observed with POPE/POPG vesicles. These data clearly suggest that cathelicidin-DM binds to negatively charged liposomes placing tryptophan in a relatively hydrophobic environment. A blue spectral shift and enhancement in fluorescence emission intensity indicate membrane binding. However, the lack of these features does not rule it out. It is possible that the peptide binds to liposomes but tryptophan is not involved in membrane binding, therefore remaining exposed to the aqueous environment. Binding of peptide to liposomes, however, often affects its accessibility to dynamic quenchers. Even when the tryptophan is exposed to aqueous environment, the quenchers approaching from vesicle side cannot reach it. Tryptophan fluorescence quenching assay, therefore, was carried out.

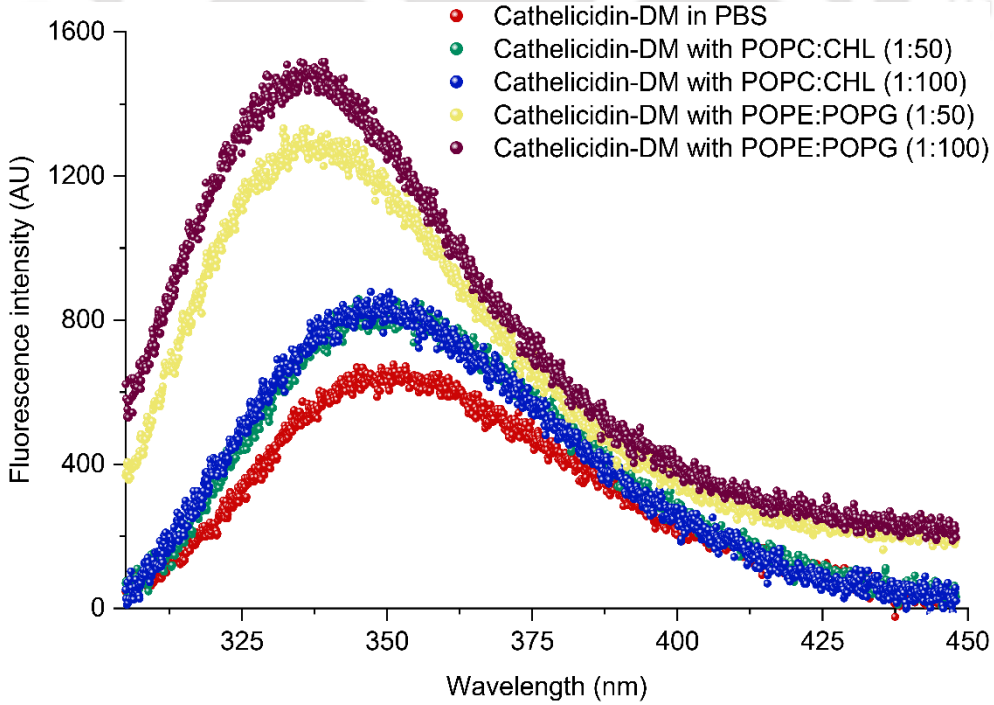

Figure 5.2. The tryptophan fluorescence emission spectra of cathelicidin-DM in the absence and presence of SUVs, POPC/CHL, and POPE/POPG with peptide/lipid ratios 1:50 and 1:100.

5.2.3. Tryptophan fluorescence quenching of cathelicidin-DM in the presence of lipid vesicles

Tryptophan fluorescence quenching assay was carried out using acrylamide as the quencher. For cathelicidin-DM in PBS, tryptophan fluorescence displays maximum quenching (Figure 5.3A), whereas little quenching is observed in the presence of POPE/POPG vesicles (Figure 5.3C). Quenching is also observed in the presence of POPC/CHL vesicles (Figure 5.3B). Fluorescence intensities at the λ_{max} for unquenched samples were extracted and Stern-Volmer plots were obtained by plotting F_0/F with respect to the concentration of acrylamide using equation 5.1 (Figure 5.3D),

$$\frac{F_0}{F} = 1 + K_{SV}[Q] \qquad (5.1)$$

F_0 is the fluorescence emission intensity in the absence of quencher, F is the fluorescence intensity in the presence of quencher at a given quencher concentration (Q).

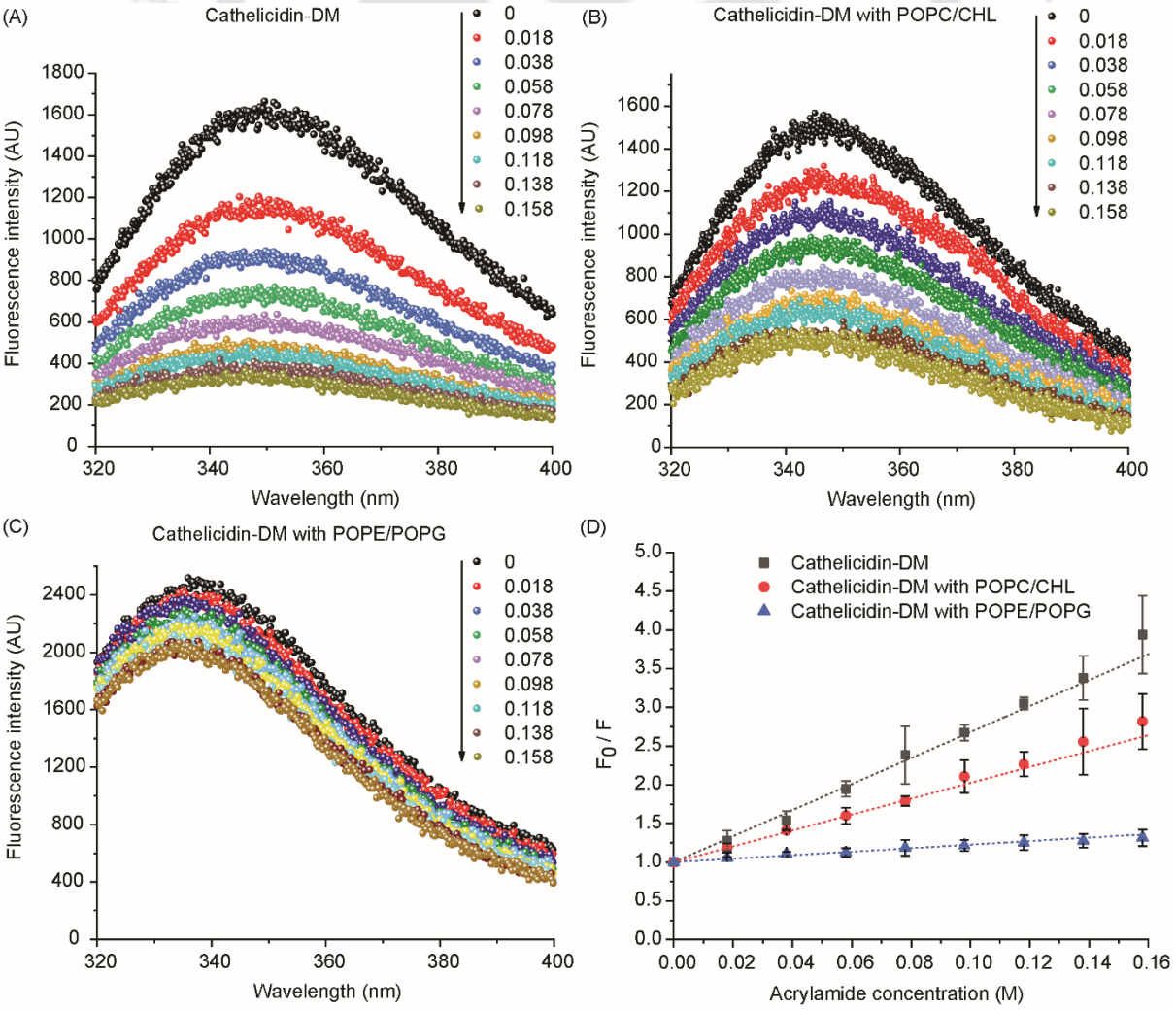

Figure 5.3. The tryptophan fluorescence quenching of cathelicidin-DM by acrylamide in the absence and presence of POPC/CHL and POPE/POPG SUVs with peptide/lipid ratio of 1:100. (A) peptide in buffer, (B) peptide with POPC/CHL, (C) peptide with POPE/POPG vesicles, and (D) Stern-Volmer plot of tryptophan fluorescence quenching of peptide in the absence and presence of SUVs.

The Stern-Volmer constants (K_{SV}) and the tryptophan's net accessibility factors are tabulated in Table 5.2. Net accessibility factor is the ratio of K_{SV} values for cathelicidin-DM with liposomes to that in the absence of liposomes.

Table 5.2. K_{SV} and NAF values of cathelicidin-DM in solution with and without SUVs

	PBS	POPC/CHL	POPE/POPG
K_{SV} (M^{-1})	17.3	9.8	2.4
NAF	1	0.57	0.14

The K_{SV} and NAF values show a dramatic decrease in tryptophan's accessibility to acrylamide in POPE/POG SUVs. The tryptophan was about 14% accessible compared to that in the absence of lipid vesicles. With POPC/CHL liposomes, tryptophan's accessibility reduces to 57%, suggesting its binding to lipid vesicles. This data corroborates with the MD simulation data where the peptide was found to bind the POPC/CHL as well as POPC vesicles. The peptide, therefore, binds to both model membranes, however, with clear preference for negatively charged vesicles, a conclusion that is in line with the lipid monolayer penetration data (Figure 4.12 and Figure 4.13).

5.2.4. Förster resonance energy transfer

Preferential binding of cathelicidin-DM was further verified using FRET. Liposomes doped with dansyl-POPE were employed. Energy transfer from tryptophan to dansyl causes decrease in tryptophan fluorescence and increase in dansyl fluorescence emission. For POPC/CHL vesicles, at 1:100 peptide/lipid ratio, both tryptophan (~350 nm) and dansyl (~518 nm) fluorescence signatures can be seen (Figure 5.4A). Addition of more peptide caused steady increase in tryptophan without any noticeable increase in dansyl fluorescence. For POPE/POPG vesicles, on the other hand, a steady increase in dansyl

fluorescence was observed as more peptide was added (Figure 5.4B). Clearly, the peptide prefers to bind to negatively charged vesicles over zwitterionic ones.

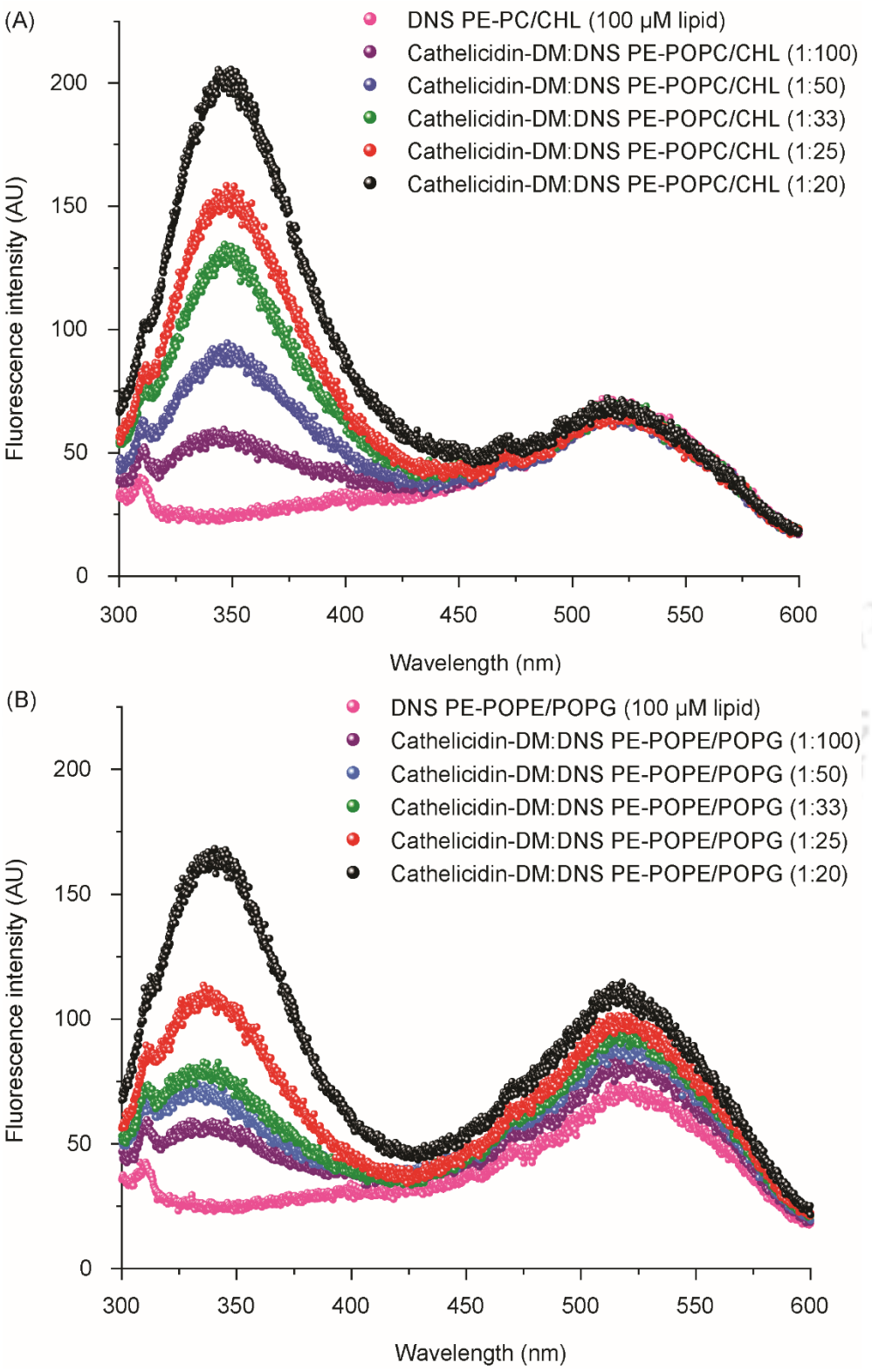

Figure 5.4. FRET assay of the peptide with dansyl-POPE (DNS PE)-doped SUVs, (A) interaction with POPC/CHL SUVs, (B) interaction with POPE/POPG SUVs.

5.2.5. Dye-release assay

Perturbation/disruption of lipid vesicles, if any, was investigated using well-established dye release assay. A fluorescent dye, calcein in this study, is encapsulated in the lipid vesicles at self-quenching concentration. Membrane destabilization allows diffusion of the encapsulated dye down the concentration gradient, causing an enhancement in fluorescence intensity (Figure 5.5A). The calcein-loaded vesicles were prepared as described in section 2.2.21, and their size verified using DLS. The vesicles were found to be around 100 nm in diameter (Figure 5.5B). The assay was carried out at 1:70 and 1:200 peptide/lipid ratio as described in section 2.2.22. Addition of peptide to POPC and POPC/CHL (10:1) vesicles caused rapid release of calcein dye (Figure 5.5C and D). Interestingly, however, no appreciable release was observed from POPE/POPG (7:3) vesicles. Replacing POPG with another negatively charged lipid POPS caused some release of calcein. The extent of release, however, was much lower than that observed for POPC and POPC/CHL (10:1) vesicles. This data came as a big surprise. The lipid monolayer penetration and tryptophan fluorescence data suggested preferential binding to POPE/POPG (7:3) vesicles, but does not perturb the membrane integrity. On the other hand, POPC and POPC/CHL vesicles are readily destabilized. No lysis of POPE/POPG vesicles is difficult to explain. One possibility is that the peptide remains bound to the negatively charged polar headgroup without gaining access to the hydrophobic core. However, a small calcein release observed for POPE/POPS vesicles suggests that cathelicidin-DM may have lipid-specific activity.

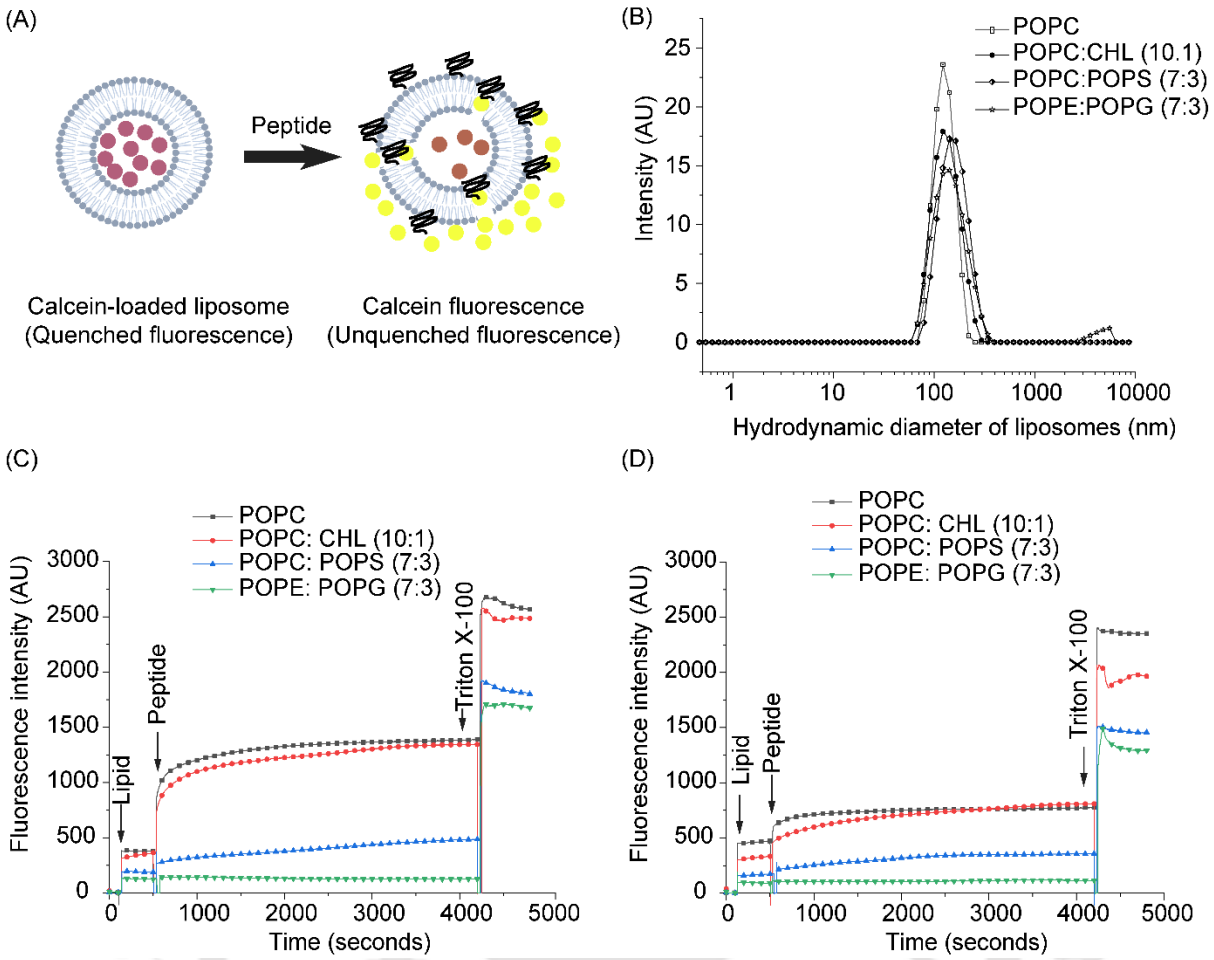

Figure 5.5. Calcein release assay. (A) A cartoon depicting the membrane perturbation of liposomes by the peptide releasing calcein dye causing calcein release with concomitant enhancement in fluorescence intensity, (B) characterisation of hydrodynamic diameter of LUVs by DLS. Calcein release data from LUVs with 1:70 (C) and (1:200) peptide/lipid ratios. The arrows indicate the time of peptide/lipid/Triton X-100 addition.

5.3. Conclusion

Cathelicidin-DM is not unstructured in PBS. CD spectrum is suggestive of a mixture of β-sheet and random coil conformations. Small changes are observed in the presence of lipid vesicles, possibly caused by the ordering of flexible regions upon membrane binding. Tryptophan fluorescence, its quenching, and energy transfer to dansyl-labeled lipid vesicles supported preferential binding to negatively charged lipid vesicles. Surprisingly, however, calcein release assay suggested rapid destabilization of POPC/CHL vesicles with no noticeable effect on POPE/POPG vesicles. Intrigued by these results, we included POPC and POPE/POPS vesicles in our study. POPC SUVs was included to rule out the

contribution of cholesterol to membrane perturbation, if any. POPE/POPS vesicles were included to substitute one anionic lipid with another one. Like POPC/CHL vesicles, POPC vesicles were also rapidly destabilized. Unlike POPE/POPG vesicles, however, POPE/POPS vesicles showed some calcein release. These data suggest that cathelicidin-DM may have lipid-specific activity. To conclude, the peptide shows preferential binding to negatively charged vesicles, but preferentially destabilizes the zwitterionic ones.

Chapter 6

Conclusions, Discussion, and Possibilities

Traditional medicines are used worldwide to treat various ailments. Such medicines, however, failed to get the recognition that modern medicine enjoys. This could partly be attributed to their non-systematic preparations that cause variations in their efficacy, the unknown molecular mechanisms, and the apprehension about potential adverse health effects. In 2018, the World Health Organization (WHO) recommended various traditional medicines, one of which was Traditional Chinese Medicine, offering hope for research into traditional medicine that could be transformed into therapeutics (WHO, 2019). *Chan su*, a traditional medication, is derived from the secretions of the toads *D. melanostictus* or *B. garganizans* (Meng et al, 2009; Qiu et al, 2013). Subsequently, various molecules have been identified from these extracts (Qi et al, 2011; Baldo et al, 2017). The bacteriostatic activity was detected in these secretions; however, this activity was lost following trypsin treatment, indicating the presence of antimicrobial peptides/proteins (Garg et al, 2007). However, the full potential of proteins/peptides found in these extracts is yet to be realized. Zhang and coworkers identified a cathelicidin from the skin secretions of *D. melanostictus* (Shi et al, 2020). They named the peptide cathelicidin-DM and reported its antimicrobial and wound-healing properties. The mechanism of antimicrobial action was not investigated, but predicted to be membrane-permeabilization. In this thesis, I delved into examining cathelicidin-DM's interfacial activity and membrane interactions.

The interfacial activity indicated that the peptide might indeed be a membrane-binding one. Interaction with lipid bilayers mimicking mammalian and bacterial membranes was investigated using molecular dynamics simulations. A transient interaction was observed with POPC/CHL vesicles that caused the unfolding of the peptide. Separation from the membrane caused rapid refolding of the peptide. This data is very intriguing. The binding of the peptide with POPC/CHL can be attributed to its intrinsic amphipathicity that facilitated its partition to the water/cyclohexane interface. The detachment from the bilayer suggests that the peptide's unfolding is associated with diminished amphipathicity. Refolding of the peptide would cause recovery of amphipathicity, and could lead to the next round of interaction. This hypothesis can probably be verified by carrying out long (microsecond) timescale simulations or using single-molecule experimental methods. MD simulation with negatively charged vesicles POPE/POPG

resulted in peptide binding at the interface without much structural changes, and the peptide remained bound till the end of the simulation.

The preferential binding to POPE/POPG bilayer is primarily attributed to the electrostatic interactions between positively-charged vesicles and negatively charged POPG. The POPC/CHL bilayer, on the other hand, has no net charge. In addition, the presence of cholesterol in POPC/CHL vesicles modulates the membrane's rigidity, making it difficult for the peptides to penetrate (Epand et al, 2010). On the other hand, the POPE/POPG membrane is more fluid and should make it easy for the peptide to penetrate the bilayer.

The membrane binding propensity of a peptide is attributed to its amphipathicity or its propensity to fold into an amphipathic structure upon membrane interaction. An amphipathic peptide displays surface activity *i.e.* partitions to air/water interface when dissolved in water (Saikia et al, 2017). Lu and coworkers explored the cationic surfactant-like peptide for their antimicrobial activity (Gong et al, 2019). A surface activity greater than 12 mN/m was needed to observe appreciable antimicrobial activity. Cationicity is required for preferential binding of the peptides to the negatively charged bacterial surface. A surface-active peptide, therefore, is expected to interact with cell membrane. Upon binding with the membrane, an AMP can disrupt the microbial cells' transmembrane potential through different mechanisms, as described in section 1.7.

The molecular dynamics simulation of cathelicidin-DM in a water/cyclohexane biphasic system showed that the peptide partitions to the interface of the two phases. No appreciable change was observed in the peptide's structure, suggesting that the native structure of the peptide is amphipathic. The interfacial activity was experimentally verified for the air/water interface. The peptide dissolved in PBS partitions to interface, causing a decrease in surface tension. The peptide (0.5 μM) showed ~10 mN/m surface pressure. Doubling the concentration caused very little (~10%) increase in surface pressure. Therefore, the surface pressure observed for cathelicidin-DM was slightly below the threshold limit observed by Lu and coworkers for their designed cationic surfactant-like peptides (Gong et al, 2019). The 12 mN/m surface pressure reported for these peptides, however, need not be applicable to all other peptides. Cathelicidin-DM demonstrates its near-maximal surface activity at about 1 μM (4.17 μg/mL) concentration. Interestingly, the MICs reported for cathelicidin-DM in the literature

against various bacteria lie between 6-12 μg/mL. The lower the concentration to obtain maximal surface activity, the lower the MIC. This presents an advantage as it signifies that only small quantities of the peptide are necessary to yield substantial antimicrobial effects, thereby diminishing the potential for toxicity and adverse effects.

The peptide monolayer was investigated using compression/expansion isotherms. A steady increase in surface pressure upon compression indicated a smooth transition from a liquid-expanded (LE) to a liquid-condensed (LC) state. The peptide monolayer could be compressed up to approximately 44-45 mN/m before collapsing, suggesting exceptional stability of the peptide monolayer. The peptide also exhibited significant hysteresis upon expansion. The hysteresis observed for protein/peptide monolayer compression/ expansion isotherms is often attributed to the compaction of the protein/peptide, their reorientation, their self-assembly, or depletion from the interface. The Blodgett-deposited films of the peptide monolayer displayed CD spectrum similar to that observed in PBS, suggesting that the conformational change does not contribute to the hysteresis. As subsequent compression isotherms display small shift towards smaller molecular area, it can be concluded that both peptide reorientation at interface and monolayer depletion might contribute to the hysteresis. The conformational changes that occur during compression at the interface have been studied for different peptides. Dannehl et al. studied two peptides, namely LL-20 and LL-32, which were derived from human cathelicidin (LL-37). Both the peptides were found to be unstructured in pure water. LL-32 adopted an α-helix conformation when lying flat at the air/aqueous buffer interface, while LL-20 formed a partially unstructured intermediate. They suggested that the perfect helix formed by LL-32 at the hydrophilic/hydrophobic interface may contribute to its increased antimicrobial activity (Dannehl et al, 2013).

The interaction of peptide with lipids was experimentally investigated using multiple methods. The peptide-lipid penetration activity was investigated by using negatively charged and zwitterionic lipid monolayers as described elsewhere (Brockman, 1999; Mohapatra et al, 2023). Cathelicidin-DM exhibited better penetration to negatively charged lipid vesicles. The critical insertion pressure for POPE/POPG monolayers was very high (50 mN/m) compared to that observed for POPC/CHL monolayers (35 mN/m). The biological membranes display an equivalent pressure of ~30-35 mN/m (Marsh,

1996). Therefore, it can be concluded that cathelicidin-DM preferentially penetrates the POPE/POPG monolayers but can also penetrate the mammalian membranes.

Intrinsic tryptophan fluorescence and its quenching in the presence of zwitterionic and negatively charged lipid vesicles resonate with the computational and lipid monolayer results. A large blue shift in tryptophan fluorescence emission spectrum in the presence of POPE/POPG vesicles compared to that with POPC/CHL vesicles confirmed preferential binding of the peptide with negatively charged vesicles. Concerning the tryptophan's accessibility in buffer, Trp with POPE/POPG vesicles was about 14% vesicles while that with POPC/CHL vesicles was ~57% vesicles. The dye (calcein) release data, however, came as a very big surprise. There was little calcein release from POPE/POPG vesicles, while rapid release was observed from POPC/CHL vesicles. As these data were contrary to the expectation, the dye release assay was carried out with POPC vesicles and POPE/POPS vesicles as well. The peptide displayed rapid release of calcein from POPC vesicles. Unlike POPE/POPG, that showed no lysis, POPC/POPS vesicles displayed some lysis. It is likely that the peptide molecules bind to the negatively charged lipid vesicles through electrostatic interactions too tightly, affecting their cooperative activity that is usually required for membranolytic action of AMPs. The weaker interaction with zwitterionic vesicles would allow the peptide molecules to bind, detach, reorient, and cooperate with each other to bring about the membranolytic effect. It is also important to mention that bacterial killing need not require large pores that are required for dye release. Small pores that disrupt the electrochemical potential of the bacterial membrane are good enough to kill the bacteria. As cathelicidin-DM did not cause calcein release from POPE/POPG vesicles, one might argue that the peptide acts through non-membranolytic pathways. Non-membranolytic antimicrobial pathways, however, are usually much slower than the membranolytic pathways. Zhang and coworkers reported that cathelicidin-DM exhibits rapid antimicrobial action, killing the bacteria within 15 minutes. Such rapid killing of bacteria supports membranolytic action underlying bacterial killing (Shi et al, 2020).

To conclude, cathelicidin-DM displays preferential binding to anionic lipid vesicles but does not disrupt them as efficiently as it does with zwitterionic vesicles. The underlying mechanism for this behavior, however, has not been elucidated in this thesis and could be an interesting extension of this work. Advanced techniques such as AFM or cryo-

electron microscopy could provide insights into the structural changes and pore formation in the membranes (Shaw et al, 2006; Hammond et al, 2021). Techniques like surface plasmon resonance or isothermal titration calorimetry could provide quantitative data on binding kinetics and affinity, helping to elucidate how binding influences membrane disruption (Thomas & Surolia, 1999; Lin et al, 2007). The peptide takes up an antiparallel β-hairpin structure flanked by highly cationic stretches that largely remain unstructured. Interestingly, the N-terminal stretch is stapled to the first β-strand *via* a disulfide bridge. The precise roles that these features play is not clear. The peptide has been reported to possess a wound-healing property as well. Structure-function studies can help elucidate the exact roles of these stretches and the core β-hairpin in peptide stability, antimicrobial activity, and wound healing.

This research can be extended to cellular systems to understand how cathelicidin-DM affects real cell membranes compared to model membranes. This could include studying cytotoxicity, cellular uptake, and the peptide's impact on cellular functions and integrity. Examining the peptide's behavior in more complex lipid environments, such as mixed lipid bilayers or biological membranes containing proteins and other components, would also provide a more realistic picture of how cathelicidin-DM interacts in natural cellular contexts. By investigating these aspects, future research can build on the current findings to provide a more comprehensive understanding of cathelicidin-DM-lipid interaction and peptide-membrane interaction in general.

References

Agerberth, B., J. Y. Lee, T. Bergman, M. Carlquist, H. G. Boman, V. Mutt and H. JÖRnvall (1991). "Amino acid sequence of PR-39: Isolation from pig intestine of a new member of the family of proline-arginine-rich antibacterial peptides." European Journal of Biochemistry **202**(3): 849-854.

Aliste, M. P. and D. P. Tieleman (2005). "Computer simulation of partitioning of ten pentapeptides Ace-WLXLL at the cyclohexane/water and phospholipid/water interfaces." BMC Biochemistry **6**(1): 30.

Anne, K. and T. Marianna (2018). "Recent Advances in the Development of Antimicrobial Peptides (AMPs): Attempts for Sustainable Medicine?" Current Medicinal Chemistry **25**(21): 2503-2519.

Baldo, E. C. F., F. A. P. Anjolette, E. C. Arantes and M. A. Baldo (2017). "Toad Poison and Drug Discovery 16." J Toxins Drug Discovery: 373.

Ballard, E., R. Yucel, W. J. G. Melchers, A. J. P. Brown, P. E. Verweij and A. Warris (2020) "Antifungal Activity of Antimicrobial Peptides and Proteins against Aspergillus fumigatus." Journal of Fungi **6** DOI: 10.3390/jof6020065.

Balls, A., W. Hale and T. Harris (1942). "A crystalline protein obtained from a lipoprotein of wheat flour." Cereal Chem **19**(19): 279-288.

Bals, R. (2000). "Epithelial antimicrobial peptides in host defense against infection." Respir Res **1**(3): 141-150.

Baumann, G. and P. Mueller (1974). "A molecular model of membrane excitability." Journal of Supramolecular Structure **2**(5-6): 538-557.

Baxter, N. J. and M. P. Williamson (1997). "Temperature dependence of 1H chemical shifts in proteins." Journal of Biomolecular NMR **9**(4): 359-369.

Bellamy, W., M. Takase, H. Wakabayashi, K. Kawase and M. Tomita (1992). "Antibacterial spectrum of lactoferricin B, a potent bactericidal peptide derived from the N-terminal region of bovine lactoferrin." Journal of Applied Bacteriology **73**(6): 472-479.

Bellamy, W., M. Takase, H. Wakabayashi, K. Kawase and M. J. J. o. A. B. Tomita (1992). "Antibacterial spectrum of lactoferricin B, a potent bactericidal peptide derived from the N-terminal region of bovine lactoferrin." **73**(6): 472-479.

Bellesia, G. and J.-E. Shea (2009). "Effect of β-sheet propensity on peptide aggregation." The Journal of Chemical Physics **130**(14): 145103.

Bensch, K. W., M. Raida, H.-J. Mägert, P. Schulz-Knappe and W.-G. Forssmann (1995). "hBD-1: a novel β-defensin from human plasma." FEBS Letters **368**(2): 331-335.

Bera, A., S. Singh, R. Nagaraj and T. Vaidya (2003). "Induction of autophagic cell death in Leishmania donovani by antimicrobial peptides." Molecular and Biochemical Parasitology **127**(1): 23-35.

Boland, M. P. and F. Separovic (2006). "Membrane interactions of antimicrobial peptides from Australian tree frogs." Biochimica et Biophysica Acta (BBA) - Biomembranes **1758**(9): 1178-1183.

Boman, H. (1981). "Microbial Control of Insects, Mites and Plant Diseases, 1970-1980." New York and London: Academic Press. p: 769-784.

Boman, H. G., B. Agerberth and A. Boman (1993). "Mechanisms of action on Escherichia coli of cecropin P1 and PR-39, two antibacterial peptides from pig intestine." Infection and Immunity **61**(7): 2978-2984.

Bowdish, D. M. E., D. J. Davidson, M. G. Scott and R. E. W. Hancock (2005). "Immunomodulatory Activities of Small Host Defense Peptides." Antimicrobial Agents and Chemotherapy **49**(5): 1727-1732.

Brillault, L. and M. J. Landsberg (2020). Preparation of Proteins and Macromolecular Assemblies for Cryo-electron Microscopy. Protein Nanotechnology: Protocols, Instrumentation, and Applications. J. A. Gerrard and L. J. Domigan. New York, NY, Springer US**:** 221-246.

Brockman, H. (1999). "Lipid monolayers: why use half a membrane to characterize protein-membrane interactions?" Current Opinion in Structural Biology **9**(4): 438-443.

Brogden, K. A. (2005). "Antimicrobial peptides: pore formers or metabolic inhibitors in bacteria?" Nature Reviews Microbiology **3**(3): 238-250.

Brötz, H., G. Bierbaum, A. Markus, E. Molitor and H. G. Sahl (1995). "Mode of action of the lantibiotic mersacidin: inhibition of peptidoglycan biosynthesis via a novel mechanism?" Antimicrobial Agents and Chemotherapy **39**(3): 714-719.
Brown, K. L. and R. E. Hancock (2006). "Cationic host defense (antimicrobial) peptides." Current opinion in immunology **18**(1): 24-30.
Bulet, P., J. L. Dimarcq, C. Hetru, M. Lagueux, M. Charlet, G. Hegy, A. Van Dorsselaer and J. A. Hoffmann (1993). "A novel inducible antibacterial peptide of Drosophila carries an O-glycosylated substitution." Journal of Biological Chemistry **268**(20): 14893-14897.
Burian, M. and B. Schittek (2015). "The secrets of dermcidin action." International Journal of Medical Microbiology **305**(2): 283-286.
Cannon, M. (1987). "A family of wound healers." Nature **328**(6130): 478-478.
Casares, D., P. V. Escribá and C. A. Rosselló (2019) "Membrane Lipid Composition: Effect on Membrane and Organelle Structure, Function and Compartmentalization and Therapeutic Avenues." International Journal of Molecular Sciences **20** DOI: 10.3390/ijms20092167.
Casteels, P., C. Ampe, F. Jacobs, M. Vaeck and P. Tempst (1989). "Apidaecins: antibacterial peptides from honeybees." Embo j **8**(8): 2387-2391.
Cen, M., J. F. Fan, D. Y. Liu, X. Z. Song, J. Liu, W. Q. Zhou and H. M. Xiao (2013). "Cyclo-hexa-peptides at the water/cyclohexane interface: a molecular dynamics simulation." Journal of Molecular Modeling **19**(2): 601-611.
Chan, Y. R. and R. L. Gallo (1998). "PR-39, a Syndecan-inducing Antimicrobial Peptide, Binds and Affects p130Cas*." Journal of Biological Chemistry **273**(44): 28978-28985.
Charlet, M., S. Chernysh, H. Philippe, C. Hetru, J. A. Hoffmann and P. Bulet (1996). "Innate Immunity: ISOLATION OF SEVERAL CYSTEINE-RICH ANTIMICROBIAL PEPTIDES FROM THE BLOOD OF A MOLLUSC, MYTILUS EDULIS*." Journal of Biological Chemistry **271**(36): 21808-21813.
Charpentier, S., M. Amiche, J. Mester, V. Vouille, J.-P. Le Caer, P. Nicolas and A. Delfour (1998). "Structure, Synthesis, and Molecular Cloning of Dermaseptins B, a Family of Skin Peptide Antibiotics *." Journal of Biological Chemistry **273**(24): 14690-14697.
Chessa, C., C. Bodet, C. Jousselin, M. Wehbe, N. Lévêque and M. Garcia (2020). "Antiviral and Immunomodulatory Properties of Antimicrobial Peptides Produced by Human Keratinocytes." Frontiers in Microbiology **11**(1155).
Chugh, J. K. and B. A. Wallace (2001). "Peptaibols: models for ion channels." Biochem Soc Trans **29**(Pt 4): 565-570.
Cociancich, S., A. Dupont, G. Hegy, R. Lanot, F. Holder, C. Hetru, J. A. Hoffmann and P. Bulet (1994). "Novel inducible antibacterial peptides from a hemipteran insect, the sap-sucking bug Pyrrhocoris apterus." Biochemical Journal **300**(2): 567-575.
Coin, I., M. Beyermann and M. Bienert (2007). "Solid-phase peptide synthesis: from standard procedures to the synthesis of difficult sequences." Nature Protocols **2**(12): 3247-3256.
Colilla, F. J., A. Rocher and E. Mendez (1990). "γ-Purothionins: amino acid sequence of two polypeptides of a new family of thionins from wheat endosperm." FEBS Letters **270**(1-2): 191-194.
Conlon, J. M. (2011). "Structural diversity and species distribution of host-defense peptides in frog skin secretions." Cellular and Molecular Life Sciences **68**(13): 2303-2315.
Conlon, J. M., J. Kolodziejek and N. Nowotny (2004). "Antimicrobial peptides from ranid frogs: taxonomic and phylogenetic markers and a potential source of new therapeutic agents." Biochimica et Biophysica Acta (BBA) - Proteins and Proteomics **1696**(1): 1-14.
Conlon, J. M., M. Mechkarska, Y. H. Abdel-Wahab and P. R. Flatt (2018). "Peptides from frog skin with potential for development into agents for Type 2 diabetes therapy." Peptides **100**: 275-281.
Conlon, J. M., M. Mechkarska, J. M. Pantic, M. L. Lukic, L. Coquet, J. Leprince, P. F. Nielsen and A. C. Rinaldi (2013). "An immunomodulatory peptide related to frenatin 2 from skin secretions of the Tyrrhenian painted frog Discoglossus sardus (Alytidae)." Peptides **40**: 65-71.
Conlon, J. M., V. Musale, S. Attoub, M. L. Mangoni, J. Leprince, L. Coquet, T. Jouenne, Y. H. A. Abdel-Wahab, P. R. Flatt and A. C. Rinaldi (2017). "Cytotoxic peptides with insulin-releasing activities from

skin secretions of the Italian stream frog Rana italica (Ranidae)." Journal of Peptide Science **23**(10): 769-776.
Conlon, J. M. and A. Sonnevend (2010). Antimicrobial Peptides in Frog Skin Secretions. Antimicrobial Peptides: Methods and Protocols. A. Giuliani and A. C. Rinaldi. Totowa, NJ, Humana Press**:** 3-14.
Cudic, M. and L. Otvos, Jr. (2002). "Intracellular targets of antibacterial peptides." Curr Drug Targets **3**(2): 101-106.
D R Storm, a. K S Rosenthal and P. E. Swanson (1977). "Polymyxin and Related Peptide Antibiotics." Annual Review of Biochemistry **46**(1): 723-763.
Dannehl, C., T. Gutsmann and G. Brezesinski (2013). "Surface activity and structures of two fragments of the human antimicrobial LL-37." Colloids and Surfaces B: Biointerfaces **109**: 129-135.
Day, L., D. G. Bhandari, P. Greenwell, S. A. Leonard and J. D. Schofield (2006). "Characterization of wheat puroindoline proteins." The FEBS Journal **273**(23): 5358-5373.
De Smet, K. and R. Contreras (2005). "Human Antimicrobial Peptides: Defensins, Cathelicidins and Histatins." Biotechnology Letters **27**(18): 1337-1347.
Deslouches, B. and Y. P. Di (2017). "Antimicrobial peptides with selective antitumor mechanisms: prospect for anticancer applications." Oncotarget **8**(28): 46635-46651.
Doole, F. T., T. Kumarage, R. Ashkar and M. F. Brown (2022). "Cholesterol Stiffening of Lipid Membranes." The Journal of Membrane Biology **255**(4): 385-405.
Dorschner, R. A., V. K. Pestonjamasp, S. Tamakuwala, T. Ohtake, J. Rudisill, V. Nizet, B. Agerberth, G. H. Gudmundsson and R. L. Gallo (2001). "Cutaneous Injury Induces the Release of Cathelicidin Anti-Microbial Peptides Active Against Group A Streptococcus." Journal of Investigative Dermatology **117**(1): 91-97.
Duarte-Mata, D. I. and M. C. Salinas-Carmona (2023). "Antimicrobial peptides´ immune modulation role in intracellular bacterial infection." Front Immunol **14**: 1119574.
Dubos, R. J. (1939). "Studies on a Bactericidal Agent Extracted from a Soil Bacillus : I. Preparation of the Agent. Its Activity in Vitro." J Exp Med **70**(1): 1-10.
Dubos, R. J. (1939). "Studies on a Bactericidal Agent Extracted from a Soil Bacillus : Ii. Protective Effect of the Bactericidal Agent against Experimental Pneumococcus Infections in Mice." J Exp Med **70**(1): 11-17.
Duclohier, H. (2007). "Peptaibiotics and Peptaibols: An Alternative to Classical Antibiotics?" Chemistry & Biodiversity **4**(6): 1023-1026.
Duplantier, A. and M. van Hoek (2013). "The Human Cathelicidin Antimicrobial Peptide LL-37 as a Potential Treatment for Polymicrobial Infected Wounds." Frontiers in Immunology **4**(143).
Edelhoch, H. (1967). "Spectroscopic determination of tryptophan and tyrosine in proteins." J Biochemistry **6**(7): 1948-1954.
Edwards, I. A., A. G. Elliott, A. M. Kavanagh, M. A. T. Blaskovich and M. A. Cooper (2017). "Structure–Activity and −Toxicity Relationships of the Antimicrobial Peptide Tachyplesin-1." ACS Infectious Diseases **3**(12): 917-926.
Edwards, I. A., A. G. Elliott, A. M. Kavanagh, J. Zuegg, M. A. T. Blaskovich and M. A. Cooper (2016). "Contribution of Amphipathicity and Hydrophobicity to the Antimicrobial Activity and Cytotoxicity of β-Hairpin Peptides." ACS Infectious Diseases **2**(6): 442-450.
Elgarhy, L. H., M. M. Shareef and S. M. Moustafa (2015). "Granulysin expression increases with increasing clinical severity of psoriasis." Clinical and Experimental Dermatology **40**(4): 361-366.
Epand, R. F., J. E. Pollard, J. O. Wright, P. B. Savage and R. M. Epand (2010). "Depolarization, bacterial membrane composition, and the antimicrobial action of ceragenins." Antimicrob Agents Chemother **54**(9): 3708-3713.
Epand, R. M. and R. F. Epand (2009). "Lipid domains in bacterial membranes and the action of antimicrobial agents." Biochim Biophys Acta **1788**(1): 289-294.
Epand, R. M., A. Thomas, R. Brasseur and R. F. Epand (2010). Cholesterol Interaction with Proteins That Partition into Membrane Domains: An Overview. Cholesterol Binding and Cholesterol Transport

Proteins: Structure and Function in Health and Disease. J. R. Harris. Dordrecht, Springer Netherlands**:** 253-278.
Falla, T. J., D. N. Karunaratne and R. E. W. Hancock (1996). "Mode of Action of the Antimicrobial Peptide Indolicidin*." Journal of Biological Chemistry **271**(32): 19298-19303.
Fan, L., J. Sun, M. Zhou, J. Zhou, X. Lao, H. Zheng and H. Xu (2016). "DRAMP: a comprehensive data repository of antimicrobial peptides." Scientific Reports **6**: 24482.
Fehlbaum, P., P. Bulet, S. Chernysh, J. P. Briand, J. P. Roussel, L. Letellier, C. Hetru and J. A. Hoffmann (1996). "Structure-activity analysis of thanatin, a 21-residue inducible insect defense peptide with sequence homology to frog skin antimicrobial peptides." **93**(3): 1221-1225.
Fehlbaum, P., P. Bulet, L. Michaut, M. Lagueux, W. F. Broekaert, C. Hetru and J. A. Hoffmann (1994). "Insect immunity. Septic injury of Drosophila induces the synthesis of a potent antifungal peptide with sequence homology to plant antifungal peptides." Journal of Biological Chemistry **269**(52): 33159-33163.
Fernandez, D. I., A. P. Le Brun, T. C. Whitwell, M.-A. Sani, M. James and F. Separovic (2012). "The antimicrobial peptide aurein 1.2 disrupts model membranes via the carpet mechanism." Physical Chemistry Chemical Physics **14**(45): 15739-15751.
Finking, R. and M. A. Marahiel (2004). "Biosynthesis of Nonribosomal Peptides1." **58**(Volume 58, 2004): 453-488.
Fjell, C. D., J. A. Hiss, R. E. Hancock and G. Schneider (2011). "Designing antimicrobial peptides: form follows function." Nat Rev Drug Discov **11**(1): 37-51.
Frederick, H., R. D. Sarah and A. P. David (2009). "Anionic Antimicrobial Peptides from Eukaryotic Organisms." Current Protein & Peptide Science **10**(6): 585-606.
Ganz, T., M. E. Selsted, D. Szklarek, S. S. Harwig, K. Daher, D. F. Bainton and R. I. Lehrer (1985). "Defensins. Natural peptide antibiotics of human neutrophils." J Clin Invest **76**(4): 1427-1435.
Garg, A. D., D. V. Kanitkar, R. V. Hippargi and A. N. Gandhare (2007). "Antimicrobial activity of skin secretions isolated from Indian toad, Bufo melanostictus Schneider 1799." Nature Precedings.
Gaspar, D., A. S. Veiga and M. A. R. B. Castanho (2013). "From antimicrobial to anticancer peptides. A review." Frontiers in Microbiology **4**(294).
Gause, G. F. and M. G. Brazhnikova (1944). "Gramicidin S and its use in the Treatment of Infected Wounds." Nature **154**(3918): 703-703.
Glukhov, E., M. Stark, L. L. Burrows and C. M. Deber (2005). "Basis for Selectivity of Cationic Antimicrobial Peptides for Bacterial Versus Mammalian Membranes *." Journal of Biological Chemistry **280**(40): 33960-33967.
Gong, H., J. Zhang, X. Hu, Z. Li, K. Fa, H. Liu, T. A. Waigh, A. McBain and J. R. Lu (2019). "Hydrophobic Control of the Bioactivity and Cytotoxicity of de Novo-Designed Antimicrobial Peptides." ACS Applied Materials & Interfaces **11**(38): 34609-34620.
Gong, W., J. Wang, Z. Chen, B. Xia and G. Lu (2011). "Solution Structure of LCI, a Novel Antimicrobial Peptide from Bacillus subtilis." Biochemistry **50**(18): 3621-3627.
Gong, W., J. Wang, Z. Chen, B. Xia and G. J. B. Lu (2011). "Solution structure of LCI, a novel antimicrobial peptide from Bacillus subtilis." **50**(18): 3621-3627.
Gottler, L. M. and A. Ramamoorthy (2009). "Structure, membrane orientation, mechanism, and function of pexiganan — A highly potent antimicrobial peptide designed from magainin." Biochimica et Biophysica Acta (BBA) - Biomembranes **1788**(8): 1680-1686.
Graf, M., M. Mardirossian, F. Nguyen, A. C. Seefeldt, G. Guichard, M. Scocchi, C. A. Innis and D. N. Wilson (2017). "Proline-rich antimicrobial peptides targeting protein synthesis." Natural Product Reports **34**(7): 702-711.
Grünewald, J. and M. A. Marahiel (2013). Nonribosomal peptide synthesis, Elsevier Inc.
Gusman, H., J. Travis, E. J. Helmerhorst, J. Potempa, R. F. Troxler and F. G. Oppenheim (2001). "Salivary Histatin 5 Is an Inhibitor of Both Host and Bacterial Enzymes Implicated in Periodontal Disease." Infection and Immunity **69**(3): 1402-1408.

H Bohlmann, a. and K. Apel (1991). "Thionins." Annual Review of Plant Physiology and Plant Molecular Biology **42**(1): 227-240.
Hallock, K. J., D.-K. Lee and A. Ramamoorthy (2003). "MSI-78, an analogue of the magainin antimicrobial peptides, disrupts lipid bilayer structure via positive curvature strain." Biophysical journal **84**(5): 3052-3060.
Hamedi, F. and D. Mohammad-Aghaie (2020). "Molecular Insight into the Mutual Interactions of Two Transmembrane Domains of Human Glycine Receptor (TM23-GlyR), with the Lipid Bilayers." J Physical Chemistry Research **8**(3): 373-397.
Hammond, K., M. G. Ryadnov and B. W. Hoogenboom (2021). "Atomic force microscopy to elucidate how peptides disrupt membranes." Biochimica et Biophysica Acta (BBA) - Biomembranes **1863**(1): 183447.
Hancock, R. E. (1997). "Peptide antibiotics." Lancet **349**(9049): 418-422.
Hancock, R. E. and G. Diamond (2000). "The role of cationic antimicrobial peptides in innate host defences." Trends Microbiol **8**(9): 402-410.
Hancock, R. E. W. and A. Rozek (2002). "Role of membranes in the activities of antimicrobial cationic peptides." FEMS Microbiology Letters **206**(2): 143-149.
Hansen, J. N. (1994). "Nisin as a model food preservative." Crit Rev Food Sci Nutr **34**(1): 69-93.
Helmerhorst, E. J., W. van't Hof, P. Breeuwer, E. I. Veerman, T. Abee, R. F. Troxler, A. V. N. Amerongen and F. G. Oppenheim (2001). "Characterization of Histatin 5 with Respect to Amphipathicity, Hydrophobicity, and Effects on Cell and Mitochondrial Membrane Integrity Excludes a Candidacidal Mechanism of Pore Formation*." Journal of Biological Chemistry **276**(8): 5643-5649.
Hendrickson, W. A. and M. M. Teeter (1981). "Structure of the hydrophobic protein crambin determined directly from the anomalous scattering of sulphur." Nature **290**(5802): 107-113.
Hilchie, A. L., K. Wuerth and R. E. Hancock (2013). "Immune modulation by multifaceted cationic host defense (antimicrobial) peptides." Nat Chem Biol **9**(12): 761-768.
Hill, C. P., J. Yee, M. E. Selsted and D. Eisenberg (1991). "Crystal structure of defensin HNP-3, an amphiphilic dimer: Mechanisms of membrane permeabilization." Science **251**(5000): 1481-1485.
Hollmann, A., M. Martínez, M. E. Noguera, M. T. Augusto, A. Disalvo, N. C. Santos, L. Semorile and P. C. Maffía (2016). "Role of amphipathicity and hydrophobicity in the balance between hemolysis and peptide–membrane interactions of three related antimicrobial peptides." Colloids and Surfaces B: Biointerfaces **141**: 528-536.
Hoover, D. M., O. Chertov and J. Lubkowski (2001). "The Structure of Human β-Defensin-1: New insights into structural properties of β-defensins." Journal of Biological Chemistry **276**(42): 39021-39026.
Hoskin, D. W. and A. Ramamoorthy (2008). "Studies on anticancer activities of antimicrobial peptides." Biochimica et Biophysica Acta (BBA) - Biomembranes **1778**(2): 357-375.
Hotchkiss, R. D. and R. J. Dubos (1940). "Bactericidal fractions from an aerobic sporulating bacillus." Journal of Biological Chemistry **136**(3): 803-804.
Hotchkiss, R. D. and R. J. Dubos (1940). "Fractionation of the bactericidal agent from cultures of a soil bacillus." Journal of Biological Chemistry **132**(2): 791-792.
Hotchkiss, R. D. and R. J. Dubos (1941). "The isolation of bactericidal substances from cultures of *Bacillus brevis*." Journal of Biological Chemistry **141**(1): 155-162.
Hsu, C.-H., C. Chen, M.-L. Jou, A. Y.-L. Lee, Y.-C. Lin, Y.-P. Yu, W.-T. Huang and S.-H. Wu (2005). "Structural and DNA-binding studies on the bovine antimicrobial peptide, indolicidin: evidence for multiple conformations involved in binding to membranes and DNA." Nucleic Acids Research **33**(13): 4053-4064.
Huang, H.-J., C. R. Ross and F. Blecha (1997). "Chemoattractant properties of PR-39, a neutrophil antibacterial peptide." Journal of Leukocyte Biology **61**(5): 624-629.
Huang, H. W. (2000). "Action of Antimicrobial Peptides: Two-State Model." Biochemistry **39**(29): 8347-8352.

Huang, Y., L. He, G. Li, N. Zhai, H. Jiang and Y. Chen (2014). "Role of helicity of α-helical antimicrobial peptides to improve specificity." Protein Cell **5**(8): 631-642.
Hughes, P., E. Dennis, M. Whitecross, D. Llewellyn and P. Gage (2000). "The Cytotoxic Plant Protein, β-Purothionin, Forms Ion Channels in Lipid Membranes*." Journal of Biological Chemistry **275**(2): 823-827.
Hultmark, D., A. Engstrom, H. Bennich, R. Kapur and H. G. Boman (1982). "Insect immunity: isolation and structure of cecropin D and four minor antibacterial components from Cecropia pupae." Eur J Biochem **127**(1): 207-217.
Hultmark, D., H. Steiner, T. Rasmuson and H. G. Boman (1980). "Insect immunity. Purification and properties of three inducible bactericidal proteins from hemolymph of immunized pupae of Hyalophora cecropia." Eur J Biochem **106**(1): 7-16.
Hwang, P. M. and H. J. Vogel (1998). "Structure-function relationships of antimicrobial peptides." Biochemistry and Cell Biology **76**(2-3): 235-246.
Hyun, Y. (2025). "Cyclotides as novel plant-derived scaffolds for orally active cyclic peptide therapeutics." Mol Cells **48**(9): 100252.
Ilić, N., M. Novković, F. Guida, D. Xhindoli, M. Benincasa, A. Tossi and D. Juretić (2013). "Selective antimicrobial activity and mode of action of adepantins, glycine-rich peptide antibiotics based on anuran antimicrobial peptide sequences." Biochimica et Biophysica Acta (BBA) - Biomembranes **1828**(3): 1004-1012.
Jarczak, J., E. M. Kościuczuk, P. Lisowski, N. Strzałkowska, A. Jóźwik, J. Horbańczuk, J. Krzyżewski, L. Zwierzchowski and E. Bagnicka (2013). "Defensins: natural component of human innate immunity." Human immunology **74**(9): 1069-1079.
Jennings, C. V., K. J. Rosengren, N. L. Daly, M. Plan, J. Stevens, M. J. Scanlon, C. Waine, D. G. Norman, M. A. Anderson and D. J. Craik (2005). "Isolation, Solution Structure, and Insecticidal Activity of Kalata B2, a Circular Protein with a Twist: Do Möbius Strips Exist in Nature?" Biochemistry **44**(3): 851-860.
Johansson, J., G. H. Gudmundsson, M. E. Rottenberg, K. D. Berndt and B. Agerberth (1998). "Conformation-dependent antibacterial activity of the naturally occurring human peptide LL-37." Journal of Biological Chemistry **273**(6): 3718-3724.
Jones, C. R., M. Kuo, hang and W. A. Gibbons (1979). "Multiple solution conformations and internal rotations of the decapeptide gramicidin S." Journal of Biological Chemistry **254**(20): 10307-10312.
Kelly, J. B., A. C. Nolan and M. S. Zeden (2024). "How can we escape the ESKAPEs: Antimicrobial resistance mechanisms and what lies ahead?" PLOS Pathogens **20**(6): e1012270.
Kiss, G. and H. Michl (1962). "On the venomous skin secretion of the orange speckled frog Bombina variegata." Toxicon **1**: 33-39.
Ko, W. S., T. Y. Park, C. Park, Y. H. Kim, H. J. Yoon, S. Y. Lee, S. H. Hong, B. T. Choi, Y. T. Lee and Y. H. Choi (2005). "Induction of apoptosis by Chan Su, a traditional Chinese medicine, in human bladder carcinoma T24 cells." Oncol Rep **14**(2): 475-480.
Kościuczuk, E. M., P. Lisowski, J. Jarczak, N. Strzałkowska, A. Jóźwik, J. Horbańczuk, J. Krzyżewski, L. Zwierzchowski and E. Bagnicka (2012). "Cathelicidins: family of antimicrobial peptides. A review." Mol Biol Rep **39**(12): 10957-10970.
Krause, A., S. Neitz, H.-J. Mägert, A. Schulz, W.-G. Forssmann, P. Schulz-Knappe and K. Adermann (2000). "LEAP-1, a novel highly disulfide-bonded human peptide, exhibits antimicrobial activity11The nucleotide sequence data reported in this paper have been submitted to the GenBank/EBI Data Bank with accession number AJ277280. Scanning of this sequence against the data base resulted in the identification of related sequences with the accession numbers AD000684 and P81172." FEBS Letters **480**(2): 147-150.
Kumar, P., J. N. Kizhakkedathu and S. K. Straus (2018). "Antimicrobial Peptides: Diversity, Mechanism of Action and Strategies to Improve the Activity and Biocompatibility In Vivo." Biomolecules **8**(1): 4.
Kuroda, K., K. Okumura, H. Isogai and E. Isogai (2015). "The Human Cathelicidin Antimicrobial Peptide LL-37 and Mimics are Potential Anticancer Drugs." Frontiers in Oncology **5**(144).

Lai, R., H. Liu, W. Hui Lee and Y. Zhang (2002). "An anionic antimicrobial peptide from toad Bombina maxima." Biochem Biophys Res Commun **295**(4): 796-799.
Lai, R., H. Liu, W. H. Lee and Y. Zhang (2002). "An anionic antimicrobial peptide from toad Bombina maxima." Biochemical and biophysical research communications **295**(4): 796-799.
Lai, R., Y. T. Zheng, J. H. Shen, G. J. Liu, H. Liu, W. H. Lee, S. Z. Tang and Y. Zhang (2002). "Antimicrobial peptides from skin secretions of Chinese red belly toad Bombina maxima." Peptides **23**(3): 427-435.
Lai, Y. and R. L. Gallo (2009). "AMPed up immunity: how antimicrobial peptides have multiple roles in immune defense." Trends Immunol **30**(3): 131-141.
Lambert, J., E. Keppi, J.-L. Dimarcq, C. Wicker, J.-M. Reichhart, B. Dunbar, P. Lepage, A. Van Dorsselaer, J. Hoffmann and J. J. P. o. t. N. A. o. S. Fothergill (1989). "Insect immunity: isolation from immune blood of the dipteran Phormia terranovae of two insect antibacterial peptides with sequence homology to rabbit lung macrophage bactericidal peptides." **86**(1): 262-266.
Landon, C., P. Sodano, C. Hetru, J. Hoffmann and M. Ptak (1997). "Solution structure of drosomycin, the first inducible antifungal protein from insects." Protein Sci **6**(9): 1878-1884.
Lauth, X., H. Shike, J. C. Burns, M. E. Westerman, V. E. Ostland, J. M. Carlberg, J. C. Van Olst, V. Nizet, S. W. Taylor, C. Shimizu and P. Bulet (2002). "Discovery and Characterization of Two Isoforms of Moronecidin, a Novel Antimicrobial Peptide from Hybrid Striped Bass*." Journal of Biological Chemistry **277**(7): 5030-5039.
Lawyer, C., S. Pai, M. Watabe, P. Borgia, T. Mashimo, L. Eagleton and K. Watabe (1996). "Antimicrobial activity of a 13 amino acid tryptophan-rich peptide derived from a putative porcine precursor protein of a novel family of antibacterial peptides." FEBS Lett **390**(1): 95-98.
Lawyer, C., S. Pai, M. Watabe, P. Borgia, T. Mashimo, L. Eagleton and K. J. F. l. Watabe (1996). "Antimicrobial activity of a 13 amino acid tryptophan-rich peptide derived from a putative porcine precursor protein of a novel family of antibacterial peptides." **390**(1): 95-98.
Lázár, V., A. Martins, R. Spohn, L. Daruka, G. Grézal, G. Fekete, M. Számel, P. K. Jangir, B. Kintses, B. Csörgő, Á. Nyerges, Á. Györkei, A. Kincses, A. Dér, F. R. Walter, M. A. Deli, E. Urbán, Z. Hegedűs, G. Olajos, O. Méhi, B. Bálint, I. Nagy, T. A. Martinek, B. Papp and C. Pál (2018). "Antibiotic-resistant bacteria show widespread collateral sensitivity to antimicrobial peptides." Nature Microbiology **3**(6): 718-731.
Lee, A. G. (2004). "How lipids affect the activities of integral membrane proteins." Biochimica et Biophysica Acta (BBA) - Biomembranes **1666**(1): 62-87.
Lee, I. H., Y. Cho and R. I. Lehrer (1997). "Effects of pH and salinity on the antimicrobial properties of clavanins." Infection and immunity **65**(7): 2898-2903.
Lee, I. H., C. Zhao, Y. Cho, S. S. L. Harwig, E. L. Cooper and R. I. Lehrer (1997). "Clavanins, α-helical antimicrobial peptides from tunicate hemocytes." **400**(2): 158-162.
Lehrer, R. and T. Ganz (2002). "Defensins of vertebrate animals." Current opinion in immunology **14**: 96-102.
Lei, J., L. Sun, S. Huang, C. Zhu, P. Li, J. He, V. Mackey, D. H. Coy and Q. He (2019). "The antimicrobial peptides and their potential clinical applications." American journal of translational research **11**(7): 3919-3931.
Lemkul, J. A., W. J. Allen and D. R. Bevan (2010). "Practical Considerations for Building GROMOS-Compatible Small-Molecule Topologies." Journal of Chemical Information and Modeling **50**(12): 2221-2235.
Lequin, O., F. Bruston, O. Convert, G. Chassaing and P. Nicolas (2003). "Helical Structure of Dermaseptin B2 in a Membrane-Mimetic Environment." Biochemistry **42**(34): 10311-10323.
Li, B.-J., H.-Y. Tian, D.-M. Zhang, Y.-H. Lei, L. Wang, R.-W. Jiang and W.-C. Ye (2015). "Bufadienolides with cytotoxic activity from the skins of Bufo bufo gargarizans." Fitoterapia **105**: 7-15.
Li, D., L. Zhang, H. Yin, H. Xu, J. S. Trask, D. G. Smith, Y. Li, M. Yang and Q. Zhu (2014). "Evolution of primate α and θ defensins revealed by analysis of genomes." Molecular Biology Reports **41**(6): 3859-3866.

Li, J., M. Post, R. Volk, Y. Gao, M. Li, C. Metais, K. Sato, J. Tsai, W. Aird, R. D. Rosenberg, T. G. Hampton, J. Li, F. Sellke, P. Carmeliet and M. Simons (2000). "PR39, a peptide regulator of angiogenesis." Nature Medicine **6**(1): 49-55.
Li, Y.-X., Z. Zhong, W.-P. Zhang and P.-Y. Qian (2018). "Discovery of cationic nonribosomal peptides as Gram-negative antibiotics through global genome mining." Nature Communications **9**(1): 3273.
Liang, Y., X. Zhang, Y. Yuan, Y. Bao and M. J. B. S. Xiong (2020). "Role and modulation of the secondary structure of antimicrobial peptides to improve selectivity." **8**(24): 6858-6866.
Libério, M. S., G. A. Joanitti, R. B. Azevedo, E. M. Cilli, L. C. Zanotta, A. C. Nascimento, M. V. Sousa, O. R. Pires Júnior, W. Fontes and M. S. Castro (2011). "Anti-proliferative and cytotoxic activity of pentadactylin isolated from Leptodactylus labyrinthicus on melanoma cells." Amino Acids **40**(1): 51-59.
Lin, M.-S., H.-M. Chiu, F.-J. Fan, H.-T. Tsai, S. S.-S. Wang, Y. Chang and W.-Y. Chena (2007). "Kinetics and enthalpy measurements of interaction between ß-amyloid and liposomes by surface plasmon resonance and isothermal titration microcalorimetry." J Colloids Surfaces B: Biointerfaces **58**: 231-236.
Loll, P. J., E. C. Upton, V. Nahoum, N. J. Economou and S. Cocklin (2014). "The high resolution structure of tyrocidine A reveals an amphipathic dimer." Biochimica et biophysica acta **1838**(5): 1199-1207.
Long, Q., L. Li, H. Wang, M. Li, L. Wang, M. Zhou, Q. Su, T. Chen and Y. Wu (2019). "Novel peptide dermaseptin-PS1 exhibits anticancer activity via induction of intrinsic apoptosis signalling." Journal of Cellular and Molecular Medicine **23**(2): 1300-1312.
Maget-Dana, R. (1999). "The monolayer technique: a potent tool for studying the interfacial properties of antimicrobial and membrane-lytic peptides and their interactions with lipid membranes." Biochimica et Biophysica Acta (BBA) - Biomembranes **1462**(1): 109-140.
Mahlapuu, M., J. Håkansson, L. Ringstad and C. Björn (2016). "Antimicrobial Peptides: An Emerging Category of Therapeutic Agents." Frontiers in cellular and infection microbiology **6**: 194-194.
Mangoni, M. L., A. M. McDermott and M. Zasloff (2016). "Antimicrobial peptides and wound healing: biological and therapeutic considerations." Exp Dermatol **25**(3): 167-173.
Mankelow, D. P. and B. A. Neilan (2000). "Non-ribosomal peptide antibiotics." Expert Opinion on Therapeutic Patents **10**(10): 1583-1591.
Mansour, S. C., O. M. Pena and R. E. W. Hancock (2014). "Host defense peptides: front-line immunomodulators." Trends in Immunology **35**(9): 443-450.
Marion, D., M. Zasloff and A. Bax (1988). "A two-dimensional NMR study of the antimicrobial peptide magainin 2." FEBS Letters **227**(1): 21-26.
Marsh, D. (1996). "Lateral pressure in membranes." Biochim Biophys Acta **1286**(3): 183-223.
Martin, P. (1997). "Wound Healing--Aiming for Perfect Skin Regeneration." Science **276**(5309): 75.
Matsuzaki, K. (2009). "Control of cell selectivity of antimicrobial peptides." Biochimica et Biophysica Acta (BBA) - Biomembranes **1788**(8): 1687-1692.
McAuliffe, O., R. P. Ross and C. Hill (2001). "Lantibiotics: structure, biosynthesis and mode of action." FEMS Microbiol Rev **25**(3): 285-308.
McBain, J. W., R. C. Bacon and H. D. Bruce (1939). "Optical surface thickness of pure water." The Journal of Chemical Physics **7**(9): 818-823.
Meng, Z., P. Yang, Y. Shen, W. Bei, Y. Zhang, Y. Ge, R. A. Newman, L. Cohen, L. Liu, B. Thornton, D. Z. Chang, Z. Liao and R. Kurzrock (2009). "Pilot study of huachansu in patients with hepatocellular carcinoma, nonsmall-cell lung cancer, or pancreatic cancer." Cancer **115**(22): 5309-5318.
Meng, Z., P. Yang, Y. Shen, W. Bei, Y. Zhang, Y. Ge, R. A. Newman, L. Cohen, L. Liu, B. Thornton, D. Z. Chang, Z. Liao and R. Kurzrock (2009). "Pilot study of huachansu in patients with hepatocellular carcinoma, nonsmall-cell lung cancer, or pancreatic cancer." Cancer **115**(22): 5309-5318.
Merrifield, R. B., L. D. Vizioli and H. G. Boman (1982). "Synthesis of the antibacterial peptide cecropin A(1-33)." Biochemistry **21**(20): 5020-5031.
Micsonai, A., F. Wien, É. Bulyáki, J. Kun, É. Moussong, Y.-H. Lee, Y. Goto, M. Réfrégiers and J. J. N. a. r. Kardos (2018). "BeStSel: a web server for accurate protein secondary structure prediction and fold recognition from the circular dichroism spectra." **46**(W1): W315-W322.

Mizukawa, N., K. Sugiyama, T. Ueno, K. Mishima, S. Takagi and T. Sugahara (2000). "Detection of human α-defensin-1, an antimicrobial peptide, in the fluid of jaw cysts." Oral Surgery, Oral Medicine, Oral Pathology, Oral Radiology, and Endodontology **90**(1): 78-81.
Mo, G.-X., X.-W. Bai, Z.-J. Li, X.-W. Yan, X.-Q. He and M.-Q. Rong (2014). "A Novel Insulinotropic Peptide from the Skin Secretions of Amolops loloensis Frog." Natural products and bioprospecting **4**(5): 309-313.
Mohapatra, A. and N. Chaudhary (2021). "N-terminal acetylation does not alter α-synuclein's interfacial properties." International Journal of Biological Macromolecules **174**: 69-76.
Mohapatra, A., A. Hans and N. Chaudhary (2023). "Interfacial properties of α-synuclein's Parkinsonian variants." Biophysical Chemistry **297**: 107006.
Mor, A. (2009). "Multifunctional host defense peptides: antiparasitic activities." The FEBS Journal **276**(22): 6474-6482.
Mordhorst, S., F. Ruijne, A. L. Vagstad, O. P. Kuipers and J. Piel (2023). "Emulating nonribosomal peptides with ribosomal biosynthetic strategies." RSC Chemical Biology **4**(1): 7-36.
Muñoz-Camargo, C., V. A. Salazar, L. Barrero-Guevara, S. Camargo, A. Mosquera, H. Groot and E. Boix (2018). "Unveiling the Multifaceted Mechanisms of Antibacterial Activity of Buforin II and Frenatin 2.3S Peptides from Skin Micro-Organs of the Orinoco Lime Treefrog (Sphaenorhynchus lacteus)." International journal of molecular sciences **19**(8): 2170.
Munshi, T., A. Sparrow, B. W. Wren, R. Reljic and S. J. Willcocks (2020). "The Antimicrobial Peptide, Bactenecin 5, Supports Cell-Mediated but Not Humoral Immunity in the Context of a Mycobacterial Antigen Vaccine Model." Antibiotics (Basel, Switzerland) **9**(12): 926.
Musale, V., B. Casciaro, M. L. Mangoni, Y. H. A. Abdel-Wahab, P. R. Flatt and J. M. Conlon (2018). "Assessment of the potential of temporin peptides from the frog Rana temporaria (Ranidae) as anti-diabetic agents." Journal of Peptide Science **24**(2): e3065.
Mygind, P. H., R. L. Fischer, K. M. Schnorr, M. T. Hansen, C. P. Sönksen, S. Ludvigsen, D. Raventós, S. Buskov, B. Christensen, L. De Maria, O. Taboureau, D. Yaver, S. G. Elvig-Jørgensen, M. V. Sørensen, B. E. Christensen, S. Kjærulff, N. Frimodt-Moller, R. I. Lehrer, M. Zasloff and H.-H. Kristensen (2005). "Plectasin is a peptide antibiotic with therapeutic potential from a saprophytic fungus." Nature **437**(7061): 975-980.
Nair, S. S., J. Romanuka, M. Billeter, L. Skjeldal, M. R. Emmett, C. L. Nilsson and A. G. Marshall (2006). "Structural characterization of an unusually stable cyclic peptide, kalata B2 from Oldenlandia affinis." Biochimica et Biophysica Acta (BBA) - Proteins and Proteomics **1764**(10): 1568-1576.
Nakamura, T., H. Furunaka, T. Miyata, F. Tokunaga, T. Muta, S. Iwanaga, M. Niwa, T. Takao and Y. Shimonishi (1988). "Tachyplesin, a class of antimicrobial peptide from the hemocytes of the horseshoe crab (Tachypleus tridentatus). Isolation and chemical structure." Journal of Biological Chemistry **263**(32): 16709-16713.
Noble, A. J., H. Wei, V. P. Dandey, Z. Zhang, Y. Z. Tan, C. S. Potter and B. Carragher (2018). "Reducing effects of particle adsorption to the air–water interface in cryo-EM." Nature Methods **15**(10): 793-795.
Oard, S. and F. Enright (2006). "Expression of the antimicrobial peptides in plants to control phytopathogenic bacteria and fungi." Plant cell reports **25**(6): 561-572.
Olson, L., A. M. Soto, F. C. Knoop and J. M. Conlon (2001). "Pseudin-2: An Antimicrobial Peptide with Low Hemolytic Activity from the Skin of the Paradoxical Frog." Biochemical and Biophysical Research Communications **288**(4): 1001-1005.
Ongpipattanakul, C., E. K. Desormeaux, A. DiCaprio, W. A. van der Donk, D. A. Mitchell and S. K. Nair (2022). "Mechanism of Action of Ribosomally Synthesized and Post-Translationally Modified Peptides." Chemical Reviews **122**(18): 14722-14814.
Oppenheim, F., T. Xu, F. McMillian, S. Levitz, R. Diamond, G. Offner and R. Troxler (1988). "Histatins, a novel family of histidine-rich proteins in human parotid secretion. Isolation, characterization, primary structure, and fungistatic effects on Candida albicans." Journal of Biological Chemistry **263**(16): 7472-7477.

Oppenheim, F. G., Y. C. Yang, R. D. Diamond, D. Hyslop, G. D. Offner and R. F. Troxler (1986). "The primary structure and functional characterization of the neutral histidine-rich polypeptide from human parotid secretion." Journal of Biological Chemistry **261**(3): 1177-1182.
Organization, W. H. (2020). "Global antimicrobial resistance surveillance system (GLASS) report: early implementation 2020."
Ouellette, A. J. (2006). "Paneth cell alpha-defensin synthesis and function." Curr Top Microbiol Immunol **306**: 1-25.
Pahr, S., C. Constantin, N. G. Papadopoulos, S. Giavi, M. Mäkelä, A. Pelkonen, C. Ebner, A. Mari, S. Scheiblhofer, J. Thalhamer, M. Kundi, S. Vrtala, I. Mittermann and R. Valenta (2013). "α-Purothionin, a new wheat allergen associated with severe allergy." Journal of Allergy and Clinical Immunology **132**(4): 1000-1003.e1004.
Pál, T., B. Abraham, Á. Sonnevend, P. Jumaa and J. M. J. I. j. o. a. a. Conlon (2006). "Brevinin-1BYa: a naturally occurring peptide from frog skin with broad-spectrum antibacterial and antifungal properties." **27**(6): 525-529.
Pantic, J. M., I. P. Jovanovic, G. D. Radosavljevic, N. N. Arsenijevic, J. M. Conlon and M. L. Lukic (2017). "The Potential of Frog Skin-Derived Peptides for Development into Therapeutically-Valuable Immunomodulatory Agents." Molecules **22**(12): 2071.
Pantic, J. M., I. P. Jovanovic, G. D. Radosavljevic, N. M. Gajovic, N. N. Arsenijevic, J. M. Conlon and M. L. Lukic (2017). "The frog skin host-defense peptide frenatin 2.1S enhances recruitment, activation and tumoricidal capacity of NK cells." Peptides **93**: 44-50.
Park, C. B., H. S. Kim and S. C. Kim (1998). "Mechanism of Action of the Antimicrobial Peptide Buforin II: Buforin II Kills Microorganisms by Penetrating the Cell Membrane and Inhibiting Cellular Functions." Biochemical and Biophysical Research Communications **244**(1): 253-257.
Park, C. B., M. S. Kim and S. C. Kim (1996). "A Novel Antimicrobial Peptide fromBufo bufo gargarizans." Biochemical and Biophysical Research Communications **218**(1): 408-413.
Park, C. B., K.-S. Yi, K. Matsuzaki, M. S. Kim and S. C. Kim (2000). "Structure–activity analysis of buforin II, a histone H2A-derived antimicrobial peptide: The proline hinge is responsible for the cell-penetrating ability of buforin II." **97**(15): 8245-8250.
Park, I. Y., J. H. Cho, K. S. Kim, Y.-B. Kim, M. S. Kim and S. C. Kim (2004). "Helix Stability Confers Salt Resistance upon Helical Antimicrobial Peptides*." Journal of Biological Chemistry **279**(14): 13896-13901.
Pasupuleti, M., A. Schmidtchen and M. Malmsten (2012). "Antimicrobial peptides: key components of the innate immune system." Critical Reviews in Biotechnology **32**(2): 143-171.
Patil, A., A. L. Hughes and G. Zhang (2004). "Rapid evolution and diversification of mammalian α-defensins as revealed by comparative analysis of rodent and primate genes." Physiological genomics **20**(1): 1-11.
Peschel, A. and H. G. Sahl (2006). "The co-evolution of host cationic antimicrobial peptides and microbial resistance." Nat Rev Microbiol **4**(7): 529-536.
Piktel, E., K. Niemirowicz, U. Wnorowska, M. Wątek, T. Wollny, K. Głuszek, S. Góźdź, I. Levental and R. Bucki (2016). "The Role of Cathelicidin LL-37 in Cancer Development." Archivum immunologiae et therapiae experimentalis **64**(1): 33-46.
Popov, C. S. F. C., B. S. Magalhães, B. J. Goodfellow, A. L. Bocca, D. M. Pereira, P. B. Andrade, P. Valentão, P. J. B. Pereira, J. E. Rodrigues, P. H. de Holanda Veloso and T. M. B. Rezende (2019). "Host-defense peptides AC12, DK16 and RC11 with immunomodulatory activity isolated from Hypsiboas raniceps skin secretion." Peptides **113**: 11-21.
Powers, J.-P. S. and R. E. W. Hancock (2003). "The relationship between peptide structure and antibacterial activity." Peptides **24**(11): 1681-1691.
Powers, J.-P. S., A. Rozek and R. E. W. Hancock (2004). "Structure–activity relationships for the β-hairpin cationic antimicrobial peptide polyphemusin I." Biochimica et Biophysica Acta (BBA) - Proteins and Proteomics **1698**(2): 239-250.

Pronk, S., S. Pall, R. Schulz, P. Larsson, P. Bjelkmar, R. Apostolov, M. R. Shirts, J. C. Smith, P. M. Kasson, D. van der Spoel, B. Hess and E. Lindahl (2013). "GROMACS 4.5: a high-throughput and highly parallel open source molecular simulation toolkit." Bioinformatics **29**(7): 845-854.
Qi, F., A. Li, Y. Inagaki, N. Kokudo, S. Tamura, M. Nakata and W. Tang (2011). "Antitumor activity of extracts and compounds from the skin of the toad Bufo bufo gargarizans Cantor." International Immunopharmacology **11**(3): 342-349.
Qi, Y., H. I. Ingólfsson, X. Cheng, J. Lee, S. J. Marrink and W. Im (2015). "CHARMM-GUI martini maker for coarse-grained simulations with the martini force field." J Journal of Chemical Theory Computation **11**(9): 4486-4494.
Qiu, D. Z., Z. J. Zhang, W. Z. Wu and Y. K. Yang (2013). "Bufalin, a component in Chansu, inhibits proliferation and invasion of hepatocellular carcinoma cells." BMC Complement Altern Med **13**: 185.
Radermacher, S. W., V. M. Schoop and H. J. Schluesener (1993). "Bactenecin, a leukocytic antimicrobial peptide, is cytotoxic to neuronal and glial cells." J Neurosci Res **36**(6): 657-662.
Raj, P. A., M. Edgerton and M. J. Levine (1990). "Salivary histatin 5: dependence of sequence, chain length, and helical conformation for candidacidal activity." Journal of Biological Chemistry **265**(7): 3898-3905.
Reddy, K. V. R., S. K. Shahani and P. K. Meherji (1996). "Spermicidal activity of Magainins: in vitro and in vivo studies." Contraception **53**(4): 205-210.
Renato, G., Z. Margherita, B. Monica, P. Elena and M. Monica (2002). "Pro-rich Antimicrobial Peptides from Animals: Structure, Biological Functions and Mechanism of Action." Current Pharmaceutical Design **8**(9): 763-778.
Riedl, S., D. Zweytick and K. Lohner (2011). "Membrane-active host defense peptides--challenges and perspectives for the development of novel anticancer drugs." Chemistry and physics of lipids **164**(8): 766-781.
Riley, M. A. and J. E. J. A. R. i. M. Wertz (2002). "Bacteriocins: evolution, ecology, and application." **56**(1): 117-137.
Rinaldi, A. C., M. L. Mangoni, A. Rufo, C. Luzi, D. Barra, H. Zhao, P. K. Kinnunen, A. Bozzi, A. d. Giulio and M. J. B. J. Simmaco (2002). "Temporin L: antimicrobial, haemolytic and cytotoxic activities, and effects on membrane permeabilization in lipid vesicles." **368**(1): 91-100.
Rodríguez, C., L. Rollins-Smith, R. Ibáñez, A. A. Durant-Archibold and M. Gutiérrez (2017). "Toxins and pharmacologically active compounds from species of the family Bufonidae (Amphibia, Anura)." Journal of Ethnopharmacology **198**: 235-254.
Rollins-Smith, L., L. Reinert, C. J O'Leary, L. E Houston and D. Woodhams (2005). Antimicrobial Peptide Defenses in Amphibian Skin.
Romeo, D., B. Skerlavaj, M. Bolognesi and R. Gennaro (1988). "Structure and bactericidal activity of an antibiotic dodecapeptide purified from bovine neutrophils." J Biol Chem **263**(20): 9573-9575.
Rossetti, P., M. F. Trollmann, C. Wichmann, T. Gutsmann, C. Eggeling and R. A. J. S. Böckmann (2024). "From Membrane Composition to Antimicrobial Strategies: Experimental and Computational Approaches to AMP Design and Selectivity." 2411476.
Rozek, T., K. L. Wegener, J. H. Bowie, I. N. Olver, J. A. Carver, J. C. Wallace and M. J. J. E. J. o. B. Tyler (2000). "The antibiotic and anticancer active aurein peptides from the Australian Bell Frogs Litoria aurea and Litoria raniformis: The solution structure of aurein 1.2." **267**(17): 5330-5341.
Sai, K. P., M. V. Jagannadham, M. Vairamani, N. P. Raju, A. S. Devi, R. Nagaraj and N. Sitaram (2001). "Tigerinins: Novel Antimicrobial Peptides from the Indian FrogRana tigerina *." Journal of Biological Chemistry **276**(4): 2701-2707.
Saikia, K. and N. Chaudhary (2018). "Antimicrobial peptides from C-terminal amphipathic region of E. coli FtsA." Biochimica et Biophysica Acta (BBA)-Biomembranes **1860**(12): 2506-2514.
Saikia, K. and N. Chaudhary (2018). "Interaction of MreB-derived antimicrobial peptides with membranes." Biochemical and Biophysical Research Communications **498**(1): 58-63.
Saikia, K., Y. D. Sravani, V. Ramakrishnan and N. Chaudhary (2017). "Highly potent antimicrobial peptides from N-terminal membrane-binding region of E. coli MreB." Scientific Reports **7**(1): 42994.

Saikia, K., Y. D. Sravani, V. Ramakrishnan and N. Chaudhary (2017). "Highly potent antimicrobial peptides from N-terminal membrane-binding region of E. coli MreB." J Scientific Reports **7**(1): 42994.
Sanderson, J. M. (2005). "Peptide–lipid interactions: insights and perspectives." Organic & Biomolecular Chemistry **3**(2): 201-212.
Sato, H. and J. B. Feix (2006). "Peptide–membrane interactions and mechanisms of membrane destruction by amphipathic α-helical antimicrobial peptides." Biochimica et Biophysica Acta (BBA) - Biomembranes **1758**(9): 1245-1256.
Savitzky, A. and M. J. J. A. c. Golay (1964). "Smoothing and differentiation of data by simplified least squares procedures." **36**(8): 1627-1639.
Schibli, D. J., L. T. Nguyen, S. D. Kernaghan, Ø. Rekdal and H. J. Vogel (2006). "Structure-function analysis of tritrpticin analogs: potential relationships between antimicrobial activities, model membrane interactions, and their micelle-bound NMR structures." Biophysical journal **91**(12): 4413-4426.
Schittek, B., R. Hipfel, B. Sauer, J. Bauer, H. Kalbacher, S. Stevanovic, M. Schirle, K. Schroeder, N. Blin, F. Meier, G. Rassner and C. Garbe (2001). "Dermcidin: a novel human antibiotic peptide secreted by sweat glands." Nature Immunology **2**(12): 1133-1137.
Schmid, N., A. P. Eichenberger, A. Choutko, S. Riniker, M. Winger, A. E. Mark and W. F. van Gunsteren (2011). "Definition and testing of the GROMOS force-field versions 54A7 and 54B7." Eur Biophys J **40**(7): 843-856.
Selsted, M. E. (2004). "Theta-defensins: cyclic antimicrobial peptides produced by binary ligation of truncated alpha-defensins." Curr Protein Pept Sci **5**(5): 365-371.
Selsted, M. E. and S. S. Harwig (1989). "Determination of the disulfide array in the human defensin HNP-2. A covalently cyclized peptide." J Biol Chem **264**(7): 4003-4007.
Selsted, M. E., M. J. Novotny, W. L. Morris, Y. Q. Tang, W. Smith and J. S. Cullor (1992). "Indolicidin, a novel bactericidal tridecapeptide amide from neutrophils." J Biol Chem **267**(7): 4292-4295.
Selsted, M. E., Y. Q. Tang, W. L. Morris, P. A. McGuire, M. J. Novotny, W. Smith, A. H. Henschen and J. S. Cullor (1993). "Purification, primary structures, and antibacterial activities of beta-defensins, a new family of antimicrobial peptides from bovine neutrophils." Journal of Biological Chemistry **268**(9): 6641-6648.
Shaw, J. E., J.-R. Alattia, J. E. Verity, G. G. Privé and C. M. Yip (2006). "Mechanisms of antimicrobial peptide action: Studies of indolicidin assembly at model membrane interfaces by in situ atomic force microscopy." Journal of Structural Biology **154**(1): 42-58.
Shi, Y., C. Li, M. Wang, Z. Chen, Y. Luo, X.-s. Xia, Y. Song, Y. Sun and A. M. Zhang (2020). ACS Omega **5**(16): 9301-9310.
Shi, Y., C. Li, M. Wang, Z. Chen, Y. Luo, X.-s. Xia, Y. Song, Y. Sun and A. M. Zhang (2020). "Cathelicidin-DM is an Antimicrobial Peptide from Duttaphrynus melanostictus and Has Wound-Healing Therapeutic Potential." ACS Omega **5**(16): 9301-9310.
Shin Ko, W., T. Yeol Park, C. Park, Y. Hee Kim, H. Jung Yoon, S. Yeon Lee, S. Hoon Hong, B. Tae Choi, Y. Tae Lee and Y. Choi (2005). Induction of apoptosis by Chan Su, a traditional Chinese medicine, in human bladder carcinoma T24 cells.
Shinnar, A. E., K. L. Butler and H. J. Park (2003). "Cathelicidin family of antimicrobial peptides: proteolytic processing and protease resistance." Bioorganic Chemistry **31**(6): 425-436.
Silva, P. I., S. Daffre and P. Bulet (2000). "Isolation and Characterization of Gomesin, an 18-Residue Cysteine-rich Defense Peptide from the Spider Acanthoscurria gomesiana Hemocytes with Sequence Similarities to Horseshoe Crab Antimicrobial Peptides of the Tachyplesin Family*." Journal of Biological Chemistry **275**(43): 33464-33470.
Simmaco, M., G. Kreil and D. Barra (2009). "Bombinins, antimicrobial peptides from Bombina species." Biochimica et Biophysica Acta (BBA) - Biomembranes **1788**(8): 1551-1555.
Simons, A., K. Alhanout and R. E. J. M. Duval (2020). "Bacteriocins, antimicrobial peptides from bacterial origin: overview of their biology and their impact against multidrug-resistant bacteria." **8**(5): 639.

Sitaram, N. and R. Nagaraj (1999). "Interaction of antimicrobial peptides with biological and model membranes: structural and charge requirements for activity." Biochimica et Biophysica Acta (BBA) - Biomembranes **1462**(1): 29-54.
Sitaram, N. and R. Nagaraj (2002). "The Therapeutic Potential of Host-Defense Antimicrobial Peptides." Current Drug Targets **3**(3): 259-267.
Sitaram, N., C. Subbalakshmi and R. Nagaraj (2003). "Indolicidin, a 13-residue basic antimicrobial peptide rich in tryptophan and proline, interacts with Ca(2+)-calmodulin." Biochem Biophys Res Commun **309**(4): 879-884.
Skerlavaj, B., R. Gennaro, L. Bagella, L. Merluzzi, A. Risso and M. Zanetti (1996). "Biological Characterization of Two Novel Cathelicidin-derived Peptides and Identification of Structural Requirements for Their Antimicrobial and Cell Lytic Activities*." Journal of Biological Chemistry **271**(45): 28375-28381.
Stec, B. (2006). "Plant thionins--the structural perspective." Cell Mol Life Sci **63**(12): 1370-1385.
Steinberg, D. A., M. A. Hurst, C. A. Fujii, A. H. Kung, J. F. Ho, F. C. Cheng, D. J. Loury and J. C. Fiddes (1997). "Protegrin-1: a broad-spectrum, rapidly microbicidal peptide with in vivo activity." Antimicrobial Agents and Chemotherapy **41**(8): 1738-1742.
Steiner, H., D. Hultmark, Å. Engström, H. Bennich and H. G. Boman (1981). "Sequence and specificity of two antibacterial proteins involved in insect immunity." Nature **292**(5820): 246-248.
Stotz, H. U., J. G. Thomson and Y. Wang (2009). "Plant defensins: defense, development and application." Plant Signal Behav **4**(11): 1010-1012.
Stuart, L. and T. Harris (1942). "Bactericidal and fungicidal properties of a crystalline protein isolated from unbleached wheat flour." Cereal Chem **19**: 288-300.
Sun, T., B. Zhan and Y. Gao (2015). "A novel cathelicidin from Bufo bufo gargarizans Cantor showed specific activity to its habitat bacteria." Gene **571**(2): 172-177.
Suresh, A. and C. Verma (2006). "Modelling study of dimerization in mammalian defensins." BMC Bioinformatics **7**(5): S17.
Tajbakhsh, M., A. Karimi, F. Fallah and M. Akhavan (2017). "Overview of ribosomal and non-ribosomal antimicrobial peptides produced by gram positive bacteria." Cellular and Molecular Biology **63**(10): 20-32.
Takahashi, T., N. N. Kulkarni, E. Y. Lee, L.-j. Zhang, G. C. L. Wong and R. L. Gallo (2018). "Cathelicidin promotes inflammation by enabling binding of self-RNA to cell surface scavenger receptors." Scientific Reports **8**(1): 4032.
Tam, J. P., Y.-A. Lu and J.-L. Yang (2002). "Correlations of Cationic Charges with Salt Sensitivity and Microbial Specificity of Cystine-stabilized β-Strand Antimicrobial Peptides*." Journal of Biological Chemistry **277**(52): 50450-50456.
Tang, Y. Q. and M. E. Selsted (1993). "Characterization of the disulfide motif in BNBD-12, an antimicrobial beta-defensin peptide from bovine neutrophils." Journal of Biological Chemistry **268**(9): 6649-6653.
Tatham, A. S., R. C. Hider and A. F. Drake (1983). "The effect of counterions on melittin aggregation." The Biochemical journal **211**(3): 683-686.
Teixeira, V., M. J. Feio and M. Bastos (2012). "Role of lipids in the interaction of antimicrobial peptides with membranes." Progress in Lipid Research **51**(2): 149-177.
Teixeira, V., M. J. Feio and M. Bastos (2012). "Role of lipids in the interaction of antimicrobial peptides with membranes." Prog Lipid Res **51**(2): 149-177.
Terwilliger, T. C., L. Weissman and D. Eisenberg (1982). "The structure of melittin in the form I crystals and its implication for melittin's lytic and surface activities." Biophysical Journal **37**(1): 353-361.
Thomas, C. J. and A. Surolia (1999). "Kinetics of the interaction of endotoxin with polymyxin B and its analogs: a surface plasmon resonance analysis." FEBS Lett **445**(2-3): 420-424.
Timmons, P. B., D. O'Flynn, J. M. Conlon and C. M. Hewage (2019). "Structural and positional studies of the antimicrobial peptide brevinin-1BYa in membrane-mimetic environments." Journal of Peptide Science **25**(11): e3208.

Tossi, A., L. Sandri and A. Giangaspero (2000). "Amphipathic, α-helical antimicrobial peptides." Peptide Science **55**(1): 4-30.
Trabi, M. and D. J. Craik (2002). "Circular proteins — no end in sight." Trends in Biochemical Sciences **27**(3): 132-138.
Troxler, R. F., G. D. Offner, T. xu, J. C. Vanderspek and F. G. Oppenheim (1990). "Structural Relationship Between Human Salivary Histatins." Journal of Dental Research **69**(1): 2-6.
Turner, J., Y. Cho, N.-N. Dinh, A. J. Waring and R. I. Lehrer (1998). "Activities of LL-37, a Cathelin-Associated Antimicrobial Peptide of Human Neutrophils." **42**(9): 2206-2214.
Tzou, P., S. Ohresser, D. Ferrandon, M. Capovilla, J.-M. Reichhart, B. Lemaitre, J. A. Hoffmann and J.-L. J. I. Imler (2000). "Tissue-specific inducible expression of antimicrobial peptide genes in Drosophila surface epithelia." **13**(5): 737-748.
Urmi, U. L., A. K. Vijay, R. Kuppusamy, S. Islam and M. D. P. Willcox (2023). "A review of the antiviral activity of cationic antimicrobial peptides." Peptides **166**: 171024.
van Zoggel, H., Y. Hamma-Kourbali, C. Galanth, A. Ladram, P. Nicolas, J. Courty, M. Amiche and J. Delbé (2012). "Antitumor and angiostatic peptides from frog skin secretions." Amino Acids **42**(1): 385-395.
Vanhoye, D., F. Bruston, P. Nicolas and M. Amiche (2003). "Antimicrobial peptides from hylid and ranin frogs originated from a 150-million-year-old ancestral precursor with a conserved signal peptide but a hypermutable antimicrobial domain." European Journal of Biochemistry **270**(9): 2068-2081.
Veldhuizen, E. J., V. A. Schneider, H. Agustiandari, A. van Dijk, J. L. Tjeerdsma-van Bokhoven, F. J. Bikker and H. P. Haagsman (2014). "Antimicrobial and immunomodulatory activities of PR-39 derived peptides." PLoS One **9**(4): e95939.
Veldhuizen, E. J. A., A. van Dijk, M. H. G. Tersteeg, S. I. C. Kalkhove, J. van der Meulen, T. A. Niewold and H. P. Haagsman (2007). "Expression of β-defensins pBD-1 and pBD-2 along the small intestinal tract of the pig: Lack of upregulation in vivo upon Salmonella typhimurium infection." Molecular Immunology **44**(4): 276-283.
Vincent, P. A. and R. D. J. C. m. c. Morero (2009). "The structure and biological aspects of peptide antibiotic microcin J25." **16**(5): 538-459.
Vlieghe, P., V. Lisowski, J. Martinez and M. Khrestchatisky (2010). "Synthetic therapeutic peptides: science and market." Drug Discov Today **15**(1-2): 40-56.
Waghu, F. H., R. S. Barai, P. Gurung and S. Idicula-Thomas (2015). "CAMPR3: a database on sequences, structures and signatures of antimicrobial peptides." Nucleic Acids Research **44**(D1): D1094-D1097.
Waghu, F. H. and S. Idicula-Thomas (2020). "Collection of antimicrobial peptides database and its derivatives: Applications and beyond." Protein Science **29**(1): 36-42.
Wang, C., L.-L. Tian, S. Li, H.-B. Li, Y. Zhou, H. Wang, Q.-Z. Yang, L.-J. Ma and D.-J. Shang (2013). "Rapid Cytotoxicity of Antimicrobial Peptide Tempoprin-1CEa in Breast Cancer Cells through Membrane Destruction and Intracellular Calcium Mechanism." PLOS ONE **8**(4): e60462.
Wang, G. (2008). "Structures of Human Host Defense Cathelicidin LL-37 and Its Smallest Antimicrobial Peptide KR-12 in Lipid Micelles*." Journal of Biological Chemistry **283**(47): 32637-32643.
Wang, G., X. Li and Z. Wang (2015). "APD3: the antimicrobial peptide database as a tool for research and education." Nucleic Acids Research **44**(D1): D1087-D1093.
Wang, G., C. Schmidt, X. Li and Z. Wang (2025). "APD6: the antimicrobial peptide database is expanded to promote research and development by deploying an unprecedented information pipeline." J Nucleic Acids Research: gkaf860.
Wang, J., M. Cheng, I. K. M. Law, C. Ortiz, M. Sun and H. W. Koon (2019). "Cathelicidin Suppresses Colon Cancer Metastasis via a P2RX7-Dependent Mechanism." Molecular Therapy - Oncolytics **12**: 195-203.
Wang, J., V. Yadav, A. L. Smart, S. Tajiri and A. W. Basit (2015). "Stability of peptide drugs in the colon." European Journal of Pharmaceutical Sciences **78**: 31-36.
Wang, L., C. Dong, X. Li, W. Han and X. Su (2017). "Anticancer potential of bioactive peptides from animal sources." J Oncology reports **38**(2): 637-651.

Wang, W., A. M. Cole, T. Hong, A. J. Waring and R. I. Lehrer (2003). "Retrocyclin, an antiretroviral θ-defensin, is a lectin." The journal of immunology **170**(9): 4708-4716.
Whitmore, L., J. K. Chugh, C. F. Snook and B. A. Wallace (2003). "The peptaibol database: a sequence and structure resource." J Pept Sci **9**(11-12): 663-665.
Whitmore, L. and B. A. Wallace (2004). "The Peptaibol Database: a database for sequences and structures of naturally occurring peptaibols." Nucleic Acids Research **32**(suppl_1): D593-D594.
WHO (2019). WHO global report on traditional and complementary medicine 2019, WHO.
Wiesner, J. and A. Vilcinskas (2010). "Antimicrobial peptides: the ancient arm of the human immune system." Virulence **1**(5): 440-464.
Willey, J. M. and W. A. v. d. Donk (2007). "Lantibiotics: Peptides of Diverse Structure and Function." Annual Review of Microbiology **61**(1): 477-501.
Wimley, W. C. (2010). "Describing the Mechanism of Antimicrobial Peptide Action with the Interfacial Activity Model." ACS Chemical Biology **5**(10): 905-917.
Wimley, W. C. and K. Hristova (2011). "Antimicrobial peptides: successes, challenges and unanswered questions." The Journal of membrane biology **239**(1-2): 27-34.
Wüthrich, K. (1986). "NMR with proteins and nucleic acids." Europhysics News **17**(1): 11-13.
Wymore, T. and T. C. Wong (1999). "Molecular Dynamics Study of Substance P Peptides in a Biphasic Membrane Mimic." Biophysical Journal **76**(3): 1199-1212.
Xia, X., L. Cheng, S. Zhang, L. Wang and J. Hu (2018). "The role of natural antimicrobial peptides during infection and chronic inflammation." Antonie van Leeuwenhoek **111**(1): 5-26.
Xu, R., H.-Q. Xie, L.-L. Deng, J.-X. Zhang, F.-M. Yang, J.-H. Liu, X.-J. Hao and Y.-H. Zhang (2014). "A new bufadienolide with cytotoxic activity from the Chinese traditional drug Ch'an Su." Chinese Journal of Natural Medicines **12**(8): 623-627.
Yi, G.-S., C. B. Park, S. C. Kim and C. Cheong (1996). "Solution structure of an antimicrobial peptide buforin II." FEBS Letters **398**(1): 87-90.
Yonezawa, A., J. Kuwahara, N. Fujii and Y. Sugiura (1992). "Binding of tachyplesin I to DNA revealed by footprinting analysis: significant contribution of secondary structure to DNA binding and implication for biological action." Biochemistry **31**(11): 2998-3004.
Yorek, M. A. (2018). Biological distribution. Phospholipids handbook, CRC Press**:** 743-775.
Yount, N. Y., A. S. Bayer, Y. Q. Xiong and M. R. Yeaman (2006). "Advances in antimicrobial peptide immunobiology." **84**(5): 435-458.
Zairi, A., C. Serres, F. Tangy, P. Jouannet and K. Hani (2008). "In vitro spermicidal activity of peptides from amphibian skin: Dermaseptin S4 and derivatives." Bioorganic & Medicinal Chemistry **16**(1): 266-275.
Zanetti, M., R. Gennaro and D. J. F. l. Romeo (1995). "Cathelicidins: a novel protein family with a common proregion and a variable C-terminal antimicrobial domain." **374**(1): 1-5.
Zasloff, M. (1987). "Magainins, a class of antimicrobial peptides from Xenopus skin: isolation, characterization of two active forms, and partial cDNA sequence of a precursor." **84**(15): 5449-5453.
Zasloff, M. (1987). "Magainins, a class of antimicrobial peptides from Xenopus skin: isolation, characterization of two active forms, and partial cDNA sequence of a precursor." Proceedings of the National Academy of Sciences of the United States of America **84**(15): 5449-5453.
Zasloff, M. (2002). "Antimicrobial peptides of multicellular organisms." Nature **415**(6870): 389-395.
Zasloff, M. (2002). "Antimicrobial peptides of multicellular organisms." Nature **415**: 389.
Zeng, B., J. Chai, Z. Deng, T. Ye, W. Chen, D. Li, X. Chen, M. Chen and X. Xu (2018). "Functional Characterization of a Novel Lipopolysaccharide-Binding Antimicrobial and Anti-Inflammatory Peptide in Vitro and in Vivo." Journal of Medicinal Chemistry **61**(23): 10709-10723.
Zhang, R., M. Zhou, L. Wang, S. McGrath, T. Chen, X. Chen and C. Shaw (2010). "Phylloseptin-1 (PSN-1) from Phyllomedusa sauvagei skin secretion: A novel broad-spectrum antimicrobial peptide with antibiofilm activity." Molecular Immunology **47**(11): 2030-2037.

Zhang, X. L., M. E. Selsted and A. Pardi (1992). "NMR studies of defensin antimicrobial peptides. 1. Resonance assignment and secondary structure determination of rabbit NP-2 and human HNP-1." J Biochemistry **31**(46): 11348-11356.
Zhou, K. and B. Liu (2022). Molecular dynamics simulation: Fundamentals and Applications, Academic Press.
Zhu, S., M. A. Sani and F. Separovic (2018). "Interaction of cationic antimicrobial peptides from Australian frogs with lipid membranes." Peptide Science **110**(3): e24061.
Zhu, X., N. Dong, Z. Wang, Z. Ma, L. Zhang, Q. Ma and A. J. A. b. Shan (2014). "Design of imperfectly amphipathic α-helical antimicrobial peptides with enhanced cell selectivity." **10**(1): 244-257.